Hochschule für Angewandte Wissenschaften Hamburg
Hamburg University of Applied Sciences

Hamburg Univertsity of Applied Sciences
Faculty of Life Sciences

Analysis of [6]-Gingerol-dependent Protein Complex Formation in HeLa Cells

Master Thesis
in Pharmaceutical Biotechnology

Submitted by
Treewut Rassamegevanon
Matriculation number: 2132287

First examiner:	Prof. Dr. Oliver Ullrich	(HAW Hamburg)
Second examiner:	Prof. Dr. Birger Anspach	(HAW Hamburg)

Date of submission: 6 June 2014

This thesis was supervised and performed in the laboratory of molecular biology and cell culture techniques at Hamburg University of Applied Sciences.

Acknowledgements

I would like to express my profound gratitude to Prof. Dr. Oliver Ullrich, who provided an opportunity to accomplish this thesis and learn in his laboratory. He provided an environment for me that exceeded all I could wish for. His inestimable generosity and patience for consistently giving guidance and assistances has been greatly appreciated. All of his advices have been invaluable.

My grateful thanks are also extended to Prof. Dr. Birger Anspach for serving as my second examiner and providing valuable information concerning experimental procedures.

I would also like to extend my thanks to the technician of the laboratory of molecular biology and cell culture techniques, Mrs. Elisabeth Schäfer, for her greatly valuable supports on cells and instrument handling and general questions in the laboratory.

I extend my appreciation to Dr. Marcus Nalaskowski (UKE, Hamburg) for giving me the possibility to use the ultracentrifuge in his laboratory.

Special thanks to Katharina Rützel, Florian Aupert, Vignesh Rajamanickam, Alexander Heller and others for their advices, encouragements, friendship and co-operation within the master program. I am grateful for the opportunity I had to study and work with them.

Words cannot express how grateful I am to my guest family here in Germany for giving me the opportunity to perform the master degree in Germany. I could not imagine my life without their love and generosity. Without any doubt, their generosity will be deeply engraved in my heart.

Finally, I would like to thank my parents, friends and my girlfriend in Thailand, who always encourage me to do my best. My parents always supported me throughout my entire education.

Table of Contents

1. Introduction

1.1 Ginger: Overview

Ginger, the rhizome of the tropical herbaceous plant *Zingiber officinale*, is a well-known culinary spice in many Asian countries. Ginger is available in markets as fresh, dried, pickled, preserved, crystallized, candied, and powdered or ground. As an alternative medicine, ginger is commonly used for alleviating gastrointestinal disorders, inflammatory arthritis, common cold, cough, nausea caused by cancer treatment, nausea and vomiting after surgery, pain remedy, upper respiratory tract infections and bronchitis (Gaoa and Zhang, 2010; National Institutes of Health, 2013; Malhotra and Singh, 2003). U.S. Food and Drug Administration (FDA) recognises ginger as food additive that is "generally recognized as safe" (GRAS). A broad range of oral doses is reported of 1 or 2 grams of powdered ginger taken with liquid over an unlimited period per day (Chrubasik *et al*., 2005). And the maximum daily dose for adult is usually 5 grams per day orally for powdered ginger (American Cancer Society, 2010).

Fresh ginger composes of 79% moisture, 2% protein, 0.75% fat, 18% carbohydrate, minerals, and vitamins. Ginger has been analysed by various analytical methods and at least 115 constituents have been identified (Bode and Dong, 2011). Additionally, at least 14 bioactive compounds have been fractionated including [4]-gingerol, [6]-gingerol, [8]-gingerol, [10]-gingerol, [6]-paradol, [14]-shogaol, [6]-shogaol, 1-dehydro-[10]-gingerdione, [10]-gingerdione, hexahydrocurcumin, tetrahydrocurcumin, gingerenone A, 1,7-bis-(4-hydroxyl-3-methoxyphenyl)-5-methoxyhepthan-3-one, and methoxy-[10]-gingerol (Koh *et al*., 2009). Up to 9% of ginger are lipids and glycolipids and about 5-8% is oleoresin. The pungent principles accounting of 25% of the oleoresin, consists mainly of gingerols (Chrubasik *et al*., 2005). Gingerols are the major constituents of fresh ginger and are found slightly reduced in dehydrated ginger, whereas shogaols, the dehydrated products of gingerol, are more abundant than gingerol in dried ginger (Jolad *et al*., 2005). [6]-gingerol is more pungent than [8]-gingerol and [10]-gingerol. It appears that [6]-gingerol is the major pungent bioactive phenolic compound in the ginger oleoresin (Wohlmuth *et al*., 2005). However, the components and the oleoresin of ginger vary according to diversity of origins, agronomical conditions, age (the ginger essential oil increases as ginger ages) and storage methods (Ekundayo, 1988; Bailey-Shaw *et al*., 2008).

Ginger shows a significant anti-oxidative effect. A very high level of total antioxidants in ginger (3.85 mmol/100 g), which is slightly lower than pomegranate and some sort of berries, has been reported (Halvorsen *et al*., 2002). The volatile ginger oil from methanolic ginger extract showed various healthy benefits such as reducing serum LDL, total cholesterol, triglyceride and phospholipid levels, as well as cellular cholesterol accumulation, reducing DPPH absorption and scavenging free radicals (Al-Tahtawy *et al*., 2011). Stoilova and colleagues (2007) reported that ginger extract from CO_2 extraction revealed a high polyphenol content and exerted comparable anti-oxidative effect with synthetic antioxidants on inhibiting lipid peroxidation at 37^{o}C. Moreover, it suppressed the initiation of hydroxylradical, which is known as the inducer of lipid peroxidation (Stoilova *et al*., 2007). The anti-oxidative effect of ginger extracts relies on the presence of gingerols and shogaols. In the absence of both bioactive phenolic compounds the anti-oxidative activity of ginger extracts decreased by 20% approximately (Zancan *et al*., 2002). In *in vivo* tests, ginger oil intraperitoneally administrated to mice inhibited phorbol-12-myristate-13-acetate from promoting the oxidative stress (Jeena *et al*., 2013).

Ginger exhibits a broad spectrum of antimicrobial activities. Commercial ginger paste exerted the complete inactivation of *Escherichia coli* O157:H7 within 2 weeks at 4 and 8^{o}C in food system models and a laboratory buffer (Gupta and Ravishankar, 2005). 10% ethanolic ginger extract was reported that it possessed antimicrobial activities against the growth of the well-known oral microorganisms *Streptococcus mutans* (*S. mutans*), *Candida albicans* (*C. albicans*) and *Enterococcus faecalis* (*E. faecalis*), which are commonly implicated in oral infections (Giriraju and Yunus, 2013). *Aspergillus flavus* (*A. flavus*), *Aspergillus niger* (*A. niger*) and *Cladosporium herbarum* (*C. herbarum*) growth were inhibited by ethanolic ginger extract, which yielded the best result compared to water-based ginger extract (Tagoe *et al*., 2009). Hasan and colleagues (2012) suggested that the inhibitory effect of ginger might be the result of monoterpene, which was reported to have a wide range of antimicrobial activities. Furthermore, the main mechanism of the inhibitory effect is the disruption of bacterial or fungal membrane integrity (Hasan *et al*., 2012).

Many reports claim that ginger has an ability to decrease inflammation, swelling and pain. By applying acute inflammation inducers (carrageenan and dextran), and chronic inflammation inducer (formalin) for investigating the anti-inflammation activity of ginger oil, the swelling of mice paws was suppressed in a dose-dependent manner (100, 500 and 1000 mg ginger oil/kg mouse) (Jeena *et al*., 2013). In human histiocyte cell line (U937) model, ginger extract and gingerol inhibited prostaglandin E2 (PGE_2), which is known as a crucial mediator of inflammation, induced by lipopolysaccharide (LPS). Furthermore, LPS induced cyclooxygenase-2 (COX-2) expression in U937 cells was completely inhibited by gingerol (0.1 μg/mL) (Lantz *et al*., 2007). It is likely that the inflammation inhibiting effect of ginger extract is related to the inhibitory effect of ginger extract against a variety of pro-inflammatory cytokines (IL-12, TNF-α, IL-1β) and chemokines (RANTES, MCP-1), which were overexpressed by LPS stimulated macrophages (Tripathi *et al*., 2008). Leukotrienes are a family of eicosanoid inflammatory mediators produced in leukocytes, mastocytoma cells, macrophages, and other tissues. Leukotrienes are involved in triggering acute asthma attack and inflammatory diseases (Berger, 1999). Gingerol shows the inhibitory effect against arachidonate 5-lipoxygenase, an enzyme of leukotriene (LT) biosynthesis, hence, the possible mechanism, which is deduced from the structure and verified by its inhibitory effect, might rely on the activity against arachidonate 5-lipoxygenase (Kiuchi *et al*., 1992).

The cancer preventive and cancer therapeutic applications of ginger and various components have been studied for a great while. Many research groups are interested in anti-tumourigenic effects from crude ginger extracts and individual components including gingerol, shogaol, zerumbone (a sesquiterpene compound), and its minor metabolite components. It has been suggested that the anti-tumourigenic activity of ginger and its components includes anti-oxidative activity and the ability to induce apoptosis, decreasing proliferation, activating cell-cycle arrest, and suppressing activator protein 1 (AP-1) and NF-κB/COX-2 signalling pathways (Bode and Dong, 2011). Especially, [6]-gingerol and [6]-shogaol have been intensively investigated for analysing the anti-tumourigenic activity. Cheng and colleagues (2011) reported that methanolic extract of streamed ginger exhibited the strongest anti-proliferative effect on human epithelial carcinoma cells (HeLa cells) compared to methanolic extract of fresh ginger and dried ginger. The possible explanation for the instance is the content of [6]-shogaol in the methanolic extract of streamed ginger was significantly higher than the others. And it was confirmed that [6]-shogaol exerted the highest cytotoxic effect on HeLa cells in comparison to [6]-gingerol (Cheng *et al*., 2011). Rützel (2012) and Renger (2013) examined the growth inhibiting effects of dried and fresh ginger for HeLa cells and reported that ginger extracts demonstrated a significant reduction of HeLa cell viability

compared to Chinese hamster ovary (CHO) cells. Furthermore, it was reported that ginger extracts altered microtubule structure causing cell-cycle arrest in telophase of mitosis (Rützel, 2012; Renger, 2013).

1.2 Pharmacological properties of [6]-gingerol

[6]-gingerol (1-(4-hydroxy-3-methoxyphenyl)-5-hydroxy-3-decanone) is the major pungent bioactive compound of ginger. The structure of [6]-gingerol is depicted on figure 1.1. [6]-gingerol has a wide range of pharmacological effects including antimicrobial, anti-tumourigenic and anti-inflammatory activity. [6]-gingerol is isolated from ginger rhizome by using organic solvents, near critical fluids or supercritical fluids. The dehydrated analogue of [6]-gingerol is [6]-shogaol. Shogaol and its degradation products and zingerone, are produced when fresh ginger is heated or cooked. [6]-gingerol is a condensation product of zingerone with saturated six straight-chain of aldehydes and it is named according to the position of the aldehyde unit (Zachariah, 2008). [6]-gingerol was analysed through structural based *in silico* studies and reported as a hydrophobic phenolic compound due to its aromatic ring and methoxy group (Saptarini *et al*., 2013).

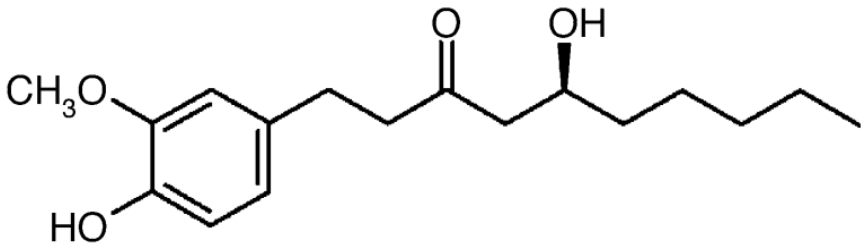

Figure 1.1 Chemical structure of [6]-gingerol (Ippoushi *et al*., 2003)

1.2.1 Anti-tumourigenic effects

Neoplasia or tumours are abnormal cells or tissues resulting from unnatural cell proliferation, which cause an abnormal growth of organs, where tumours are located. Depending on the type of tumour, benign tumour, pre-malignant (carcinoma *in vivo*) or malignant tumour, the growth of tumour behaves differently. Benign tumours, the non-cancerous tumours, do not cause severe or life threatening problems unless the tumours govern excessive space and affect nearby vital organs. They have slow growth rate and do not spread to other nearby or remote organs. The malignant tumours, the cancerous tumours, behave differently since they are able to grow faster and invade to nearby or remote tissues (metastasis), which threat patients' life differently. The evolution of cancer cells or carcinogenesis is a multistep process involving three distinct steps; initiation, promotion and progression. The carcinogenesis involves numerous signal transduction pathways. Initiation occurrs when normal cells are exposed or damaged by carcinogens and their suffered genomic DNA remain unrepaired or misrepaired resulting in irreversible changes of genomic DNA (mutation). Promotion is a step where mutated cells expand to give rise of a mutated cell population (pre-malignant tumour). Progression is termed as the promotion of pre-malignant tumour to a neoplasm and to the malignancy increasing proliferation rate, invasiveness and metastatic potential (Surh, 1999). The carcinogenesis process is depicted in figure 1.2

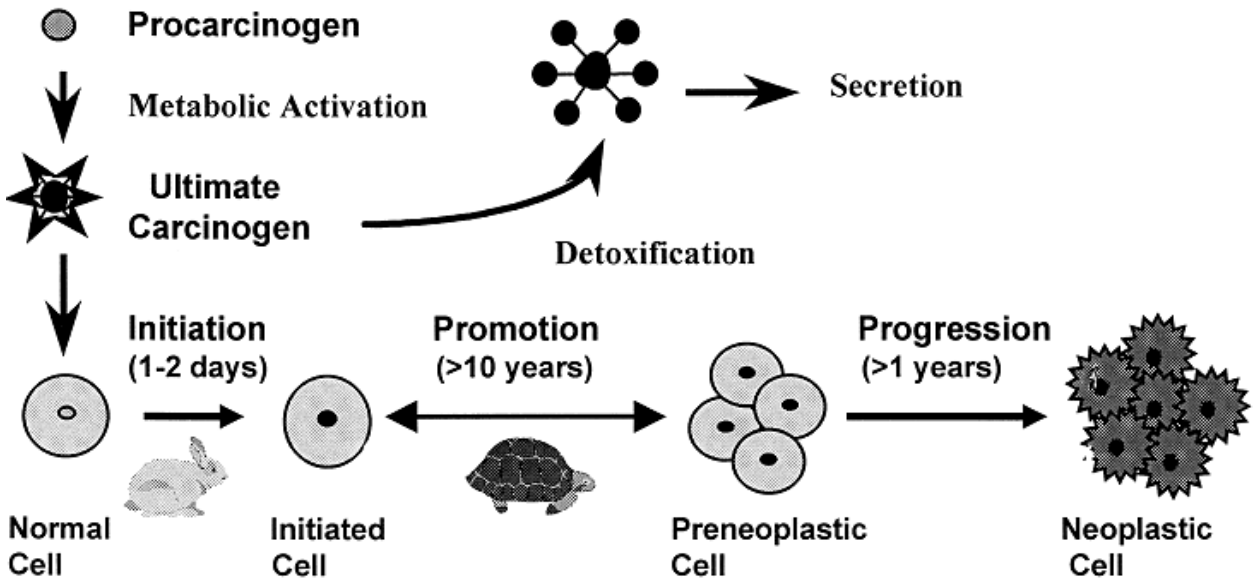

Figure 1.2 Schematic illustration of multistep carcinogenesis
A procarcinogen is metabolised resulting in an ultimate carcinogen. The ultimate carcinogen is either detoxificated or damages the normal cells causing permanent changes in genomic DNA. The mutated cells or initiated cells carrying damaged or misrepaired genomic DNA divide to create mutated daughter cells so called preneoplastic cells. A bunch of preneoplastic cells are promoted to become neoplastic cells during promotion phase resulting in highly uncontrolled growth rate and metastatic potential (Surh, 1999).

[6]-gingerol is predominantly involved in an anti-tumourigenic activity of ginger extract. The proposed action of [6]-gingerol on carcinogenic process is to suppress either the promotion or the progression of initiated cells into malignant cells (Surh, 1999). Lee and colleagues (2008) investigated effects of [6]-gingerol on human colorectal cancer cells. They have found that [6]-gingerol reduced cell growth in a concentration-dependent fashion (0, 50, 100, 150, and 200 μM). The cell cycle was arrested by [6]-gingerol at G_1 phase inducing apoptosis of cells. G1/S-specific cyclin D1, an important protein for cell cycle transition, was suppressed after incubating with [6]-gingerol in a concentration-dependent manner. The downregulation of cyclin D1 expression is due to the inhibition of the transcriptional regulation via β-catenin signalling pathways and the activation of the proteolysis of cyclin D1. The protein kinase C (PKC-ε) has been proposed to serve dual purposes as a tumour suppressor and a tumour promoter via multiple steps. Glycogen synthase kinase-3 (GSK-3) is one of the primary target genes of the PI3K/AKT pathway that mediates apoptotic signals. NAG-1 expression, which was reported to inhibit the development of intestinal tumours and prostate tumours in animal models (Wang *et al*., 2013), was increased in a concentration-dependent fashion after incubating cells with [6]-gingerol. For the NAG-1 expression, it has been proposed that [6]-gingerol activated NAG-1 expression occurs through the activation of PKC-ε and GSK-3 pathways (Lee *et al*., 2008).

To investigate the potential binding partner(s) of [6]-gingerol in human colorectal cancer cells, Joeng and colleagues (2009) conducted an *in silico* prediction using a reverse-docking approach and confirmed the results by conducting *in vivo* (mice model) and *ex vivo* tests. They demonstrated that Leukotriene A_4 Hydrolase (LTA_4H), which is a bifunctional zinc enzyme with the activities of epoxide hydrolase and aminopeptidase and has become a promising therapeutic target against cancer and chronic

inflammation (Chen *et al*., 2004; DuBois, 2003), might be a potential target of [6]-gingerol. The binding potential of [6]-gingerol and LTA_4H was confirmed by pull-down assay using [6]-gingerol-Sepharose 4B beads and subsequently western blot analysis. Moreover, [6]-gingerol inhibited the cancer cell growth and decreased LTA_4H activity based on ELISA test. *In vivo* tests in mice model indicated that [6]-gingerol treated mice demonstrated significantly prolonged life by suppressing LTA_4H activity as compared to mice that were treated with ethanol (vehicle) (Jeong *et al*., 2009).

p53 protein is a tumour suppressor protein that is crucial for multicellular organisms. The p53 protein is encoded by *TP53* gene responding to a diverse cellular stresses, by which the expression of the protein is regulated. The tumour suppressive activity of p53 protein is involved in various processes including cell-cycle arrest, apoptosis, senescence, DNA repair, or changes in metabolism. Park and colleagues (2006) investigated effects of [6]-gingerol on human pancreatic cancer cells, HPAC with wild-type p53 and BxPC3 with mutant p53. The results from their work showed that [6]-gingerol inhibited the cell growth of both BxPC3 and HPAC cells in a concentration- and a time-dependent fashion. Cell-cycle arrest induced by [6]-gingerol was observed in BxPC-3 cells causing the cells to accumulate in G_1 phase within 24 hours. In contrast to HPAC cells, the cell-cycle arrest was slightly higher in the [6]-gingerol treated group. Moreover, the expression levels of proteins that affect the cell division cycle (Cyclin A, Cyclin E, Cyclin D1, Cdk-2, Cdk-4, Cdk-6, Rb, pRb) were investigated. The results indicated that [6]-gingerol downregulated the expression of Cyclin A and Cdks including Cdk-2, Cdk-4, Cdk-6 in BxPC-3 cells and Cyclin A, Cdk-6 in HPAC cells. The cell-cycle arrest by [6]-gingerol has been proposed to be due to the lack of Cyclin or Cdk expression leading to the obstacle of Cyclin-Cdk complex formation and lowering the level of pRb. The cells failed to enter S phase since Rb protein was unphosphorylated leading to no activation of E2F, a group of genes that plays a crucial role in the control of cell cycle. [6]-gingerol induced apoptosis of BxPC-3 cells was observed 24 hours after [6]-gingerol treatment. On the other hand, HPAC resisted highly to the apoptosis induced by [6]-gingerol, which was suppressed through the PI3K/AKT pathway (Park *et al*., 2006).

In HeLa cells, Chakraborty and colleagues (2012) demonstrated the mechanism of anti-tumourigenic properties of [6]-gingerol. HeLa cells altered dramatically their morphology after treatment with [6]-gingerol and the mitochondrial membrane potential of the cells was lost indicating the mitochondrial membrane-dependent apoptosis. Autophagy, the self-degradation process through the action of lysosomes, was induced by [6]-gingerol and [6]-gingerol showed notable affinity towards binding nuclear DNA and circulating tumour DNA (ctDNA) in a concentration-dependent fashion. HeLa cells treated by [6]-gingerol showed the condensation of nuclei and isolated DNA. The [6]-gingerol treated cells revealed the ladder formation of DNA indicating cleavage of chromosomal DNA into oligonucleosomal size fragments. Those three phenomena, alteration of morphology, DNA degradation into oligonucleosomal size fragments and condensation of nuclei, are biochemical characteristics of apoptosis (Bortner *et al*., 1995). Moreover, it was reported that [6]-gingerol treated HeLa cells upregulated the expression of TNF-α, Bax and cytochrome C, but downregulated the expression of NF-κβ, AKT (total AKT) and Bcl2. The upregulation of TNF-α, downregulation of NF-κβ and imbalance of Bax/Bcl2 ratio trigger the apoptosis of cancer cells (Chakraborty *et al*., 2012).

1.2.2 Anti-inflammation effects

Inflammation is a response of the immune system to infection or harmful stimuli such as pathogens, damaged cells or irritants. The response of the immune system to inflammation requires a communication between various classes of immune cells. Inflammation can be classified into acute inflammation and chronic inflammation. Acute inflammation is a short-term response, usually resulting in healing: leukocytes infiltrate the damaged region, removing the stimulus and repairing the tissue. In contrast, chronic inflammation is a prolonged, dysregulated and maladaptive response that involves active inflammation, tissue destruction and attempts in tissue repair (Weiss, 2008). Chronic inflammation is involved in many human diseases such as allergic rhinitis, atherosclerosis, rheumatoid arthritis and development of cancer (Rakoff-Nahoum, 2006). Numerous cytokines (e.g. IL-1, IL-6 and TNF-α), chemokines (e.g. IL-8, CXC- and CC-groups), enzymes (e.g. COX-2 and Protein kinease C (PKC)) and inflammation mediators (e.g. reactive oxygen species (ROS) and inducible nitric oxide synthase (iNOs)) are involved in the induction of chronic and acute inflammation processes.

The pharmacological properties of [6]-gingerol against inflammation have been reported. (Bode and Dong, 2011). Pain relief and anti-inflammatory effects of [6]-gingerol were confirmed by Young and co-workers (2005) with a nociception test induced by acetic acid and formalin, and a mice paw oedema model induced by λ-carrageenin. Mice were pre-treated intraperitoneally with different doses of [6]-gingerol (12.5, 25 and 50 mg [6]-gingerol/kg mouse). The writhing activity induced by 1% acetic acid of the [6]-gingerol pre-treated mice was significantly decreased in a concentration-dependent manner compared to untreated mice. As well as the reaction of mice to 1% formalin, the [6]-gingerol pre-treated mice suffered from formalin significantly shorter than the untreated mice. Furthermore [6]-gingerol effectively reduced the mouse's hind paw oedema induced by λ-carrageenin in a dose-dependent fashion (Young *et al*., 2005).

Prostaglandin-endoperoxide synthase 2 (COX-2) is an enzyme that presents an elevated level during inflammation. [6]-gingerol showed an ability to suppress ROS production and COX-2 expression using *in vivo* and *in vitro* models. Kim and co-workers (2007) demostrated that [6]-gingerol suppressed ROS production in human keratinocyte (HaCaT) cells induced by UVB radiation. ROS has been found to be a mediator of COX-2 expression and NF-κβ activation. Thus, the suppression of ROS by [6]-gingerol leading to the downregulation of COX-2 expression and NF-κβ activation in HaCaT cells and mouse skin (Kim *et al*., 2007).

Lee and colleagues (2009) demonstrated effects of [6]-gingerol in lipopolysaccharide (LPS) stimulated mouse macrophages. [6]-gingerol did not show significant cytotoxicity to mouse macrophage cells and suppressed the production of iNOs (protein and mRNA levels) in LPS-treated cells in a dose- and a time-dependent manner. [6]-gingerol also efficiently decreased TNF-α level and IL-10 expression in the LPS-treated cells. LPS induces Ca^{2+} overload in mouse macrophage cells and consequently induces the generation of ROS. By incubation of the LPS treated cells with [6]-gingerol, the intracellular Ca^{2+} overload was suppressed as well as the ROS production. [6]-gingerol also prevented the disruption of the mitochondrial membrane potential, which is one of the critical actions in oxidative stress pathways. [6]-gingerol induced migration of PKC-α protein from cytosolic fraction to membrane fraction in a concentration-dependent manner. Moreover, the level of NF-κβ proteins in nuclear extract was significantly reduced in a concentration-dependent manner. Thus, the production of iNOs and ROS in the

LPS-treated cells was effectively downregulated by [6]-gingerol through PKC-α and NF-κβ, which both are key elements of triggering pro-inflammation signal transduction (Lee *et al*., 2009). In addition, Tripathi and colleagues (2007) investigated [6]-gingerol suppression effect on pro-inflammatory cytokines (TNF-α, IL-12 and IL-β) and chemokines (RANTES and MCP-1) in LPS-induced mouse macrophages. Most of the analysed cytokine and chemokine expressions were significantly suppressed by [6]-gingerol except MCP-1. As well as NF-κβ expression, the LPS-induced mouse macrophages treated by [6]-gingerol showed significant reduction of the NF-κβ expression in nuclear extract. Major histocompatibility complex II (MHC II) expression, an activation state of macrophages, was not affected by [6]-gingerol indicating that [6]-gingerol selectively inhibits pro-inflammatory lymphokine production in activated macrophages (Tripathi *et al*., 2007).

1.2.3 Antimicrobial and anti-parasitic effects

Ginger shows a broad spectrum of pharmacological properties, antimicrobial and anti-parasitic effects are two of them. [6]-gingerol is one of the pungent bioactive compounds that act against pathogenic microbes and parasites (Saha *et al*., 2013; Lin *et al*., 2010; Mahady *et al*., 2003). Mahady and colleagues (2003) investigated the antimicrobial effect of methanolic ginger extract and isolated gingerols (e.g. [6]-shogaol, [6]-gingerol) against *Helicobacter pylori* (*H. pylori*), a group 1 carcinogen gram-negative bacterium and a cause of gastric cancer in humans. For 19 strains of *H. pylori* including 5 *CagA*$^{+}$ strains, susceptibility testing was conducted. CagA is the strain specific *H. pylori* gene that has been linked to the development of pre-malignant and malignant histological lesions. The minimum inhibitory concentration (MIC) was measured and [6]-gingerol inhibited the growth of 5 *H. pylori CagA*$^{+}$ strains at a concentration range of 3.125-12.5 µg/mL (Mahady *et al*., 2003).

Anti-parasitic properties of [6]-gingerol were also investigated. *Angiostrongylus cantonensis* (*A. cantonensis*), also known as the rat lungworm, is a nematode parasite that dwells in the rat pulmonary artery. It has been related to *A. cantonensis* infection in humans. [6]-gingerol exhibited larvicidal activity (lethal efficacy) against *A. cantonensis* larvae in a concentration- and a time-dependent manner. Their spontaneous movement was also reduced when the worms were exposed to [6]-gingerol in a concentration- and a time-dependent manner (Lin *et al*., 2010).

Saha and co-workers (2013) demonstrated the effects of [6]-gingerol on *Vibrio cholera* (*V. cholera*), a major gram-negative pathogenic bacterium. Cholera toxin produced by *V. cholera* during infection causes potentially life-threatening diarrhoeal disease. Although [6]-gingerol was not able to reduce the viability and adherence of *V. cholera* to the intestinal epithelial cell, cholera toxin was dramatically reduced by [6]-gingerol in a dose-dependent manner based on ELISA analysis. Furthermore, p*I* of cholera toxin of [6]-gingerol treated *V. cholera* changed from 6.8 to 7.5 indicating remarkable cholera toxin-[6]-gingerol interaction. This was supported by fluorescence spectroscopic results that [6]-gingerol quenched cholera toxin emitted signals in a dose-dependent manner. Cholera toxin induced the elongation of CHO cells, which was inhibited by [6]-gingerol. And [6]-gingerol reduced cholera toxin induced intracellular cAMP expression in CHO cells suggesting the reduction of pathogenic activity (Saha *et al*., 2013).

1.2.4 Anti-oxidative effects

ROS are reactive molecules or free radicals that are derived from oxygen molecules including superoxide anion ($\bullet O_2^-$), peroxide ($\bullet O_2^{2-}$), hydrogen peroxide (H_2O_2), hydroxyl radical ($\bullet OH$) and hydroxyl ion (OH^-). These molecules are produced as by-products of aerobic metabolism, primarily in mitochondria. ROS have been regarded as toxic by-products of metabolism, which potentially cause damage to proteins and DNA. ROS potentially cause oxidative stress in cells, which has been implicated in a large number of human diseases including atherosclerosis, pulmonary fibrosis, cancer, neurodegenerative diseases, and aging (Thannickal and Fanburg, 2000). Nitric oxide is an important cellular signalling free radical generated by constitutive and inducible nitric oxide synthase (cNOS and iNOS). NOS-derived NO plays an important role in numerous physiological (e.g. blood pressure regulation, wound repair and host defence mechanisms) and pathophysiological (inflammation, infection, neoplastic diseases, liver cirrhosis, diabetes) conditions (Lechner *et al*., 2005). [6]-gingerol has been reported that it has anti-oxidative properties that reduce oxidative stress in cells.

Dugasani and colleagues (2010) demonstrated anti-oxidative activity of [6]-gingerol in scavenging DPPH, ROS including superoxide radical, hydroxyl radical, and reduction of nitrite and prostaglandin E_2 (PGE_2) in mouse macrophage cells. Scavenging actions of [6]-gingerol against stable free radical (DPPH), superoxide and hydroxyl radical were investigated and the results exhibited that [6]-gingerol exerted ROS scavenging potential in a dose-dependent manner. In LPS stimulated mouse macrophage cells, [6]-gingerol inhibited the expression of nitrite and the release of prostaglandin E_2 in a dose-dependent fashion. Nevertheless, it was reported that [6]-shogaol exerted higher free radicals scavenging activity and preferable inhibition of the expression of nitrate and PGE_2 (Dugasani *et al*., 2010). In addition, [6]-gingerol treatment demonstrated the inhibition of iNOS induction and the protective effects against intracellular NO and potent oxidizing and nitrating molecule, peroxynitrite ($ONOO^-$). Intracellular NO and peroxynitrite have been proposed as the cause for damage of DNA and proteins contributing to carcinogenic processes (Ippoushi *et al*., 2003).

[6]-gingerol was also reported by Chakraborty and colleagues (2012) to improve insulin secretion and reduce oxidative stress *in vivo* and *in vitro*. *In vitro* tests, using isolated hepatocytes and pancreatic β-cells intoxicated by inorganic arsenic, which is suggested to contribute to diabetes type 2, were treated with [6]-gingerol. The cell viability was monitored and [6]-gingerol showed to have a protective effect against cytotoxicity of arsenic by improving the cell viability and reducing cell death at a concentration of 50 µg/mL and 75 µg/mL. Moreover, the intoxicated cells generated significantly less ROS accumulation and increased the insulin-regulated glucose transporter (GLUT4) content when the cells were treated by [6]-gingerol. *In vivo* testing showed that [6]-gingerol treatment enhanced activity of cellular defence mechanisms against ROS (super oxide dismutase (SOD)), catalase (CAT), glutathione peroxidase (GPx) and glutathione (GSH)) and reduced elevated blood glucose level. Intoxicated mice treated by [6]-gingerol exhibited an upregulation of protein expressions that are involved in the activation of downstream signal cascades leading to glucose uptake and metabolism in cells compared to intoxicated untreated mice. Inflammation related protein expressions as TNF-α and IL-6 were also downregulated by treating the intoxicated mice with [6]-gingerol (Chakraborty *et al*., 2012).

1.3 Pharmacokinetics of [6]-gingerol

Naora and colleagues (1992) demonstrated pharmacokinetics of [6]-gingerol in acute renal or hepatic failure rats. For bilaterally nephrectomised (acute renal failure) rats, 3 mg/kg of [6]-gingerol was administrated intravenously and plasma of nephrectomised rats and control was collected at different time points. Analysis was done by HPLC. The concentration of [6]-gingerol in the plasma declined biexponentially in a two compartment model with time and no significant difference in pharmacokinetic parameters was observed indicating that the [6]-gingerol elimination was not proceeded in kidney. Rats with hepatic failure was administered intravenously with 1.5 mg/kg of [6]-gingerol and plasma were collected at different time points. [6]-gingerol in plasma was eliminated in a two compartment model with time. [6]-gingerol in hepatic failure rats had longer half-life at terminal phase and total clearance of [6]-gingerol was reduced compared to control. Those results implied that kidney did not participate in elimination but rather the liver (Naora *et al*., 1992).

Nakazawa and Ohsawa (2002) demonstrated metabolites of oral administration of [6]-gingerol in urine and bile in a rat model. Seven of [6]-gingerol-derived metabolites were isolated by HPLC: 1.) (*S*)-[6]-gingerol-4′-*O*-β-glucuronide from the bile, 2.) vanillic acid, 3.) ferulic acid, 4.) (*S*)-(+)-4-hydroxy-6-oxo-8-(4-hydroxy-3-methoxyphenyl)octanoic acid, 5.) 4-(4-hydroxy-3-methoxyphenyl)butanoic acid, 6.) 9-hydroxy [6]-gingerol, 7.) (*S*)-(+)-[6]-gingerol from the urine. These findings indicated that [6]-gingerol orally administrated to rat was metabolised by ω-oxidation and β-oxidation of a phenolic side chain. In bile, the major metabolite was (*S*)-[6]-gingerol-4′-*O*-β-glucuronide, which corresponded to 48% of the applied dose indicating the major role of liver in [6]-gingerol elimination (Nakazawa and Ohsawa, 2002). In cancer cells, biotransformation of [6]-gingerol was observed in human and mouse cancer cells (lung and colon). [6]-gingerol was extensively metabolised by four cancer cell types and the products were (3R,5S)-gingerdiol and (3S,5S)-gingerdiol (Lv *et al*., 2012).

In a clinical trial, 2.0 g of ginger powder capsule was administered orally into healthy human participants and participants with high risk of colon cancer. In a single dose study, the healthy human participants ingested the single dose ginger capsule and blood was collected at different time points and analysed by LC-MS/MS method. [6]-gingerol was not detected in plasma indicating a rapid [6]-gingerol metabolic rate. [6]-gingerol glucuronide conjugate, a [6]-gingerol-derived metabolite, was detected between 0.25-10 hours with peak concentration of 0.47±0.31 μg/mL after one hour. Sulfate conjugated [6]-gingerol was detected from 0.25 to 8 h with the highest concentration of 0.28±0.15 μg/mL after one hour. In a multiple doses study (2.0 g ginger extract per day/ 24 days), blood samples from healthy human participants were collected within 24 hours. No [6]-gingerol was accumulated in the participants blood. Low levels of 6-gingerol glucuronide (ranging from 5.43 to 13.6 ng/mL) and 6-gingerol sulfate (ranging from 6.19 to 7.29 ng/mL) were observed in 4 of 12 participants that received ginger extract. For high risk participants with multiple doses of ginger extract, no free [6]-gingerol was observed in participants' colon tissue. It can be concluded that [6]-gingerol does not accumulate in blood plasma due to its short half-life and fast clearance (Yu *et al*., 2011).

1.4 Aim of the study

Möbus (2013) demonstrated potential binding partners of [6]-gingerol by applying an affinity precipitation technique and analysing the captured factors by LC-MS. [6]-gingerol coupled matrix (Epoxy- and CNBr-matrix) precipitated [6]-gingerol potential interacting proteins from HeLa cytosol. Proteins were separated by SDS-PAGE and identified by LC-MS. A prominent band turned out to be migration inhibitory factor (MIF). MIF is one of the major cytokine that possesses a number of physiological properties (inflammatory mediator, cell-mediated immunity, immunoregulation) and pathogenic properties (tumour promoting, angiogenesis, chronic and acute inflammation) (Mitchell and Bucula, 2000; Xu *et al*., 2013). Furthermore, the affinity precipitation with [6]-gingerol-conjugated matrix precipitated two other potential interacting partners of MIF and [6]-gingerol, which were tubulin and actin.

Based on the findings of Möbus (2013), the aim of this study is to analyse [6]-gingerol induced protein complex formation of MIF with other cellular binding partners by using a number of protein-protein interaction analytical methods: 1.) Blue native electrophoresis, 2.) Clear native electrophoresis 3.) Co-immunoprecipitation with anti-MIF IgG, 4.) Dot blotting analysis and 5.) Stabilisation of protein-protein interactions by chemical crosslinkers. Known proteins such as MIF, tubulin and actin are detected by western blot, unknown proteins are visualised by silver and coomassie staining.

2. Methods

2.1 Cell cultures

The HeLa cell line (human epithelial carcinoma cell line) is the first continuous cancer cell line that was isolated from an aggressive glandular cervical cancer of a young female African-American named Henrietta Lacks on February 8, 1951 (Scherer *et al*., 1953) in Baltimore, Maryland. For more than 60 years, HeLa cells have been used in research facilities around the world and more than 60,000 scientific research articles were published since the HeLa cell line was isolated (Williams, 2010). It is the first human immortal cell line that can survive *in vitro* under laboratory conditions. HeLa cells proliferate indefinitely in adequate medium, culture surface and culture condition with 24 hours as the generation time (Puck *et al*., 1956). Furthermore, because of the immortal nature of cancer cells, they show lack of contact inhibition (Stephenson, 1982). Once the surface of culture vessel is covered, they continue to divide, piling up into mounds. Like many cancer cells, HeLa cells express high telomerase activity during cell division preventing incremental shortening of telomeres, which hinders cells entering senescence and apoptosis (Ivanković *et al*., 2007).

HeLa cells were preserved in a cryovial in liquid nitrogen (-196^{o}C). After removing the cryovial containing frozen HeLa cells from liquid nitrogen, the vial was immediately placed into a 37^{o}C water bath and then gently swirled for 1 minute until a small bit of ice was left in the vial. Subsequently, prior to transfer of the cryovial containing thawed HeLa cells into a sterile laminar-flow hood, the vial was wiped with 70% ethanol. HeLa medium (see Table 2.1) was added dropwise into a reaction tube containing thawed HeLa cells. The HeLa cell suspension was centrifuged at $200 \times g$ for 10 minutes and the supernatant was aseptically aspirated without disturbing cell pellets. The HeLa cell pellets were resuspended in HeLa medium and the suspension was carefully transferred into a T75 culture flask. Because HeLa cells are mostly cultured as adherent monolayer, a culture vessel with sufficient surface is required. HeLa cells were cultivated in a CO_2 incubator that supplied sterile air with 5% CO_2. Atmospheric carbon dioxide is supplied during mammalian cell cultivation to regulate pH levels in culture media through the bicarbonate buffer system. After thawing, HeLa cells were subcultered for several times until a constant growth rate was reached. To avoid contaminations, working under sterile conditions was achieved by working in a laminar-flow hood, where air is drawn through a HEPA filter and flowed in laminar manner. The inner room of the hood was regularly disinfected with 70% ethanol and ultraviolet (UV) light. Prior to placing all required equipments, chemicals and biochemicals, they had to be disinfected by spraying with 70% ethanol and wiping clean. All solutions, buffers and equipments that were used under the laminar-flow hood were sterilised by autoclaving at 121^{o}C or using sterile filters.

Because of toxic metabolites, exhaustion of nutrients in medium or cells occupying all available surface, cells enter the stationary phase that greatly reduces cell proliferation. Therefore, cells have to be subcultured and fresh medium must be supplied to maintain an optimal density for persistent growth, stimulating further proliferation and preventing cells dying. For adherent cells, removal of medium and dissociation of cells in warm trypsin was performed. Trypsinization or trypsin proteolysis is a common enzymatic dissociation method for adherent cell cultures. Trypsin, which cleaves peptides at the c-terminal side of lysine and argenine, gently separates cell-cell and cell-matrix contacts resulting in a single cell suspension. EDTA, a divalent cation chelator, is included to bind the remaining calcium and

magnesium ions supporting cell binding. Since HeLa medium contains calcium and magnesium ions and proteins from fetal bovine serum, cells should be washed with PBS without Ca^{2+} and Mg^{2+}. HeLa cells were cultivated in a T75 culture flask until the cell confluency reached 80-90%, which usually requires around 3-5 days. The medium was removed and cells were washed twice with 10 mL pre-warmed PBS^- (37^oC) to remove traces of serum and deplete divalent cations. 5 mL of warm trypsin/EDTA (37^oC) was added to cover cell monolayer thoroughly and 4 mL trypsin/EDTA solution was discarded afterwards. Cells overlaid with 1 mL trypsin/EDTA were incubated at 37^oC (5% CO_2) for ~10 minutes. The incubation time should not exceed 10 minutes to avoid the risk of enzymatic damage to cells. The trypsin/EDTA activity was then inactivated by supplying 9 mL of HeLa medium and cells were dispersed by repeated pipetting over the surface carrying the monolayer. Subsequently, the cell suspension was disaggregated by gentle repeated pipetting. The suspension was divided into 10X T75 culture flasks (1:10 splitting ratio) and further cultivated for 5 days. Large quantities of HeLa cells were needed for cytosol production. To facilitate cell removal by scarping, HeLa cells in 10X T75 culture flasks were further split into 100X culture dishes (Ø 100 mm) (1:10 splitting ratio) and cells were cultivated for 3 days.

Table 2.1 Composition of medium, buffer, and dissociation agent for HeLa cell culture

Medium, buffer and dissociation agent (Dilute all components in sterile pyrogen-free ddH_2O)	**Composition**
HeLa medium	1x Dulbecco's Modified Eagle's Medium (Biochrom F0455) 1x Non-essential amino acid (Biochrom K0293) 0.225% $NaHCO_3$ (Biochrom L1713) 2 mM L-Glutamine (Biochrom K 0282) 50,000 U Penicillin-Streptomycin (Gibco 15140-114) 1 mM Na-Pyruvate (Biochrom L0473) 10% Fetal bovine serum decomplemented for 30 minutes at 56^oC (Sigma F-7524)
PBS without Ca^{2+}, Mg^{2+} (L182-50)	NaCl (8 g/L) KCl (0.2 g/L) Na_2HPO_4 (1.15 g/L) KH_2PO_4 (0.2 g/L)
Trypsin/EDTA solution (0.05%/0.02 % in PBS, without Ca^{2+}, Mg^{2+}) (Biochrom L2153)	NaCl (8 g/L) KCl (0.2 g/L) Na_2HPO_4 (1.15 g/L) KH_2PO_4 (0.2 g/L) EDTA-Na_2 (0.2 g/L) Trypsin (0.5 g/L)

2.2 Preparation of HeLa cell cytosol

2.2.1 Cell harvesting

To produce HeLa cytosol, HeLa cells were not detached with proteolytic enzymes that would hydrolyse proteins in cytosol. Therefore, cells were gently detached from cell culture dishes through the alternative mechanical dissociation method so called cell scraping. This method produces a cell suspension faster than by enzymatic dissociation, however the method may cause mechanical damage. Thus, gentle scraping is essential to maintain the cell viability. After HeLa cells in 100 culture dishes had reached

80-90% cell confluency, the medium was removed and discarded. Approximately 10 mL of warm PBS^- (37^oC) was immediately poured into culture dishes. Washing was conducted for two times, 5 minutes on a rocking shaker. Prior to cell scraping, PBS^- was carefully removed and approximately 1 mL PBS^- was added into the dish. Cell monolayers were carefully detached using a cell scraper at an angle of 45^o. Cell layers should come off as sheets indicating that cell breakage was prevented. From this point, all steps had to be done on ice to prevent protein degradation and enzymatic proteolysis. The cell suspension of 12-14 plates was transferred into a 15 mL conical centrifuge tube by using a 3 mL disposable pasteur pipette and centrifuged at 1200 rpm for 5 minutes at 4^oC in a Multifuge 3SR Plus (swing-out rotor).

2.2.2 Cell homogenisation and fractionation

Table 2.2 Composition of homogenisation buffer

Buffer	Composition
Homogenisation buffer	250 mM Saccharose 3 mM Imidazole (from 1 M Imidazol-stock solution; pH 7.4) adjust volume with pyrogen-free ddH_2O and pass through 0.22 µm sterile filter.

Cell homogenisation was achieved by shear forces passing cells through the narrow needle of a syringe. First, the supernatant of the cell pellets (**Subheading 2.2.1**) was discarded and 500 µL of ice-cold sterile homogenisation buffer (see Table 2.2) was added. The homogenisation buffer is composed of isotonic saccharose (250 mM saccharose) that prevents osmotic rupture of cellular membranes and preserves normal cell structure (Lodish *et al*., 2003). The cell pellets were resuspended gently with 1 mL pipette tip. The cell suspension was then homogenised by using a 1 mL syringe and 22.5 gauge syringe needle. The cell suspension was passed firmly 5 times through the needle or until 70 % of broken cells were observed under an inverted microscope as depicted in figure 2.1. In this step, nuclei must not be broken because DNA inside nucleus might be released. The cell homogenate was centrifuged at 3,000 rpm for 15 minutes at 4^oC to remove intact cells along with other large cell debris and nuclei. The supernatant (post nuclear supernatant, PNS) with a milky whitish appearance was collected very carefully. The PNS was centrifuged at $100{,}000 \times g$ for one hour at 4^oC with an ultracentrifuge (Beckman Optima TL Ultracentrifuge, Rotor TLA 100) and the supernatant (cytosolic fraction) was collected and aliquoted into 200 µL samples. The cytosol samples were shock-frozen in liquid nitrogen and stored at -70^oC. Along the process of cytosol production, the differential centrifugation was employed. It is one of the widely-used methods to fractionate cellular fraction. Based on different sedimentation rate of various cellular components, cells are able to be separated partially under different centrifugal force. Size, density and shape affect the movement (sedimentation) of cellular components. Under applied centrifugal force, relatively large and dense components are sedimented more rapidly than the smaller and lighter components. The cytosol preparation procedure is illustrated schematically in figure 2.2.

.

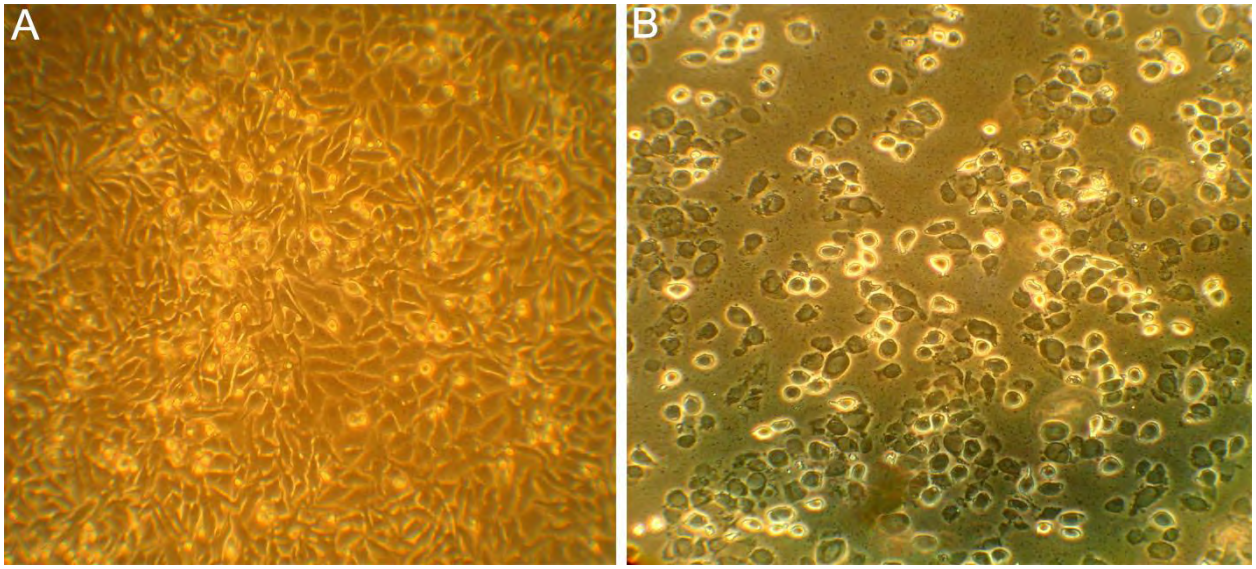

Figure 2.1 Morphology of HeLa cells A) before and B) after homogenisation

Inverted microscopic images before homogenisation (A) shows a monolayer of HeLa cells (~90% confluence). Cells have a slightly elongated shape at low density and round up upon increasing cell density. After homogenisation by forcing cells through a narrow passage of syringe needle (B), ~30% were intact cells (shiny round shaped cells), ~70% was broken cells (dark irregular shaped cells) and less than 5% of nuclei were disrupted. The magnifications are 100X (A) and 400X (B).

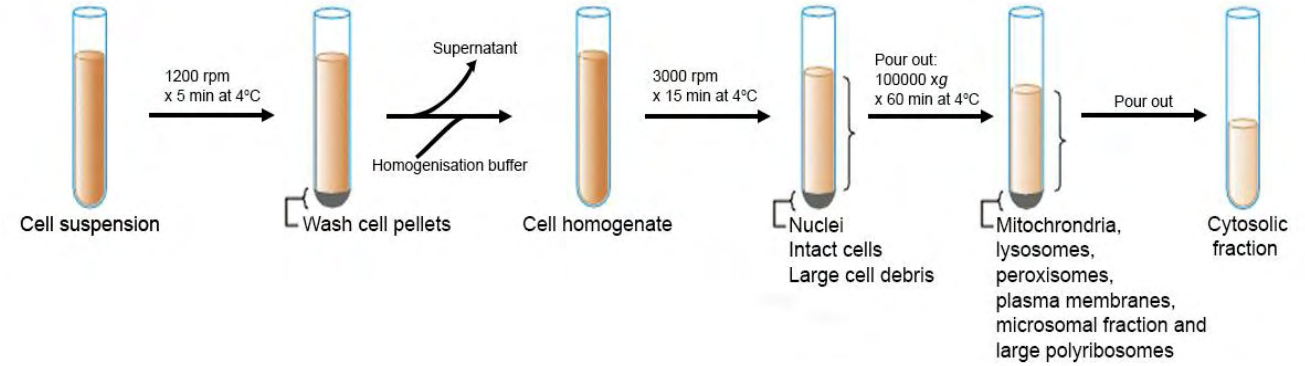

Figure 2.2 Schematic illustration of the cytosol preparation procedure

HeLa cells were washed, scraped out from the culture plates and transferred into a conical centrifuge tube. Later the cell pellets were obtained by spinning the cell suspension at 1200 rpm for 5 minutes at 4^{o}C. The cell pellets were resuspended and homogenised as described above (**Subheading 2.2.2**). The cell homogenate was centrifuged at 3000 rpm for 15 minutes at 4^{o}C to remove nuclei, intact cells and cell debris. The resulting supernatant was centrifuged at 100,000 × *g* for one hour at 4^{o}C to separate cytosolic fraction from other cellular materials. Cell fractionation starts with a low centrifugation force to separate nuclei, intact cells and large cell debris. By increasing centrifugal force and duration, various organelles can be separated owing to different density of organelles. (Adapted from Lodish *et al*., 2003)

2.3 Preparation of HeLa cell lysate

Lysis buffers that were applied to analyse [6]-gingerol-dependent protein complex formation depended on the chosen analytical approach. Table 2.3 shows the list of lysis buffers that were used in this study. First, HeLa cells were proliferated in a T75 culture flask in an incubator at 37°C with 5% exogenous CO_2 until 80-90% cell confluency had been reached.

Table 2.3 Composition of lysis buffers

Buffer	Composition	Experimental approaches
Lysis buffer	50 mM Tris 150 mM NaCl, 1 mM Pefabloc 0.1% NP-40; pH 7.5	*in vivo* analysis of [6]-gingerol-dependent protein complexes by BN-PAGE
Lysis buffer	50 mM NaCl 50 mM Imidazole/HCl (Stock 1 M Imidazole/HCl; pH 7.0) 2 mM ε-Aminocaproic acid 1 mM EDTA 0.1% NP-40 pH 7.0 (check pH before adding NP-40)	CN-PAGE Low-dye BN-PAGE
Lysis buffer	20 mM HEPES 150 mM NaCl 0.05% NP-40; pH 7.08	Chemical crosslinking (DSS)
Lysis buffer	50 mM NaCl 20 mM HEPES 1 mM EDTA 0.1% NP-40; pH 7.0 (Check pH before adding NP-40)	Chemical crosslinking (for further analysis by low dye BN-PAGE)
Lysis buffer	20 mM HEPES 150 mM NaCl 0.1% NP-40 1 mM Pefabloc; pH 7.08 add NP-40 and Pefabloc prior to use	Chemical crosslinking (DSS followed by BN-PAGE)
4X Laemmli sample buffer	250 mM Tris-HCl; pH 6.8 40% (v/v) Glycerol 8% SDS 0.04% (wt/v) Bromophenol Blue add 8% 2-Mercaptoethanol prior to use	Chemical crosslinking

In case of culturing cells in a culture dish (Ø 96 mm), cells from a T75 culture flask were split into a culture plate with 1:2 as a splitting ratio. Cells were proliferated for 24 hours in the incubator at 37°C with 5% CO_2 until 80% cell confluency was obtained. HeLa medium was removed and discarded. Cells were washed once with PBS^-, and 1 mL PBS^- was added. Cells were scarped with a cell scraper. The cell aggregates were transferred with a disposable pasteur pipette into a 2 mL reaction tube. Cells were centrifuged at 1,200 rpm for 5 minutes at 4°C resulting in washed cell pellets. The supernatant was carefully discarded, and then 500 µL of lysis buffer was added to the cell pellets. The cell pellets were resuspended gently by inverting the tube and incubated in lysis buffer on ice for 30 minutes with periodic mixing on a rocking shaker. Cell lyste was centrifuged at 12,000 × *g* for 10 minutes to pellet cell debris.

The supernatant was transferred to a new reaction tube and cell debris was discarded. The resulting cell lysate was stored at -20°C for a short time prior to use or directly applied for further analysis.

In case of culturing cells in a 24-well culture plate (Ø 21.4 mm), cells from a T75 culture flask were split into a 24-well culture plate with splitting ratio of 1:25 or 1:50. Cells were grown for 24 hours in the incubator at 37°C with 5% CO_2 resulting in a 80% confluence. Cells were either incubated with 500 µL HeLa medium without FBS containing 25 µg of [6]-gingerol in the incubator (37°C, 5% CO_2) for 24 hours or directly lysed by lysis buffer. Prior to lysis cells, HeLa medium was removed and cells were washed once briefly with PBS^- and lysed in ice-cold lysis buffer containing nonionic detergent NP-40 or Laemmli sample buffer containing 2-mercaptoethanol. For lysis of cells with ice-cold lysis buffer containing NP-40, cells were lysed in lysis buffer on ice for 30 minutes with periodic mixing on a rocking shaker. The lysate was mixed by pipetting carefully up and down and was transferred to a microcentrifuge tube. The HeLa cells were photographed before and after lysis. The lysate was centrifuged at 12,000 × *g*, 4°C for 10 minutes to pellet the cell debris. The resulting cell lysate was stored at -20°C for a short time prior to use or directly applied for further analysis. For lysis of cells with Laemmli sample buffer containing 2-mercaptoethanol, the sample buffer was added to cells and lysed by thorough pipetting at RT.

2.4 Protein determination by Bradford assay

10 µL of HeLa cytosol was used for determining protein concentration according to Bradford assay. Bradford assay is a simple widely-used spectroscopic analytical method to measure the total protein concentration in solution based on three appearance states of coomassie brilliant blue dye G-250 (CBB G-250): acidic (red), neutral (green) and basic (blue). In commercial reagent solution, the dye is predominantly in acidic form (double protonated form) that has absorbance maxima at 470 nm. The other two forms of CBB G-250 are neutral (single protonated) and anionic (unprotonated), which have absorbance maxima at 650 nm and 595 nm respectively. The formation of dye-protein complexes, which is based on Van der Waals force and hydrophobic interaction (Compton and Jones, 1985), converts the dye into the anionic blue form (Bradford, 1976). The dye binds most readily to arginyl and lysyl residues (Compton and Jones, 1985), thus the determination of total protein concentration can be achieved by measuring the absorbance of the solution at 595 nm. Several limitations of Bradford assay are due to basic samples, surfactants and proteins with poor acid-solubility. First, a BSA standard curve has to be established. 1 mg/mL of Albumin Fraction V was prepared and diluted with ddH_2O and 200 µL 5X Roti Quant (Carl Roth GmbH, Germany) to a final volume of 1 mL to obtain final concentrations of 1-11 µg/mL. The absorbance of standard solutions was spectroscopically measured at 595 nm. After the BSA standard curve was plotted, 1, 2 and 3 µL of cytosol were diluted as described before and measured at 595 nm. The measurement was carried out in duplicates for better accuracy and precision.

2.5 Direct visualisation of protein complexes on blotting membrane

Table 2.4 Composition of buffers and chemicals for dot blotting

Buffer and chemical	Composition
2X Reaction buffer; pH 7.5	100 mM Tris 10 mM EDTA 300 mM NaCl 2 mM DTT 0.02% NP-40
Homogenisation buffer	250 mM Saccharose 3 mM Imidazole (from 1 M Imidazole-stock solution; pH 7.4) adjust volume with pyrogen-free ddH_2O and filter sterilised.
[6]-Gingerol	10 mg/mL [6]-Gingerol in 100% DMSO

Since the hypothesis of this study is that MIF forms complexes with unknown proteins, which is induced by [6]-gingerol, complexes might be visualised as punctuated structures after dot blotting and immunodetection. Dot blot is one of the techniques in biochemistry that is used to detect, analyse and identify an antigen or protein depending on the detection method. As sample proteins are not electrophoretically resolved, this technique offers no information on the size of proteins and complexes. 200 µL of HeLa cytosol was incubated with 0.5 mg [6]-gingerol or without [6]-gingerol (DMSO instead) as control for 2 hours at 4^{o}C. The buffer system and the ratio of [6]-gingerol to cytosol proteins were taken from Möbus (2013). In order to facilitate pipetting and to obtain an identical protein concentration of each sample, the samples were diluted with homogenisation buffer. The samples were pipetted on a glass slide and a stripe of dry nitrocellulose membrane was laid on top of the dotted samples and the samples were allowed to absorb to the membrane for 15 minutes. The membrane was further used for detecting MIF by western blot according to general immunodetection procedure **(Subheading 2.11)**.

2.6 Sodium dodecyl sulfate polyacrylamide gel electrophoresis (SDS-PAGE)

Table 2.5 Composition of buffers for SDS-PAGE

Buffer	Composition
4X Laemmli sample buffer	250 mM Tris-HCl; pH 6.8 40% (v/v) Glycerol 8% SDS 0.04% (wt/v) Bromophenol Blue add 8% 2-Mercaptoethanol prior to use
Tris-glycine electrophoresis buffer	25 mM Tris 192 mM Glycine 0.1% SDS (10X stock solution can be prepared, stored at RT)

SDS-PAGE is the most frequently used method for separating and analysing protein mixtures according to their molecular size as they move through a polyacrylamide gel towards the anode. The method can be used to determine the relative molecular mass of proteins. The polyacrylamide gel is formed from acrylamide crosslinked by a bifunctional agent named N, N´-methylene bis-acrylamide (bis-acrylamide). Acrylamide monomers are polymerised in head to tail fashion into long chains known as vinyl addition polymerisation. Bis-acrylamide crosslinks these chains and introduces a second site of chain extension in

presence of free radicals (Figure 2.3). Free radicals are initiated by addition of ammonium persulfate (APS) and the base N,N,N',N'-tetramethylenediamine (TEMED). TEMED decompose APS resulting in persulfate ions as free radical source (Walker, 2002):

$$S_2O_8^{2-} + e^- \rightarrow SO_4^{2-} + SO_4^{-\bullet}$$

The polymerisation of acrylamide monomer can be represented as follows (Walker, 2002):

$R^\bullet + M$	$\rightarrow RM^\bullet$	R: Free radical
$RM^\bullet + M$	$\rightarrow RMM^\bullet$	M: Acrylamide monomer
$RMM^\bullet + M$	$\rightarrow RMMM^\bullet$, and so on	

By doing so, acrylamide monomers are polymerised into long chains in a reaction initiated by free radicals. Bis-acrylamide in small amounts is introduced to crosslink these chains forming a gel whose porosity depends on length of the chains and degree of crosslinking that occurs during polymerisation (Sambrook and Russell, 2001). Sodium dodecyl sulphate (SDS), a strongly anionic detergent, is used in combination with reducing agent (e.g. 2-mercaptoethanol, DTT) and heat (95^{o}C for 5 minutes) to ensure the dissociation of proteins into individual polypeptides without cleavage of peptide bonds. Reducing agent cleaves disulfide bonds that support high level protein structures (i.e. secondary, tertiary, and quaternary structure) and intermolecular bonds. SDS binds strongly to polypeptides at an approximate ratio of 1.4 gram detergent per gram polypeptides (Sambrook and Russell, 2001) and completely converts the original native charge of proteins to negatively charge allowing the proteins to migrate to the anode side. Since the amount of SDS bound to polypeptides is proportional to the molecular size and is independent of their sequence, the migration of polypeptides is based on the size of polypeptides. The sample buffer contains bromophenol blue as an ionisable tracking dye during electrophoresis. Glycerol is included to increase the sample density, thus allowing the samples to settle down in a gel pocket while loading sample.

To increase the resolution of separation during SDS-PAGE, a discontinuous buffer system, in which the buffer in the gel and in the tank are different, was applied. The sample and the stacking gel contain Tris-HCl (pH 6.8), the resolving gel contains Tris-HCl (pH 8.8) and the lower and upper buffer reservoirs contain Tris-glycine (pH 8.3). All components of the system are supplied with 0.1% SDS. When the current is applied to electrophoresis, glycinate anions at pH 8.3 are forced into the stacking gel. In the stacking gel, glycinate anions are protonated and change predominantly into glycine zwitterions, which cause slower movement in the electric field, forming the trailing edge. Chloride ions present in the stacking gel migrate ahead of the glycine zwitterions in the electric field forming the leading edge. In between the trailing and the leading edge of the moving boundary is a zone of low conductivity and steep voltage gradient, where proteins are trapped in a sharp band. As proteins enter the resolving gel, glycine zwitterions are deprotonated at pH 8.8 forming glycinate anions. Both chloride ions and glycinate anions migrate immediately through the stacked proteins towards the anode and leave the proteins behind. The voltage gradient is dissipated and the proteins are resolved based on molecular weight in a zone of uniform voltage and pH (Sambrook and Russell, 2001). The stacking gel ensures the simultaneous deposition of proteins into the resolving gel, hence the proteins with the same molecular weights will migrate as sharp bands.

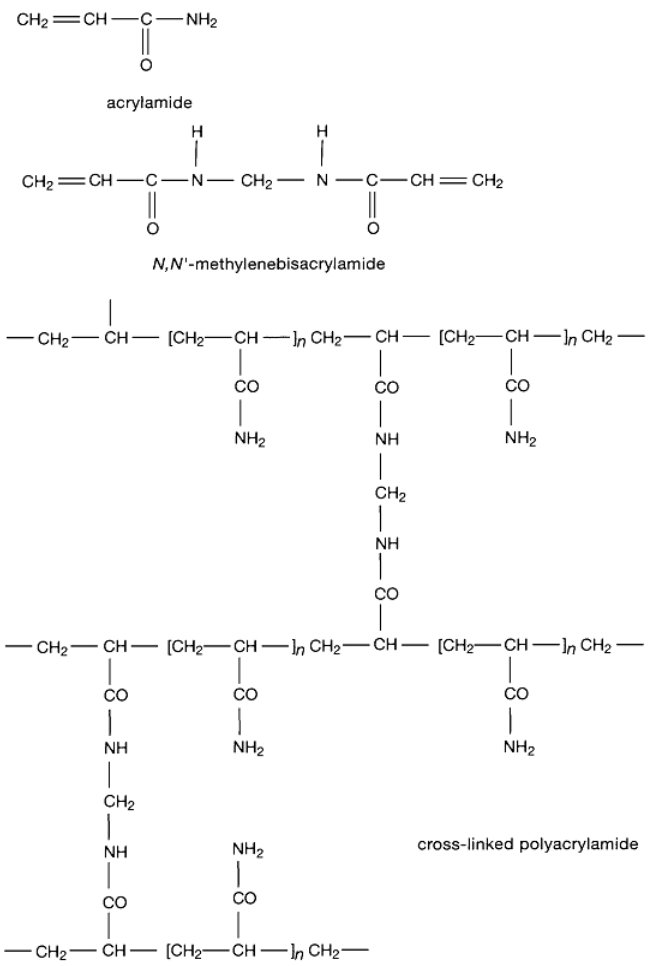

Figure 2.3 Chemical structure of polyacrylamide
Acrylamide monomers are polymerised into long chains in a reaction initiated by free radicals. Bis-acrylamide is supplied in small amounts to bridge these chains forming a gel. The porosity of the resulting gel depends on length of the chains and degree of crosslinking that occurs during polymerisation (Sambrook and Russell, 2001).

In general, 4X Laemmli sample buffer containing 8% 2-mercaptoethanol was added to samples to a final concentration of 1X containing 2% 2-mercaptoethanol. The samples were boiled at 95^{o}C for 5 minutes and loaded into a gradient SDS-gel or an uniform SDS-gel. The SDS-PAGE was carried out with limited current and conditions depending on gel apparatus as described in table 2.6. After the bromophenol blue front had reached the end of the gel, the electrophoresis was stopped. The relevant part of the gel was excised and blotted onto a nitrocellulose membrane or stained by silver or coomassie staining. The SDS gel recipes are described in table 2.7 (Large gel and Mini-gel), and table 2.8 (16x18x1.5 cm gel (SE 600 RUBY)). The general handling procedures of vertical SDS gel casting are described:

1.) Glass plates and all equipments should be cleaned with detergent and rinsed thoroughly with ddH_2O to facilitate the polymerisation reaction. For better cleaning, glass plates should be sprayed with 70% ethanol and wiped with clean tissue paper. In case of a gradient SDS-PAGE, gradient mixer is required and the handlings procedures are described in BN-PAGE methodical part (**Subheading 2.7**).

2.) TEMED and APS must be added prior to pouring gel solutions into a gel cassette.
3.) APS should be prepared freshly as persulfate in solution decomposes rapidly.
4.) After resolving gel solution is poured into the cassette, 1-2 mL ddH_2O is carefully overlaid to prevent contact of gel solution with oxygen, which retards the polymerisation reaction.
5.) Polymerisation of the resolving gel should not exceed 60-90 minutes (only for one dimensional SDS-PAGE) otherwise the gel might be rarely polymerised.
6.) After the resolving gel is polymerised, the overlaid ddH_2O is removed and the stacking gel solution is poured on the top of the resolving gel. Subsequently, a gel comb is inserted.
7.) Polymerisation of the stacking gel should be completed after 30-60 minutes.
8.) Final APS and TEMED concentrations of 0.05% in the resolving gel solution are generally adequate for obtaining complete polymerisation within 90 minutes.
9.) Stacking gel has large pore sizes; the gel can be rapidly polymerized in shorter times (~15 minutes). Hence, for increasing polymerisation reaction kinetics, ~0.1% TEMED, which expedites the conversion of persulfate to sulfate radicals (sulfate radicals is major component of the gel polymerisation reaction), is preferred with 0.05% APS
10.) The casted gel can be stored for 3 days at 4^oC by wrapping in wet tissue papers and storing in a plastic bag to prevent evaporation.

Table 2.6 Applied limited current or voltage for different gel apparatuses

Gel apparatus	Voltage (V)	Current (mA)	Duration (hours)	Temperature (^oC)
Large gel (~22x40x1 cm)	unlimited	35-45	3-8	RT
SE 600 RUBY (16x18x1.5 cm)	unlimited	35	5	4
Mini gel (10.1x7.3x0.75 cm)	200	unlimited	0.75	RT

Table 2.7 SDS-PAGE gel recipe for large gel (~22x40x1 cm) and Mini gel (10.1x7.3x0.75 cm)

Solution	Large gel			Mini gel		
	5% Stacking gel	12% Resolving gel	16% Resolving gel	5% Stacking gel*	12% Resolving gel*	16% Resolving gel
37.5:1 Acrylamide	8 mL	32 mL	34.1 mL	1.7 mL	4 mL	5.3 mL
3 M Tris-HCl pH 8.8	-	11.2 mL	11.2 mL	-	1.3 mL	1.3 mL
1 M Tris-HCl pH 6.8	4 mL	-	-	1.3 mL	-	-
10% SDS	0.6 mL	0.8 mL	0.8 mL	0.1 mL	0.1 mL	0.1 mL
60% Saccharose	15 mL	20 mL	20 mL	-	-	-
ddH_2O	32 mL	16 mL	13.5 mL	7.2 mL	4.6 mL	3.3 mL
Total Volume	60 mL	80 mL	80 mL	10 mL	10 mL	10 mL
10% APS	300 µL	300 µL	300 µL	50 µL	50 µL	50 µL
TEMED	30 µL	40 µL	40 µL	10 µL	5 µL	5 µL

* The recipe is based on manufacturer's instructions (Bio-Rad Laboratories, Inc.)

Table 2.8 SDS-PAGE gel recipe for SE 600 RUBY (16x18x1.5 cm)

Solution	Gradient gel			Fixed concentration gel		
	3.5% Stacking gel	4% Resolving gel	20% Resolving gel	5% Stacking gel	12% Resolving gel	16% Resolving gel
37.5:1 Acrylamide	1.4 mL	1.9 mL	9.3 mL	1.6 mL	9 mL	12 mL
3 M Tris-HCl pH 8.8	-	2 mL	1.96 mL	-	3.9 mL	3.9 mL
1 M Tris-HCl pH 6.8	0.8 mL	-	-	0.8 mL	-	-
10% SDS	120 µL	140 µL	140 µL	0.12 mL	0.28 mL	0.28 mL
60% Saccharose	3 mL	-	2.3 mL	3 mL	7 mL	7 mL
ddH_2O	6.5 mL	9.9 mL	0.18 mL	6.3 mL	7.6 mL	4.7 mL
Total Volume	12 mL	14 mL	14 mL	12 mL	28 mL	28 mL
10% APS	12 µL	80 µL	80 µL	120 µL	50 µL	140 µL
TEMED	120 µL	8 µL	8 µL	12 µL	5 µL	14 µL

2.7 Blue native electrophoresis (BN-PAGE) and clear native electrophoresis (CN-PAGE)

The hypothesis is that [6]-gingerol might induce MIF and potential partner proteins to form complexes, which reduce cell proliferation and decrease viability of HeLa cells. Thus, BN-PAGE and CN-PAGE might provide information to the hypothesis of [6]-gingerol induced complex formation. BN-PAGE and CN-PAGE are non-denaturing gel based techniques for detecting and analysing protein-protein and macromolecule interactions in biological samples (Krause, 2006). Both methods show a reliable ability to preserve protein complexes in protein mixtures, which allows researchers to elucidate functions of proteins being part of complexes (Ladig *et al*., 2011; Schägger *et al*., 1994; Krause, 2006).

Schägger and von Jagow originally established BN-PAGE, a charge-shift based method, in 1991 to resolve multiprotein complexes of the oxidative phosphorylation system of solubilised mitochrondria extracts in micro scale (Schägger and von Jagow, 1991). Proteins within the mass range of 20 kDa to 10 MDa (Schägger, 2001) can be separated depending on the gradient gel type as exemplified in table 2.9. The electrophoretic mobility of the blue native electrophoresis system is determined by the negative charges of bound anionic dye CBB G-250 (Wittig *et al*., 2006). As CBB G-250 binds most readily to arginyl and lysyl residues via Van der Waals force and hydrophobic interaction (Compton and Jones, 1985), the charge of proteins is shifted to negative charge by binding a large number of dye molecules causing even basic proteins to migrate towards the anode (Wittig *et al*., 2006). Furthermore, after CBB G-250 binds to proteins shifting the surface charge of the proteins, the excess of negative charges on the surface repel each other resulting in considerably reducing of the protein aggregation (Tulp *et al*., 1999). Detergent can be excluded from the gel minimising the risk of denaturation of detergent-sensitive proteins since dye-associated proteins are negatively charged and, therefore, soluble in detergent free solution (Schägger, 2001). BN-PAGE offers a broad range of applications, since all membrane and most of water-soluble proteins are likely to bind CBB G-250 (Schägger *et al*., 1994). In general, BN-PAGE can be applied to determine the molecular masses if one of both condition is fullfilled: (i) protein species with

p*I*s at or below 5.4 (ii) analysed protein species bind CBB G-250 and p*I*s are below 8.6 (Schägger *et al*., 1994). The binding affinity of anionic CBB G-250 differs, but in the case of membrane proteins, the dye binds uniformly in ratio of ~1g/g (dye/protein) as a rule of thumb (Heuberger *et al*., 2002). However, the resolving of protein mixtures is not based on charge/mass ratio but according to the decreasing porosity of acrylamide gradient gels (Wittig *et al*., 2010). CBB G-250 bound proteins migrate towards the anode until the specific pore size limitation has been reached. Native proteins and protein complexes travel along the BN-gel as blue bands, which can simply be observed during electrophoresis.

Table 2.9 Gel types for BN-PAGE

Molecular mass range (kDa)	Sample gel (%T)	Gradient gel (%T)
100-10,000	3.0	$3 \rightarrow 13$
100-3,000	3.5	$4 \rightarrow 13$
100-1,000	4.0	$5 \rightarrow 13$
20-500	4.0	$6 \rightarrow 18$

Source: (Schägger, 2001)

CN-PAGE was developed shortly after the development of BN-PAGE in 1994 (Schägger *et al*., 1994). CN-PAGE differs from BN-PAGE since CBB G-250 is omitted from the system (i.e. during sample preparation and in cathode buffer). The absence of CBB G-250 diminishes the advantages of the charge-shift of proteins in contrast to BN-PAGE, hence the protein species that migrate into the gel are limited (Krause, 2006). The electrophoretic migration of proteins in CN-PAGE system relies on the intrinsic charge of proteins, and only acidic proteins, especially p*I*s equal or less than the pH of the system, are able to enter the gel (Wittig *et al*., 2007). Moreover, it was reported that the determination of molecular mass is only suitable for acidic proteins whose p*I*s are at 5.4 or below (Schägger *et al*., 1994). Therefore, the separation of proteins in CN-PAGE does not only depend on the sieving effect but also on their p*I*s in comparison to BN-PAGE. Furthermore, it is obvious that CN-PAGE has a lower resolving resolution than BN-PAGE (Schägger *et al*., 1994). Thus, the versatility of CN-PAGE is limited. Despite the limitation of CN-PAGE, it is conducted under milder conditions (i.e. without CBB G-250) that can preserve some protein-protein interactions since CBB G-250 can cause the dissociation of protein complexes into smaller units (Wittig and Schägger, 2005; Neff and Dencher, 1999). Another advantage of CN-PAGE is that there is no interference of CBB G-250 during in-gel activity staining (Wittig *et al*., 2007).

Samples from cell lysate containing NP-40 were either supplied with 5% CBB G-250 after [6]-gingerol treatment to obtain a detergent/dye ratio of 8 (g/g) for enhancing the solubility of the samples or directly loaded onto BN-gel. For cytosol, samples were diluted with 3X gel buffer to obtain 1X gel buffer as a final concentration (Bériault *et al*., 2005; Singh *et al*., 2005) instead of adding 5% (wt/v) CBB G-250 since it contains soluble proteins (Schägger *et al*., 1994). For CN-PAGE, 0.1% ponceau S in 50% glycerol was added to all samples to a final concentration of ~2% glycerol to increase the samples density, and for low-dye BN-PAGE, glycerol was added to all samples to a final concentration of ~2%.

Both CN-PAGE and BN-PAGE require low temperatures (4^{o}C) during the run otherwise a broadening of bands is observed at RT (Schägger, 2001). They were conducted in a vertical electrophoresis apparatus (SE 600 RUBY) connected to a water-circulating temperature control unit (GE Healthcare). Buffers for BN-PAGE and CN-PAGE are listed in table 2.10. Gradient gel was casted according to analysis

approaches, the recipes are shown in table 2.11. Generally, the gradient separation gel was casted with a gradient mixer at 4^{o}C to avoid untimely polymerisation in the tubing and the gradient mixer. Gel solutions were prepared and placed on ice to obtain cold gel solutions at ~4^{o}C. The gel cassette and the gradient mixer were placed in the fridge. Before casting a BN-gel or CN-gel, the gradient mixer was connected with a flexible tube attached to a 1 mL pipette tip and placed on a magnetic stirrer positioned on a lifting table. The lifting table was adjusted to an adequate height that allows the gel solutions to flow by gravitational force with a proper velocity (i.e. casting of separation gel should be finished within 3-5 minutes, otherwise a non-linear gradient gel might be obtained). The low percentage acrylamide gel solution was poured into the column, which is directly connected to the connecting valve, whereas the high percentage acrylamide gel solution was poured into the column that is directly connected to the output of the gradient mixer. A stirrer bar was put into the column containing the high percentage acrylamide gel solution. The connecting valve was opened allowing the gel solution to flow from the top of the gel cassette to the bottom with a proper velocity. The separation gel was overlaid with ~1-2 mL ddH_2O and allowed to polymerise around 90 minutes. Subsequently, the sample gel solution was poured into the cassette, a gel comb could be inserted before or after pouring and the sample gel was allowed to polymerise around 60-90 minutes. This step might be faster or longer (overnight) depending on the percentage of the sample gel. It is recommended to polymerise the gel overnight at 4^{o}C for complete polymerisation. The casted gel can be stored for 3 days at 4^{o}C. The protein concentration in samples seems does not interfere with the resolving resolution (Wittig *et al*., 2006). BN-PAGE and CN-PAGE are continuous buffer system gel electrophoreses, which have the same pH throughout the system (gel, sample, electrode buffers). The system is simple and its buffer composition and pH is known, with the pH remains constant during resolving (Shi and Jackowski, 1998). The disadvantage of the continuous buffer system, however, is that sample volumes must be as low as possible to keep a thin starting zone since no stacking of proteins occurs (Booz, 2007). The gel could be run under two conditions; 1.) starting with a constant voltage of 100 V until the samples have entered the gel. The run is continued with a constant current of 15 mA and voltage limited to 500 V. 2.) beginning with voltage limited to 50 V until the samples have entered the separation gel. The run is continued with current limited to 15 mA and voltage limited to 120 V. The run was stopped as the coomassie front (BN-PAGE) or ponceau S front (CN-PAGE) had reached the end of the gel, which typically requires 4-6 hours for condition 1 and 14-18 hours for condition 2. During the run of BN-PAGE, for better visualisation and reducing the competition of coomassie dye during electrotransfer, cathode buffer B was removed and replaced by cathode buffer B/10 when one-third of the total running distance had been reached (Wittig *et al*., 2006). Or the cathode buffer B was replaced by colourless cathode buffer when half of the total running distance had been reached (Singh *et al*., 2005; Bériault *et al*., 2005). In the case of low-dye BN-PAGE, the run was performed with cathode buffer B/10 throughout the run (Neff and Dencher, 1999). For CN-PAGE, colourless cathode buffer was applied throughout the run under the constant voltage and current as described above. Figure 2.4 shows time course of BN-PAGE run. After the run, the resolved proteins were transferred onto PVDF or nitrocellulose membranes or were stained by silver staining. The procedures for silver staining for BN-gel **(Subheading 2.12)** and protein transfer from BN-gel and CN-gel onto membranes **(Subheading 2.10)** are described. The membranes were probed for MIF, tubulin or actin by western blot analysis according to general western blot procedure **(Subheading 2.11)**.

Table 2.10 Electrode buffer, gel buffer and acrylamide stock solution for BN- and CN-PAGE

Electrode and gel buffer	Composition
Cathode buffer B	50 mM Tricine (stock: 1 M Tricine) 7.5 mM Imidazole (stock: 1 M Imidazole) 0.02% Coomassie brilliant blue G-250 (stock: 5% (wt/v) CBB G-250 suspended in 500 mM ε-aminocaproic acid) pH ~7.0 (adjust pH with 1 M Tricine or 1 M Imidazole, if necessary) store at RT since dye tends to aggregate at low temperature stir for several hours before use.
Cathode buffer B/10	50 mM Tricine (stock: 1 M Tricine) 7.5 mM Imidazole (stock: 1 M Imidazole) 0.002% Coomassie brilliant blue G-250 (stock: 5% (wt/v) CBB G-250 suspended in 500 mM ε-aminocaproic acid) pH ~7.0 (adjust pH with 1 M Tricine or 1 M Imidazole, if necessary); store at 7°C
Colourless cathode buffer	50 mM Tricine (stock: 1 M Tricine) 7.5 mM Imidazole (stock: 1 M Imidazole) pH ~7.0 (adjust pH with 1 M Tricine or 1 M Imidazole, if necessary); store at 7°C
Anode buffer	25 mM Imidazole (stock: 1 M Imidazole) pH 7.0 (adjust pH with HCl); store at 7°C
3X Gel buffer	25 mM Imidazole (stock: 1 M Imidazole) 1.5 M ε-Aminocaproic acid (stock: 2 M ε-aminocaproic acid) pH 7.0 (adjust pH with HCl); store at 7°C
AB-3 mix (49.5% T, 3% C)	48 g Acrylamide 2X 1.5 g bis-Acrylamide 2X dissolve in 100 mL ddH_2O; store at 7°C

* 1 M Tricine: dissolve 89.59 g tricine in 400 mL ddH_2O, adjust volume to 500 mL after dissolving, store at 7°C
* 1 M Imidazole: dissolve 34.04 g imidazole in 400 mL ddH_2O, adjust volume to 500 mL after dissolving, store at 7°C
* 2 M ε-aminocaproic acid: dissolve 13.12 g ε-aminocaproic acid in 40 mL ddH_2O, adjust volume to 50 mL after dissolving, store at 7°C
* 5% (wt/v) CBB G-250 suspended in 500 mM ε-aminocaproic acid: dissolve 0.5 g CBB G-250 in 5 mL ddH_2O supplemented with 2.5 mL, adjust volume to 10 mL after dissolving, store at 7°C.

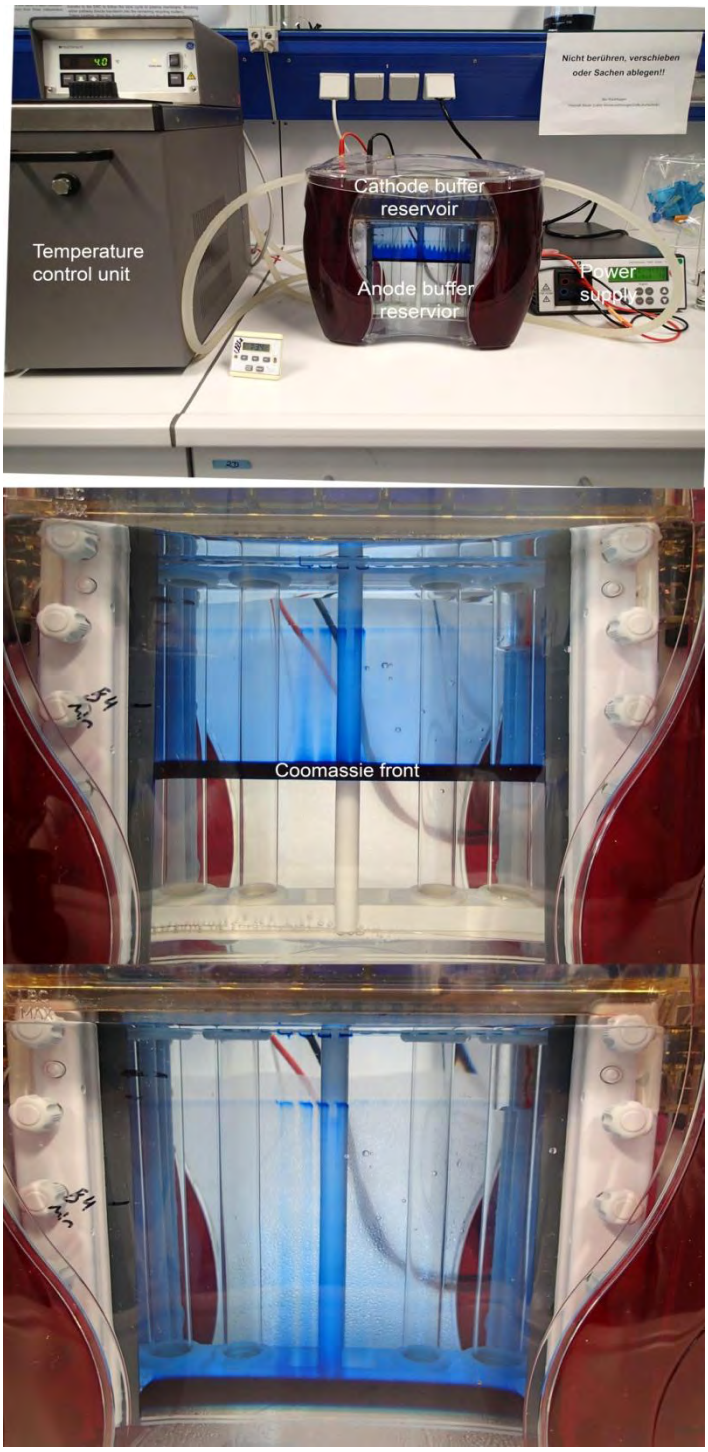

Figure 2.4 Progess of events during a blue native electrophoresis

Representative pictures of a blue native electrophoresis at different time points. The vertical electrophoresis apparatus consists of anode buffer (bottom), cathode buffer (top) and a coolant unit, which is connected to a temperature control unit. After the coomassie front reaches half of the total gel distance, cathode buffer is changed to colourless cathode buffer, or cathode buffer B/10 when the front reaches one-third of the gel for better visualisation and reducing the competition of coomassie dye during electrotransfer. Blue native electrophoresis is stopped as the coomassie front has reached the end of the gel.

Table 2.11 BN- and CN-PAGE gel recipe for SE 600 RUBY (16x18x1.5 cm)

Solution	4-16% Gradient separation gel			8-16% Gradient separation gel		
	3.5 % Sample gel	4% Separation gel	16% Separation gel	4 % Sample gel	8% Separation gel	16% Separation gel
AB-3 mix	0.9 mL	1.1 mL	4.5 mL	1 mL	2.3 mL	4.5 mL
Gel buffer (3X)	4 mL	4.7 mL	4.7 mL	4 mL	4.7 mL	4.7 mL
Glycerol	-	-	2.8 g	-	-	2.8 g
ddH_2O	7 mL	8 mL	1.9 mL	6.9 mL	7 mL	2 mL
Total volume	12 mL	14 mL	14 mL	12 mL	14 mL	14 mL
10% APS	100 µL	80 µL	80 µL	120 µL	70 µL	70 µL
TEMED	10 µL	8 µL	8 µL	12 µL	7 µL	7 µL
Solution	4-20% Gradient separation gel			8-20% Gradient separation gel		
	3.5 % Sample gel	4% Separation gel	20% Separation gel	3.5 % Sample gel	8% Separation gel	20% Separation gel
AB-3 mix	0.9 mL	1.1 mL	5.7 mL	1 mL	2.3 mL	5.7 mL
Gel buffer (3X)	4 mL	4.7 mL	4.7 mL	4 mL	4.7 mL	4.7 mL
Glycerol	-	-	2.8 g	-	-	2.8 g
ddH_2O	7 mL	8 mL	0.8 mL	6.9 mL	7 mL	0.8 mL
Total volume	12 mL	14 mL	14 mL	12 mL	14 mL	14 mL
10% APS	100 µL	80 µL	80 µL	240 µL	80 µL	80 µL
TEMED	10 µL	8 µL	8 µL	24 µL	8 µL	8 µL

* 10% APS must be prepared freshly. 10% APS and TEMED are added immediately into gel solution before casting a gel.

2.8 Co-immunoprecipitation

Co-immunoprecipitation (Co-IP) is a powerful technique to analyse physiological protein-protein interactions (Sambrook and Russell, 2001). The principle of Co-IP is based on immunoprecipitation assays, in which a target protein is captured selectively by a specific antibody. However, Co-IP focuses on additional molecules or proteins that bind directly to the target protein by inherent interactions in samples. This technique offers a possibility to identify new binding partners, structural proteins, co-factors, or signalling molecules that interact with the target protein (Johansen and Svensson, 2002; Lukas *et al*., 2006). Figure 2.5 shows a schematic illustration of a conventional Co-IP workflow. The target protein is termed as the bait protein and proteins that interact with the bait are called prey proteins. Generally, the specific antibody for the bait protein is incubated with a protein mixture or cell homogenate to form antibody-bait protein complexes. The bait protein might interact with one or more prey proteins for the complex formation. Subsequently, the antibody becomes captured on protein A or protein G gel support. Nevertheless, the pitfall of the traditional Co-IP method is the interference of co-eluted antibody light chain (25 kDa) and heavy chain (50 kDa), which hampers the interpretation of the results. Hence, chemical crosslinking of antibodies to protein A/G gel or solid support shows a significant improvement compared to the traditional Co-IP method. By applying a chemical crosslinker

such as disuccinimidyl suberate (DSS) or dimethylpimelimidate (DMP) to crosslink antibodies to protein A/G gel support, the problem of co-eluted antibodies is satisfyingly circumvented (Ren *et al*., 2003; Elmore and Coaker, 2011). Alternatively, for analysing the target protein by western blot, HRP-conjugated protein A can be used instead of HRP-conjugated secondary antibody since protein A predominately binds to the Fc region of antibodies. Thus, the background by light and heavy chains can be deminished (Lal *et al*., 2005).

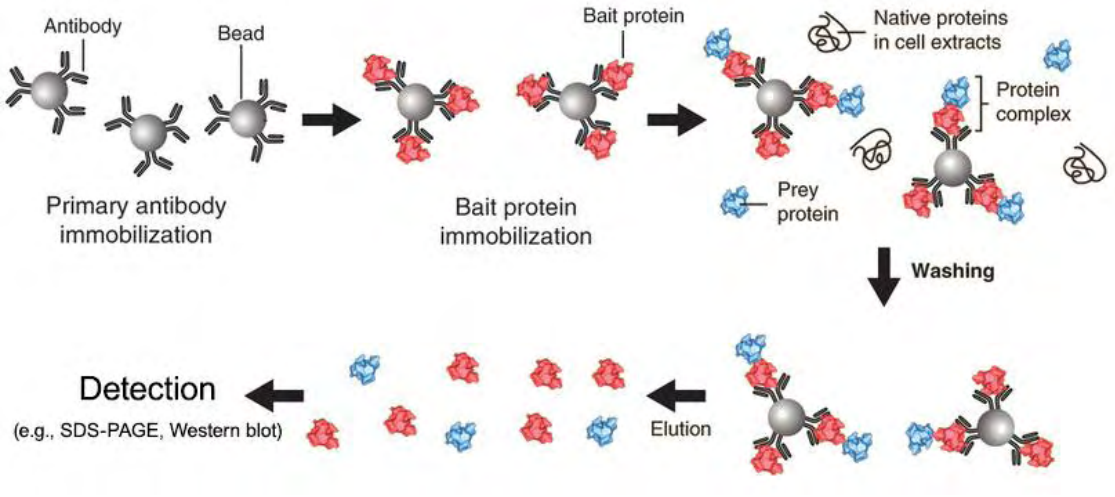

Figure 2.5 Schematic illustration of a conventional co-immunoprecipitation procedure
A cell lysate or protein mixture that contains an antigen and protein(s) interacting with antigen, thus forming a protein complex, is incubated with antibody-immobilised resin, which binds specifically to the antigen protein. After forming antibody-antigen complexes, unbound proteins are washed away and the antigen is co-eluted with the interacting protein(s) by elution buffer (adapted from Lee *et al*., 2013).

2.8.1 Co-immunoprecipitation using crosslink magnetic IP/Co-IP Kit

Co-immunoprecipitation using crosslink magnetic IP/Co-IP Kit (Thermo scientific, Inc. # 88805) was carried out according to manufacturer's instructions.

1.) 10 mg/mL of Pierce Protein A/G Magnetic Beads were resuspended by vortexing until a homogenous solution was acquired. 250 µg of Protein A/G magnetic beads, which have the rabbit IgG binding capacity ratio of 55 to 85 µg rabbit IgG per mg magnetic particles, were used per one IP reaction.
2.) The beads were collected by placing the reaction tube on a magnetic stand. The storage solution was removed and discarded.
3.) The beads were pre-washed twice with 500 µL 1X modified coupling buffer by placing on a rotating platform for 1 minute with a slow rotating rate. The beads were collected by placing the tube on a magnetic stand and the supernatant was removed and discarded.
4.) 100 µL of 0.002 % (wt/v) antibody solution (i.e. add 10 µL of 0.2 mg/mL polyclonal rabbit anti-MIF IgG to 5 µL of 20X coupling buffer, 5 µL of IP Lysis/Wash buffer and 80 µL ddH_2O) was prepared
5.) The beads (250 µg) were incubated with the antibody solution (100 µL) and the control solution to immobilise the antibody on the beads by placing on the rotating platform for 15 minutes at RT

with a slow rotating rate. The beads with the antibody immobilised were collected with the magnetic stand and the supernatant was removed and discarded.

6.) The beads were resuspended and washed with 1X modified coupling buffer for three times by gentle inverting the tube. The beads with antibody immobilised were collected with the magnetic stand, then the supernatant was removed and discarded.

7.) 2 mg DSS was dissolved in DMSO to obtain a 10X solution (25 mM). The 10X DSS was diluted with DMSO to a final concentration of 0.25 mM. The crosslinking solution was prepared by mixing 2.5 µL of 20X coupling buffer, 4 µL of 0.25 mM DSS and 43.5 µL of ultra pure water to a total volume of 50 µL.

8.) The beads with antibody immobilised were incubated with the crosslinking solution for 30 minutes at RT on the rotating platform.

9.) The beads with antibody immobilised were collected with the magnetic stand and the supernatant was removed and discarded.

10.) 100 µL of elution buffer was added to the beads and gently mixed for 5 minutes on the rotating platform to remove non-crosslinked antibody and to quench the cross-linking reaction. The beads were collected with the magnetic stand, then the supernatant was removed and discarded.

11.) 100 µL of elution buffer was added to the beads and the tube was gently inverted. The beads were collected with the magnetic stand, then the supernatant was removed and discarded.

12.) The antibody-crosslinked beads were washed twice with 200 µL of cold IP Lysis/Wash buffer and gently mixed by inverting the tube. The beads were collected with the magnetic stand, then the supernatant was removed and discarded.

13.) The antibody-crosslinked beads were now ready for use and could be stored at 4^{o}C or directly used for Co-IP of MIF-protein complexes.

14.) HeLa cytosol was incubated with [6]-gingerol (2.5 µg [6]-gingerol/µL cytosol) for 2 hours at 4^{o}C.

15.) The [6]-gingerol treated cytosol was diluted with or without 2X reaction buffer to 1X final concentration.

16.) The samples were diluted with IP Lysis/Wash buffer to obtain a final volume of 500 µL.

17.) Diluted sample solutions were incubated with 250 µg antibody-crosslinked beads for one hour at RT on the rotating platform.

18.) The beads were collected with the magnetic stand and the supernatant was removed and collected to analyse the unbound proteins.

19.) The beads were washed with 500 µL of IP/Lysis buffer by gently inverting the tube. The beads were collected with the magnetic stand and the supernatant was removed and collected to analyse the stringency of the washing buffer. This step was repeated once without saving the supernatant.

20.) The beads were washed again with ultra pure water by gently inverting the tube. The beads were collected with the magnetic stand and the supernatant was removed and discarded.

21.) Bound proteins were eluted with 100 µL of elution buffer for 5 minutes at RT on the rotating platform. The beads were separated magnetically and the supernatant containing eluted proteins was collected. For optimal protein-recovery, this step might be repeated once.

22.) The supernatant was neutralised with neutralisation buffer (10 µL of neutralisation buffer for each 100 µL of eluate).

23.) After elution, the remaining beads were boiled at 95°C for 5 minutes in reducing Laemmli sample buffer to prove the efficiency of elution. The beads were separated and the supernantant was collected.
24.) The analysis was performed with a 16% SDS-PAGE followed by western blot with anti-MIF IgG, anti-tubulin and anti-actin IgG.

Table 2.12 Composition of buffers and chemicals for Co-IP using Crosslink Magnetic IP/Co-IP Kit

Buffers and chemicals	Composition
Pierce Protein A/G Magnetic Beads (#88805)	10 mg/mL in water containing 0.05% NaN_3
IP Lysis/Wash buffer; pH 7.4 (#88805)	25 mM Tris 150 mM NaCl 1 mM EDTA 1% NP-40 5% glycerol
20X Coupling buffer (#88805)	200 mM sodium phosphate, 3 M NaCl (when diluted:10 mM sodium phosphate, 150 mM NaCl; pH 7.2)
1X Modified coupling buffer (#88805)	1X Coupling buffer 1/20X IP Lysis/Wash buffer
DSS (disuccinimidyl suberate) (#88805)	No-Weigh Format, 2 mg microtubes
Neutralisation buffer; pH 8.5 (#88805)	Undefined
Elution buffer; pH 2.0 (#88805)	Undefined
2X Reaction buffer; pH 7.5	100 mM Tris 10 mM EDTA 300 mM NaCl 2 mM DTT 0.02% NP-40
[6]-Gingerol	10 mg/mL [6]-Gingerol in 100% DMSO
Polyclonal rabbit-anti-MIF IgG (sc-20121)	200 µg/mL in PBS containing <0.1% sodium azide and 0.1% gelatine
2X Laemmli sample buffer	125 mM Tris-HCl; pH 6.8 20% (v/v) Glycerol 4% SDS 0.02% (wt/v) Bromophenol Blue add 4% 2-Mercaptoethanol prior to use

2.8.2 Co-immunoprecipitation using protein A-agarose

250 mg of protein A-agarose beads were swollen in 10 mL PBS^- overnight at 4°C. The swollen beads were collected by centrifugation (2500 × *g*, 2-3 minutes) and the supernatant was discarded. Then, the beads were washed thoroughly with 10 mL PBS^- by inverting the tube or gentle shaking. The bead suspension was spun at 2500 × *g* for 2-3 minutes at 4°C. The washing step was repeated 4 times. One bead volume of PBS^- was added to obtain a 50% bead slurry and the beads were stored at 4°C. Antigen-antibody complexes were formed by mixing 215 µL IP buffer with 30 µL cytosol and 5 µL of polyclonal rabbit anti-MIF IgG (136.59 µg protein/µg antibody). The formation of the complexes was carried out overnight at 4°C with gentle periodic mixing (on a rocking shaker). 50 µL of protein A-agarose (50% slurry) was introduced for each immunoprecipitation by using a wide-orifice

yellow tip (i.e. cut 2-3 mm at the end of the tips off). Antigen-antibody complexes were precipitated with protein A-agarose for 2 hours at 4°C with gentle periodic mixing (on a rocking shaker). Unbound antibodies and cytosolic proteins were separated from the beads by centrifugation at 2500 × *g* for 2-3 minutes at 4°C, the supernatant was carefully discarded to avoid losses of beads. The beads were washed with washing buffer by gentle inverting the tube 20 times. The beads were pelleted by centrifugation at 2500 × *g* for 2-3 minutes at 4°C and the supernatant was discarded. The washing step was carried out 3 times. The beads were then washed with mild washing buffer for 2 times. After the last washing step, 50 µL of 2X Laemmli sample buffer containing 2-mercaptoethanol was subjected to the beads and the beads were heated up to 95°C for 5 minutes. The beads were discarded and the supernatant was transferred to a new microcentrifuge tube. The samples were stored prior to analysis by SDS-PAGE at -20°C or directly loaded onto a 12% SDS-PAGE.

Table 2.13 Composition of applied buffers and chemicals for Co-IP with protein A-agarose

Buffers and chemicals	Composition
IP buffer	50 mM Tris, 150 mM NaCl, 0.1% NP-40; pH 7.5
Washing buffer	50 mM Tris, 150 mM NaCl, 0.02% NP-40; pH 7.5
Mild washing buffer	50 mM Tris, 150 mM NaCl; pH 7.5
2X Laemmli sample buffer	125 mM Tris-HCl; pH 6.8 20% (v/v) Glycerol 4% SDS 0.02% (wt/v) Bromophenol Blue Add 4% 2-Mercaptoethanol prior to use

2.9 Crosslinking of protein complexes

Upon manipulations of cell lysis and sample preparation, protein-protein interactions might destabilise and protein complexes will dissociate. Thus, chemical crosslinking is a method of choice for stabilising the interactions through covalent binding. Chemical crosslinking reagents provide a tool for inter- or intra-molecular crosslinking. Chemical crosslinking reagents can be categorised into 2 groups as homobifunctional and heterobifunctional reagents. The homobifunctional reagents contain an identical reactive group at both ends of a spacer arm such as disuccinimidyl suberate (DSS) and dimethyl pimelimidate (DMP). They are able to bind covalently to adjacent molecules containing the same functional groups. For example, subjecting the homobifunctional crosslinker with amine-amine reactive groups to protein mixtures results in random conjugation of protein subunits, interacting proteins and other polypeptides whose lysine side chains appear close to each other in the protein mixtures. However, applying a homobifunctional reagent for protein crosslinking potentially leads to poorly defined products (Avramease, 1969). The crosslinker reacts initially with a protein forming an intermediate, which might bind covalently to a second protein. Alternatively, the crosslinker could react intramolecularly with a neighbour functional group within the same polypeptide chain. Conversely, heterobifunctional reagents have different reactive groups on each arm of the crosslinker. This difference offers heterobifunctional reagents to conjugate the molecules that have respective functional groups in the single-step

conjugations(i.e. all reagents are added at the same time). Furthermore, heterobifunctional reagents can be used for the sequential conjugation, which minimise self-conjugated proteins and undesirable polymerisation.

In this study, the single-step conjugation approaches were carried out since the aim was to stabilise [6]-gingerol-dependent protein complexes. Thus, glutaraldehyde, an amine-reactive homobifunctional crosslinker, dissuccinimidyl suberate (DSS), a water insoluble, non cleavable amine-reactive homobifunctional crosslinker, and paraformaldehyde were applied. Glutaraldehyde is a membrane permeable crosslinker that can react with α-amino groups of amino acids, the N-terminal amino groups of some peptides, the sulfhydryl group of cysteine, as well as the phenolic side chain of tyrosine and the imidazole rings of histidine derivatives (Habeeb and Hiramoto, 1968). Dissuccinimidyl suberate (DSS), also a membrane permeable crosslinker, has identical N-hydroxysuccinimide (NHS)-ester reactive groups that react predominantly towards amine groups. Paraformaldehyde (PFA) is a simple, inexpensive crosslinker, which binds primarily to lysine residues (Miernyk and Thelen, 2008). PFA has been used for long times in many biological approaches (e.g. histology, hematology, immunohistochemistry) to fix the native states of tissues or cells. PFA is known as zero-length crosslinker although the actual spacer arm length is 2.3-2.7 Å. Thus, one can be implied that only close-proximity associated proteins are able to be stabilised covalently minimising non-specific protein interactions. Proteins crosslinked by PFA dissociate when boiling in SDS sample buffer at high temperature (99^{o}C), whereas the reaction is preserved if the proteins in SDS sample buffer are heated at lower temperature (65^{o}C) (Klockenbusch and Kast, 2010).

2.9.1 Crosslinking of protein complexes by DSS

For *in vivo* crosslinking, HeLa cells pre-treated with [6]-gingerol in a 24-well culture plate were washed once with PBS^{-} (37^{o}C). 2 mg DSS (Thermo Fisher Scientific, IL) was dissolved in DMSO to a final concentration of 100 mM. It was further diluted to 5 mM in lysis buffer without NP-40 (20 mM HEPES 150 mM NaCl) and DMSO was used instead of DSS for control. 50 µL of lysis buffer without NP-40 containing 5 mM DSS was subjected to each well. Cells were incubated for 60 minutes at RT. Subsequently, the NHS reaction was quenched with 50 mM Tris-HCl pH 7.5 for 30 minutes at RT. Cells were lysed in 2X Laemmli sample buffer containing 4% 2-mercaptoethanol by pipetting carefully up and down for several times. For *in vitro* crosslinking, HeLa cell lysate in lysis buffer (20 mM HEPES, 150 mM NaCl, 0.05% NP-40; pH 7.08) was incubated with [6]-gingerol at 4^{o}C for 2 hours. After that, 100 mM DSS was added to obtain a final concentration of 5 mM and the reaction was allowed to continue for 60 minutes at RT. For control, DMSO was used instead. The NHS reaction was quenched with 50 mM Tris-HCl pH 7.5 for 30 minutes at RT. The samples were diluted in 2X Laemmli sample buffer containing 4% 2-mercaptoethanol. The samples from both types of crosslinking (*in vivo* and *in vitro*) were resolved by a 12% SDS-PAGE. For resolving crosslinked samples by BN-PAGE, lysis buffer (20 mM HEPES, 150 mM NaCl, 0.1% NP-40 1 mM Pefabloc; pH 7.08) was applied for lysing cells. The same procedure was conducted as described before. In addition, 5% (wt/v) CBB G-250 was added to the supernatants to obtain a detergent/dye ratio of 8 (g/g). The samples were diluted with 3X gel buffer to 1X. The samples were subjected to a 4-16% BN- gel. Silver staining and electrophoretic transfer onto nitrocellulose membrane (for SDS-gel) or PVDF (for BN-gel) was carried out after resolving proteins.

2.9.2 Crosslinking of protein complexes by glutaraldehyde *in vitro*

HeLa cell lysate in lysis buffer (20 mM HEPES, 150 mM NaCl, 0.1% NP-40; pH 7.08) or HeLa cytosol was incubated with [6]-gingerol at 4^{o}C for 2 hours. After that, glutaraldehyde was added into the samples to a final concentration of 1% (Mischke *et al*., 1998) or 0.1% and incubated at RT for one hour or 10 minutes. For control, ddH_2O was used instead. The crosslinking reaction with glutaraldehyde was quenched with ice-cold 100 mM Tris-HCl pH 7.5 for 30 minutes or 10 minutes at RT. For resolving proteins by SDS-PAGE, the samples were diluted with 2X Laemmli sample buffer containing 4% 2-mercaptoethanol and boiled at 95^{o}C for 5 minutes. The samples were electrophoretically resolved by a 12% SDS-PAGE. After electrophoresis, the resolved proteins were transferred onto nitrocellulose membrane and further analysed by western blot with anti-MIF antibody. For resolving proteins by low-dye BN-PAGE, the samples were added with glycerol to a final concentration of ~2% to increase the samples density. The cell lysate samples were either added with 5% CBB G-250 to obtain a detergent/dye ratio of 8 (g/g) or directly loaded onto BN-gel. There was no addition of CBB G-250 to cytosol. The samples were electrophoretically separated in the native forms with a 4-16% BN-gradient gel under low dye condition. After electrophoresis, separated proteins were transferred onto PVDF membrane by the tank blot system and analysed by western blot with anti-MIF antibody.

2.9.3 Crosslinking of protein complexes by paraformaldehyde *in vivo*

HeLa cells pre-treated with [6]-gingerol in a 24-well culture plate were washed once with PBS^- (37^{o}C). The pre-treated cells were exposed to 200 µL of 0.4% PFA in PBS^+ (PBS^- supplemented with 0.1 M $CaCl_2$ and 0.1 M $MgCl_2$) for 10 minutes at RT with periodic mixing on a rocking shaker. For control, cells were exposed to PBS^+ instead. PFA solution was removed and discarded, and 50µL of 1.25 M glycine/PBS^- was supplied to quench the crosslinking reaction for 5 minutes at RT with periodic mixing. The cells were lysed with 2X Laemmli sample buffer. The samples were heated up to 65^{o}C or 99^{o}C for 5 minutes or 10 minutes respectively. The samples were subjected to a 12% SDS-PAGE. After resolving proteins by SDS-PAGE, the proteins were blotted onto nitrocellulose membrane by the tank blot system. By using specific antibodies, the membrane was probed for MIF, tubulin and actin by western blot analysis.

2.10 Protein blotting

After proteins are resolved by polyacrylamide electrophoresis, protein bands in the gel have to be transferred onto a solid support (e.g. nitrocellulose, polyvinylidene fluoride or cationic nylon membrane) prior to immunodetection. Today, there are two traditional electrotransfer procedures for proteins, which are the semi-dry transfer system and the tank blotting system. The semi-dry transfer system is a system where protein bands are perpendicularly transferred onto a membrane that covers the entire area of the gel with blotting papers serving as ion reservoir in a horizontal configuration. The tank blotting system is a transfer system where the gel/membrane stack is fully submerged in a buffer reservoir and current is applied across the stack. Since the tank transfer blot system show a higher efficiency for broad range protein samples, thus it was used in this study. The advantages and disadvantages of the semi-dry and the tank transfer system are described in table 2.14. Trans-Blot cell (Bio-Rad Laboratories, CA) is a tank blot system with two electrode panels composed of a platinum-coated titanium anode and a stainless steel

cathode. It conducts the electrophoretic transfer in a standard vertical configuration. Figure 2.6 shows the tank blot system.

Since three different polyacrylamide electrophoresis techniques were conducted, the buffers that were employed were also different as described in table 2.15. In case of BN-PAGE, nitrocellulose membrane is not recommended because CBB G-250 binds strongly to this membrane and cannot be destained with organic solvents (i.e. nitrocellulose is dissolved in a mixture of organic solvent). However, nitrocellulose

Table 2.14 Advantages and disadvantages of semi-dry and tank system

Type	Advantages	Disadvantages
Semi-dry	• Shortest transfer duration (15-30 minutes) • Less buffer requirement • Instrument has a large surface area for transferring • Low cost maintenance	• Extended transfer duration is impossible due to buffer depletion • Low buffering capacity • Variable transfer efficiencies for low and high molecular weight proteins
Tank	• Greatest flexibility for optimisation • More complete elution of protein • High compatibility for broad range of proteins resulting in more antibody recognition • Many options available to alternate transfer equipment	• Long transfer duration (1-16 hours) • Large volume of buffer requirement • Cooling require for several systems

(Adapted from LI-COR, 2008)

was used to compare the transfer efficiency between nitrocellulose and PVDF, which is compatible with most organic solvents. The membranes and 2-3 pieces of filter paper were cut to the gel dimension. For the best results, the filter papers and the membrane should be slightly larger than the gel. PVDF was immersed in methanol for 30 seconds and equilibrated in electroblotting buffer (Wittig *et al*., 2006) for ~15 minutes, whereas nitrocellulose was moistened shortly with ddH_2O and equilibrated in electroblotting buffer. The filter papers and 2 fibre pads were wet directly with electroblotting buffer. The gel was excised and equilibrated in electroblotting buffer before performing the electrotransfer. The gel sandwich was assembled in this order: fibre pad, 2 pieces of filter paper, membrane, gel, 2 pieces of filter paper, fibre pad (Figure 2.6). Air bubbles, which hinder the protein transfer, must be removed at every layer of the sandwich by rolling the bubbles out with a glass tube or glass rod. The gel sandwich was inserted into a cassette and the cassette was firmly closed. The cassette was placed in the tank that contained electroblotting buffer with the membrane orientated towards the anode. The gel sandwich has to be submerged entirely in electroblotting buffer. The electrotransfer was carried out overnight with limited current of 100 mA at RT according to manufacturer's instructions. After transfer, the gel sandwich was disassembled and the orientation of the membrane was documented. To visualise protein bands and to remove background, the membrane was destained in destaining solution for several hours for better visuality (only for PVDF). During destaining, destaining solution was exchanged for several times. After background was reduced, PVDF membrane was rinsed with PBS^- and documented with an image scanner (GE Healthcare). Alternatively, PVDF membrane was allowed to dry and was then documented. Prior to western blot, PVDF membrane was completely destained by immersing in 99% methanol for several minutes and washing once with PBS^-.

Table 2.15 Composition of blotting buffers, staining and destaining solutions

Buffers and chemicals	Composition
10X Transfer buffer (SDS-PAGE)	200 mM Tris base 1.5 M Glycine stored at RT
1X Blotting buffer (SDS-PAGE)	1X Transfer buffer (20 mM Tris, 150 mM Glycine) 200 mL 98% Ethanol 700 mL distilled water pre-cool the buffer to 4^{o}C prior to transfer.
Electroblotting buffer (BN-PAGE)	50 mM Tricine (stock: 1 M Tricine) 7.5 mM Imidazole (stock: 1 M Imidazole) pH ~7.0 (adjust pH with 1 M Tricine or 1 M Imidazole, if necessary) stored at 4^{o}C
Destaining solution (BN- and CN-PAGE)	25% Methanol 10% Acetic acid
SDS-transfer buffer (CN-PAGE)	300 mM Tris base (stock: 1 M Tris) 100 mM Acetic acid (stock: 1 M Acetic acid) 1% SDS pH 8.6 (adjust pH with 1 M Tris or 1 M Acetic acid, if necessary, correct pH before adding 1% SDS)
SDS-free transfer buffer (CN-PAGE)	150 mM Tris base (stock: 1 M Tris) 50 mM Acetic acid (stock: 1 M Acetic acid) pH 8.6 (adjust pH with 1 M Tris or 1 M Acetic acid, if necessary)
Staining solution (CN-PAGE)	25% Methanol 10% Acetic acid 0.02% Coomassie brilliant blue G-250

For the electrotransfer of proteins resolved by SDS-PAGE onto nitrocellulose membrane, 1X blotting buffer was used and the identical procedure was applied as described for BN-PAGE. The efficiency of the electrotransfer was examined by staining the membrane with ponceau S solution. Ponceau S is a rapid and reversible stain compatible with organic solvent sensitive membranes (nitrocellulose). Ponceau S staining, which generates reddish protein bands, was destained with distilled water or PBS^{-} until clear protein bands appeared. Subsequently, the membrane was documented and completely destained by immersing in distilled water or PBS^{-} for several minutes prior to western blot. Only when proteins were resolved by SDS-PAGE with Mini-PROTEAN Tetra Cell (Bio-Rad Laboratories, CA), Mini Trans-Blot (Bio-Rad Laboratories, CA), which is a smaller tank transfer apparatus, was used and the applied voltage was set constantly to 90 mA at RT for overnight according to manufacturer's instructions.

For CN-PAGE, after running the gel, it has to be handled with a different procedure prior to transfer (Wittig *et al*., 2007). To facilitate protein electrotransfer, the gel was incubated for 20 minutes in 3-fold gel volume with SDS-transfer buffer. During incubation, the gel was flipped several times. Subsequently, the gel was placed between two glass plates and stored for one hour at 20-25^{o}C allowing SDS to diffuse in the gel and to denature proteins. The identical procedure was applied as described for BN-PAGE and the denatured proteins in the gel were transferred overnight onto PVDF membrane with limited current of 100 mA by using the tank blot system with SDS-free transfer buffer at RT. The protein bands on the membrane after electrotransfer were visualised by incubating in staining solution for 5 minutes and

destaining with two changes of destaining solution for 10 minutes each. Later, the membrane was documented and destained entirely with 99% methanol for several minutes. The remaining methanol was removed by washing once with PBS^- and western blot was conducted afterwards.

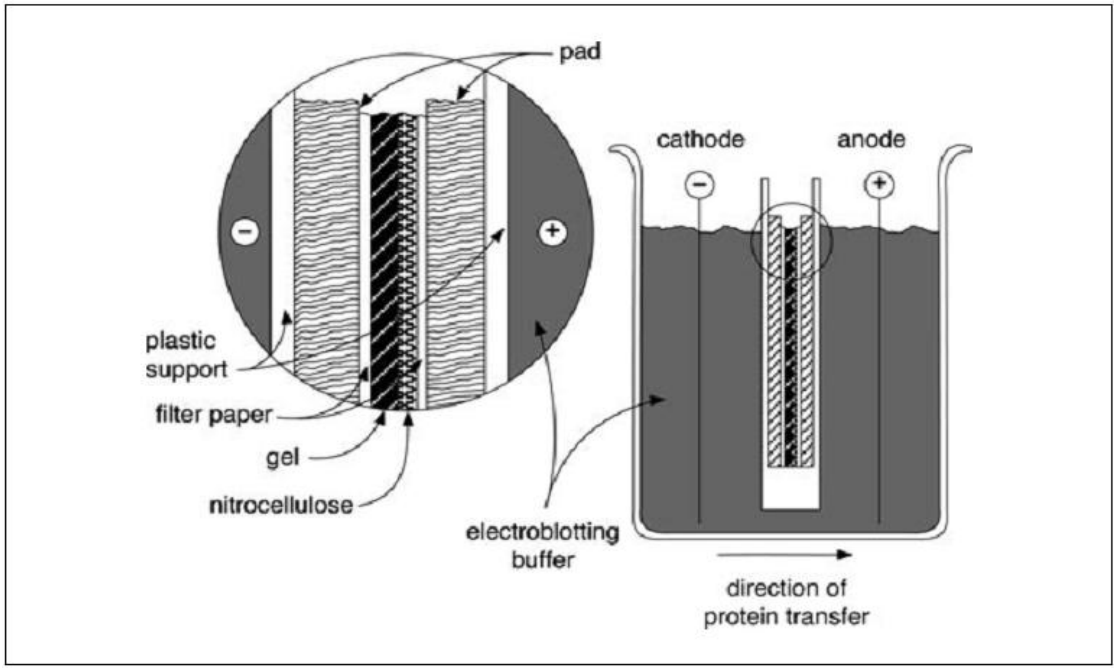

Figure 2.6 Illustration of the tank blot system
The polyacrylamide gel is positioned in between sheets of filter papers and the membrane as depicted above. The resulting stack is sandwiched between fibre pads and placed into a gel holder cassette. The cassette is inserted into a buffer tank containing transfer buffer (Gallagher *et al*., 2008).

2.11 Immunodetection

Western blot or immunodetection is a widely-used analytical method in cell and molecular biology. This method allows researchers to detect a specific protein in a mixture of proteins. Proteins are first resolved through electrophoresis techniques, then transferred onto a membrane (nitrocellulose or PVDF) by electrophoretic transferring **(Subheading 2.10**) or blotted onto a membrane through absorption or vacuum. After transfer, blocking of the membrane is necessary to prevent unspecific binding of antibody. Then, the blocked membrane is incubated with unlabelled primary antibody (monoclonal or polyclonal), which specifically binds to antigen. Following incubation, unbound primary antibody is washed away and secondary antibody is added, which specifically binds to primary antibody. The secondary antibody is conjugated to reporter enzymes, or fluorophores that produce light or colour. In this study, secondary antibodies conjugated to horseradish peroxidise (HRP) were employed. Horseradish peroxidise is an enzyme, which catalyses a reaction leading to the emission of light as depicted in figure 2.7. Finally, the unbound secondary antibody is washed away and chemiluminescence signals are detected and documented.

Protein samples were resolved by BN-, CN- or SDS-PAGE and electrophoretically transferred onto PVDF or nitrocellulose membrane. Alternatively, protein samples were directly applied onto

nitrocellulose membrane in the case of dot blotting. Unoccupied sites on blots were blocked for one hour at RT with blocking buffer (PBST containing 5% skim milk powder). Primary antibodies recognising MIF, tubulin or actin were diluted with blocking buffer to the desired concentration (see Table 2.16) and blots were incubated in diluted antibodies for one hour at RT. Unbound primary antibodies were thoroughly washed away with PBST (PBS^- supplemented with 0.1% Tween 20) 3 times for 5 minutes each. HRP-conjugated secondary antibodies recognising mouse or rabbit IgG or HRP-conjugated protein A (for analysis of Co-IP) were diluted in blocking buffer and incubated with the blots for one hour at RT. Again, unbound secondary antibodies or protein A were thoroughly washed away with PBST 3 times for 5 minutes each and once for 5 minutes with PBS^- before adding chemiluminescent reagent. The chemiluminescent reagent was diluted in a ratio of 1:1. The remaining PBS^- on the blots was allowed to drain, then the chemiluminescent reagent mixture was added to the blots and incubated for 5 minutes. The excess reagent mixture was drained to prevent background problems. Images were generated with various exposure times by using FUSION-FX7 Advance-Multi-Imaging Instrument (Vilber Lourmat, Germany) or exposing to high performance chemiluminescence films (GE Healthcare) in a dark room. In case of high background, blots can be additionally washed with high salt buffer (HSB) for 30 minutes and rinsed with ddH_2O afterwards (EMD Millipore Corporation, 2014). The chemiluminescent reagent mixture can be added onto the blots and images can be generated again.

Table 2.16 Buffers and antibodies for western blot

Buffer and antibodies	**Composition**
Washing buffer (PBST)	1X PBS^- 0.1% Tween 20
Blocking buffer	1X PBS^- 0.1% Tween 20 5% Powdered milk (non-fat)
High salt buffer (HSB)	1X PBS^- 0.5 M NaCl 0.2% SDS
Chemiluminescent reagent	Supersignal WestDura, Thermo Scientific, Inc.
Monoclonal mouse anti-actin (DLN-07274)	1:2000 (0.1 µg/mL) (Primary antibody)
Monoclonal mouse anti-tubulin (T6199)	1:2000 (0.5 µg/mL) (Primary antibody)
Polyclonal rabbit anti-MIF (sc-20121)	1:1000 (0.2 µg/mL) (Primary antibody)
Polyclonal HRP-goat anti-mouse (115-035-146)	1:3000 (0.27 µg/mL) (Secondary antibody)
Polyclonal HRP-goat anti-rabbit (111-035-144)	1:3000 (0.27 µg/mL) (Secondary antibody)
Protein A–HRP (P8651)	1:5000 (0.2 µg/mL)

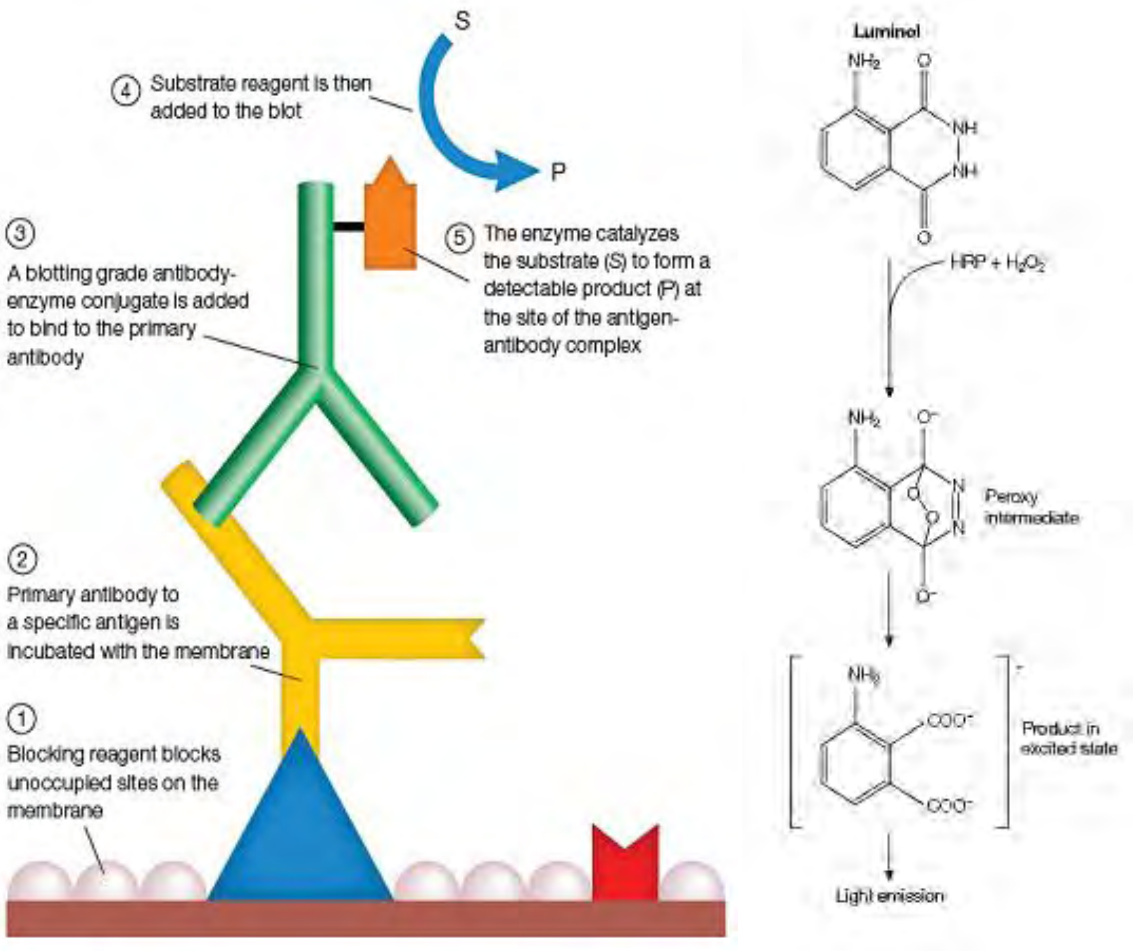

Figure 2.7 Protein detection on blotting membrane by chemiluminescence using HRP-conjugated secondary antibodies

Membrane bound proteins are specifically detected by primary antibody followed by HRP-conjugated secondary antibody. Luminol, which is the luminescence reagent, reacts with hydrogen peroxide in presence of HRP producing 3-amino phthalic acid in the excited stage (3-aminophthalate dianion), then emitting light at 425 nm. (Bio-Rad Laboratories, n.d.)

2.12 Silver staining

Silver staining is a highly sensitive staining method to detect proteins following gel electrophoresis. Switzer and colleagues reported the first successfully detection of proteins by silver staining following gel electrophoresis in 1979 (Switzer *et al*., 1979). The principle of silver staining is akin to developing photographs. However, the precise chemical mechanism of protein staining by silver ions is ambiguous. It has been presumed that Ag^+ ions bind preferentially to basic amino acids, particularly the ε-amino group of lysine, sulphur residues of cysteine and methionine, carboxyl group of glutamate and aspartate and imidazole ring of histidine (Dunn, 2002; Heukeshoven and Dernick, 1985), leading to the formation of silver-protein complexes. Proteins become visible when unbound Ag^+ ions are removed and bound Ag^+ ions are reduced to elementary state (Winkler *et al*., 2007). The silver staining protocol generally starts with: (1) Fixation and removing any interfering compounds, (2) Increasing the sensitivity and contrast of

the staining by sensitisation, (3) Impregnation of Ag^+ ions with either silver nitrate solution or ammoniacal silver solution, (4) Removing unbound Ag^+ ions and developing the silver metal image and (5) Stopping the staining process and removing the excess Ag^+ ions. Both silver nitrate solution and ammoniacal silver solution produce a ~100-1000 fold higher sensitivity than staining with coomassie brilliant blue R-250 and allowing to detect as little as 0.1-10 ng of protein in a single band. Nevertheless, silver nitrate is easier to prepare and does not produce any explosive by-product compared to ammoniacal silver solution (Sambrook and Russell, 2001).

Table 2.17 shows the solutions applied for silver staining. In sensitising solution, glutaraldehyde and sodium thiosulfate are used since both are well-known aldehyde enhancer and sulfiding agent enhancer respectively. Glutaraldehyde binds covalently to free amino groups of proteins and generates the reactive reducing aldehyde group bound to proteins (Rabilloud, 1990) covering the free aldehyde moieties of the proteins that can react with Ag^+ ions. This greatly improves the sensitivity of silver staining. Furthermore, glutaraldehyde crosslinks proteins chemically in the gel matrix and thereby improves fixation and uniformity of staining (Chevallet *et al*., 2006). Sodium thiosulfate serves as source of S^{2+} that reacts directly with Ag^+ ions accelerating the development stage and thiosulfate ions form complexes with Ag^+ ions hindering its reduction to metallic state (Amersham Biosciences, n.d.). Alcoholic sodium acetate serves for dual purposes: 1.) pH control of the glutaraldehyde reaction and 2.) pH control of the reduction of thiosulfate and hindering the degradation of thiosulfate (Heukeshoven and Dernick, 1985). Formaldehyde acts as a reductant to convert Ag^+ to metallic silver and sodium carbonate is used to shift pH to ~12 in order to facilitate the reducing reaction of formaldehyde. EDTA is a chelator that forms strong complexes with Ag^+ ions stopping their further reduction to metallic state.

Because silver staining is a highly sensitive staining method that is susceptible to a variety of interferences (e.g. dirtiness, water purity, gloves), it should be operated properly. All solutions have to be prepared freshly before use with ddH_2O since impurities have strong effects on the staining. All equipments used to run gel electrophoresis and silver staining have to be cleaned with detergent and rinsed thoroughly since detergents can interfere the staining. Gloves must be worn as keratin on hands can produce background. Touching gel during staining, even though gloves are worn, can produce a blemish on the gel. Therefore, the gel should be handled only on the edge or without touching. The staining procedure is done on a rocking shaker inside a fume hood due to the toxicity of glutaraldehyde and formaldehyde.

Table 2.17 Solutions for silver staining

Solution	Composition and concentration
Fixative solution	40% (v/v) Ethanol 10% (v/v) Acetic acid
Sensitising solution	30% (v/v) Ethanol 2 mg/mL Sodium thiosulphate pentahydrate 68 mg/mL Sodium acetate 0.5% (v/v) Glutaraldehyde (stock: 25% (wt/v))
Silver nitrate solution	2.5 mg/mL Silver nitrate 0.04% (v/v) Formaldehyde (stock: 37% (v/v))
Developing solution	25 mg/mL Sodium carbonate 0.02% (v/v) Formaldehyde (stock: 37% (v/v))
Stopping solution	146 mg/mL EDTA

Table 2.18 Protocol for silver staining

Step	Solution	Gel thickness (mm)		
		0.75	1	1.5
		Duration (minutes)		
1	Fixative solution	15	30	60
2	Sensitising solution	15	30	60
3	ddH_2O	10	10	10
4	ddH_2O	10	10	10
5	ddH_2O	10	10	10
6	Silver nitrate solution	15	30	60
7	ddH_2O	1	1	1
8	ddH_2O	1	1	1
9	Developing solution	Depending on the signal intensity	Depending on the signal intensity	Depending on the signal intensity
10	Stopping solution	15	30	60
11	ddH_2O	5	5	5
12	ddH_2O	5	5	5

* In the case of BN-PAGE, the gel has to be destained in fixative solution overnight to remove nearly entire CBB G-250 from the gel and during destaining, fixative solution should be exchanged for several times.

** At step 1, gels can be maintained in fixative solution or in ddH_2O (after fixing the gel following indicated duration) for several days.

*** After silver staining, the gel can be stored in a sealed bag containing an adequate volume of ddH_2O at 4^oC.

3. Results

3.1 Visualisation of MIF by dot blot analysis

The total protein concentration of cytosol was estimated by Bradford assay resulting in 4.55 mg/mL. The potential of [6]-gingerol inducing formation of protein complexes of MIF with other binding partners, which was hypothesised based on a previous report (Möbus, 2013), was tested by direct visualising after dot blotting. HeLa cytosol was incubated with [6]-gingerol at a concentration of 2.5 µg [6]-gingerol/µL cytosol for 2 hours at 4°C. One sample was diluted with 2X reaction buffer to a final concentration of 1X (50 mM Tris, 5 mM EDTA, 150 mM NaCl, 1 mM DTT, 0.01% NP-40; pH 7.5) to mimic the affinity purification conditions used by Möbus (2013), under which complexes were observed. As control, HeLa cytosol was incubated with DMSO instead. 2 µg protein from each sample was pipetted onto a microscopic slide with an identical volume (5 µL). The samples were allowed to bind to the nitrocellulose membrane. MIF was specifically detected through immunodetection by polyclonal anti-MIF IgG and HRP-conjugated secondary antibody, followed by a chemiluminescence reaction (Figure 3.1). The chemiluminescence signals showed that none of the samples demonstrated a significant spot-like signal that might be expected in case of large protein complexes. Even after zooming into dots, no punctuate MIF-distribution was observed. In addition, the intensity of chemiluminescence signal from dot 1 is obviously weaker compared to the others (dot 2 and 3).

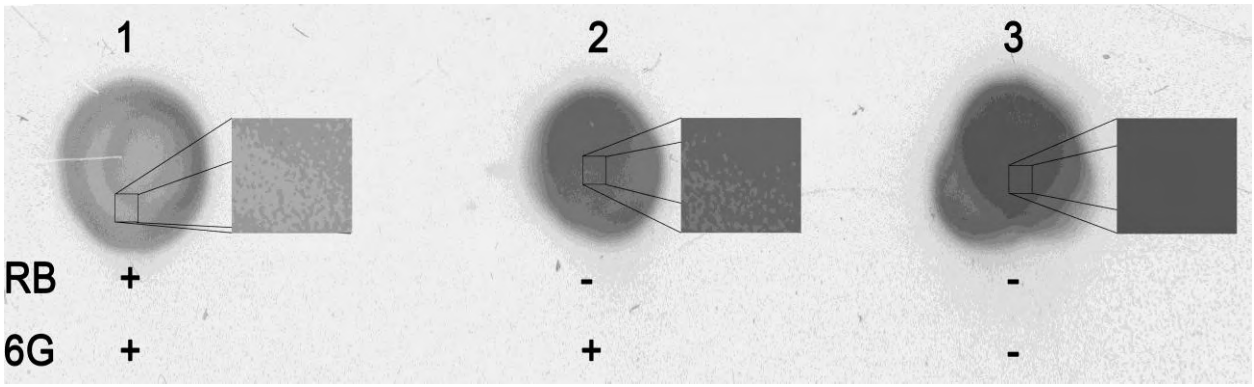

Figure 3.1 Visualisation of potential MIF-protein complexes by dot blotting
Samples were prepared by incubating cytosol with [6]-gingerol at a concentration of 2.5 µg [6]-gingerol/µL cytosol for 2 hours at 4°C and diluting with reaction buffer (RB) (dot 1), without reaction buffer (dot 2) and DMSO control (dot 3). 2 µg protein of each sample was dotted onto a nitrocellulose membrane. MIF was detected by western blot with polyclonal rabbit anti–MIF IgG and HRP-anti-rabbit IgG, followed by a chemiluminescence reaction. Signals were captured using an imaging system. Squares represent zooms into the dot.

3.2 Analysis of MIF-protein complexes by blue native electrophoresis (BN-PAGE)

Since BN-PAGE has been reported to separate proteins in their native state including protein complexes, it was a promising method to qualitatively analyse the possible formation of MIF-protein complexes induced by [6]-gingerol. First, the presence of MIF, tubulin and actin in HeLa cytosol was tested by SDS-PAGE. Additionally, it was investigated whether [6]-gingerol would have an effect on the stability and modification of the proteins. 114 µg protein of cytosol (25 µL) was incubated with 62.5 or 6.25 µg of [6]-gingerol for 2 hours at 4°C. As control, HeLa cytosol was incubated with DMSO instead. The samples were diluted with 2X reaction buffer to a final concentration of 1X to mimic the affinity purification conditions from Möbus (2013), under which complexes were observed. The treated samples were diluted in 2X Laemmli sample buffer and heated up to 95°C for 5 minutes. 20 µg protein of each sample was resolved with a 4-20% SDS-PAGE. The resolved proteins were electrophoretically transferred onto a nitrocellulose membrane. The presence of the target proteins was specifically detected by western blot with anti-MIF IgG, anti-tubulin IgG or anti-actin IgG, and HRP-conjugated secondary antibodies, followed by chemiluminescence reaction

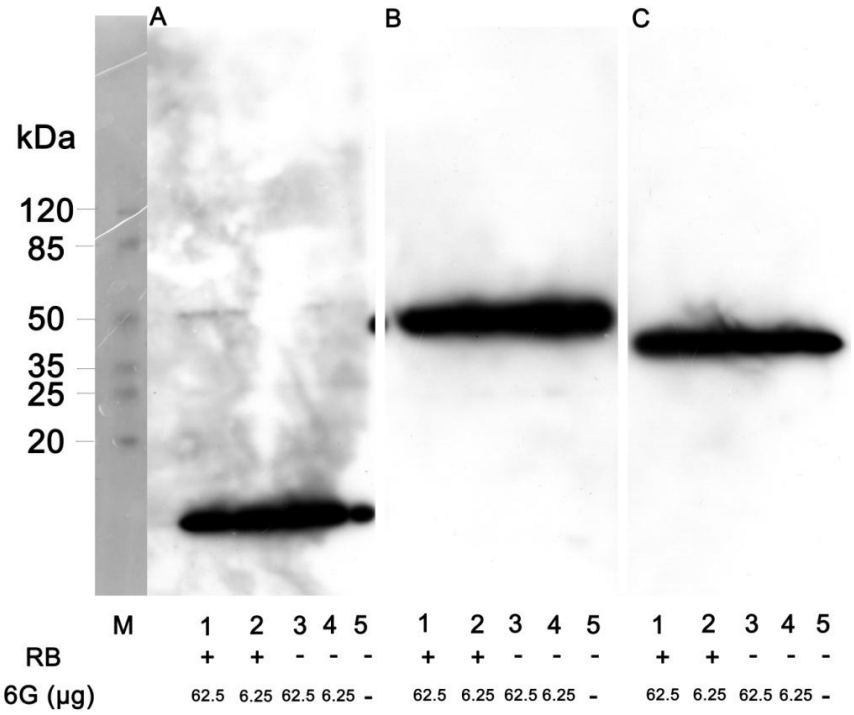

Figure 3.2 Analysis of MIF, tubulin and actin in [6]-gingerol treated cytosol by SDS-PAGE and western blot

25 µL HeLa cytosol (114 µg) was incubated with 62.5 or 6.25 µg [6]-gingerol (6G) for 2 hours at 4°C and subsequently diluted in reaction buffer (RB). For control, DMSO was added instead of [6]-gingerol without RB. 20 µg of protein of each sample was separated by a 4-20% gradient SDS-PAGE and blotted onto a nitrocellulose membrane. MIF, tubulin and actin were immunologically detected by primary antibodies, anti-MIF (A), anti-tubulin (B) and anti-actin (C), and HRP-conjugated secondary antibodies, followed by a chemiluminescence reaction. Condition 1: 62.5 µg [6]-gingerol with addition of reaction buffer; Condition 2: 6.25 µg [6]-gingerol with addition of reaction buffer; Condition 3: 62.5 µg [6]-gingerol without addition of reaction buffer; Condition 4: 6.25 µg [6]-gingerol without addition of reaction buffer; Condition 5: DMSO without addition of reaction buffer; M: marker.

Figure 3.2 shows the presence of all three proteins in HeLa cytosol. HeLa cytosol contains significant amounts of MIF (12.5 kDa), tubulin (50 kDa) and actin (42 kDa) that migrate at the position of the monomer. There are no reductions of the signal intensities in the target proteins in +/- [6]-gingerol incubated samples. Moreover, no influence of the reaction buffer was observed. Therefore, it seems that [6]-gingerol does not affect the expression and modification of MIF, tubulin and actin.

To determine the presence of a [6]-gingerol induced MIF-protein complexes in HeLa cytosol, 114 µg protein from cytosol (25 µL) was incubated with 62.5 or 6.25 µg of [6]-gingerol or DMSO as control for 2 hours at 4^{o}C. After [6]-gingerol incubation, the samples were divided into 2 groups: 1.) diluted with 2X reaction buffer to a final concentration of 1X, 2.) no addition of 2X reaction buffer. All samples were diluted with 3X gel buffer. The final concentration of the gel buffer in the samples was 1X. 18 µg protein of each sample was loaded onto a 4-20% BN-PAGE. The highest polyacrylamide concentration was 20% because of the low molecular weight of MIF monomer (12.5 kDa). Protein bands on the gel were visible during the run of BN-PAGE system. The resolved proteins were directly transferred onto PVDF membrane with the tank blot system. The detection of the target proteins was carried out by western blot with anti-MIF IgG, anti-tubulin IgG or anti-actin IgG, and HRP-conjugated secondary antibodies, followed by a chemiluminescence reaction. Figure 3.3 depicts the proteins resolved by the gradient 4-20% BN-PAGE and the presence of tubulin, MIF and actin after western blot analysis. Obviously, there is no significant band shift or differences in the pattern of bands in condition 1-5.

Because of the various sizes of tubulin structures in the native state (length and complexes with other proteins), the western blot with anti-tubulin IgG (Figure 3.3B) shows a wide range of molecular weight forms of tubulin. Tubulin in its native state can be found at the top of the gel (sample gel) and several extremely large structures, which were larger than 3,000 kDa, were even retained in the gel pockets. In the sample that was incubated with 62.5 µg [6]-gingerol and diluted with reaction buffer (condition 1), tubulin monomer signal (50 kDa) was almost completely gone. Reducing the dose of [6]-gingerol by 10-fold and diluting it with reaction buffer (condition 2), the signal intensity from tubulin monomer was slightly higher than from the sample treated with the high dose of [6]-gingerol. MIF showed a broad molecular weight range of 21-272 kDa with maximal intensity around 67-272 kDa (Figure 3.3C). However, the signals from MIF showed no detectable shift or changes in the expression for the conditions +/- [6]-gingerol and +/- reaction buffer. In addition, for the protein mixtures resolved with 4-20% BN-PAGE, MIF monomer was not present (12.5 kDa), even though the polyacrylamide concentration was high enough to resolve it properly. For actin (42 kDa), both the high and the low dose of [6]-gingerol with reaction buffer exhibited lower actin signal intensities compared to controls (Figure 3.3D). Nevertheless, there was no significant shift in molecular weight between +/- [6]-gingerol and +/- reaction buffer sample.

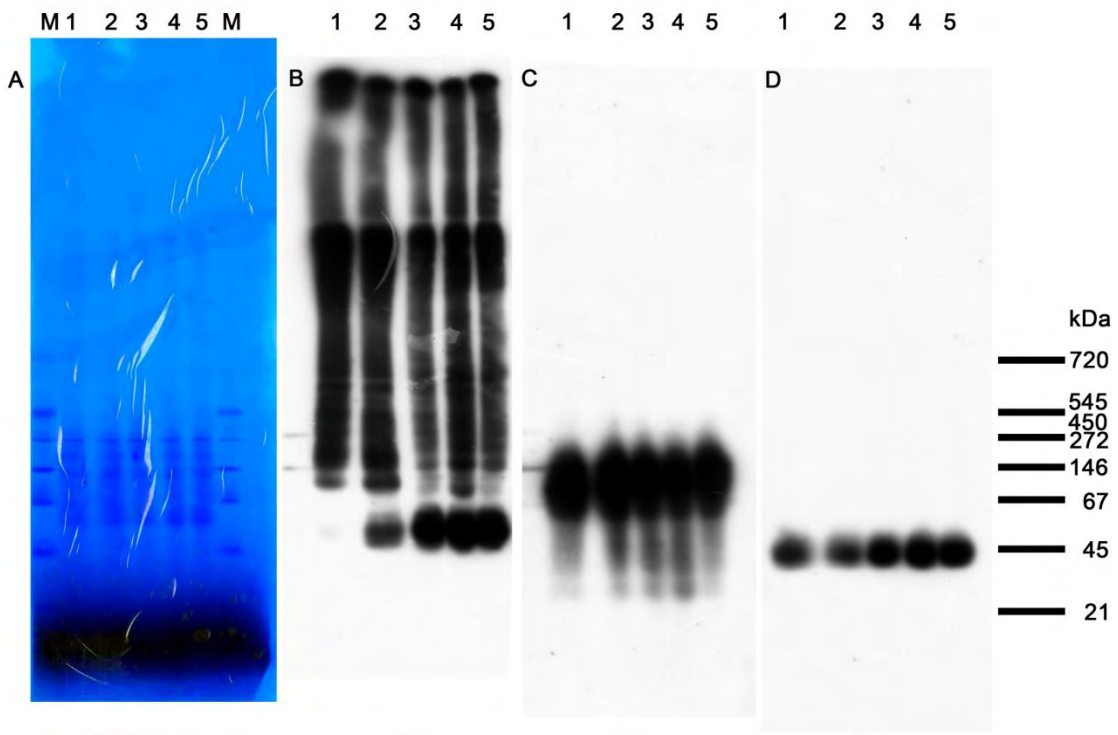

Condition	1	2	3	4	5
RB	+	+	-	-	-
6G (µg)	62.5	6.25	62.5	6.25	-

Figure 3.3 Analysis of [6]-gingerol-dependent protein complexes by 4-20% gradient BN-PAGE
25 µL HeLa cytosol (114 µg) was incubated with 62.5 or 6.25 µg of [6]-gingerol (6G) for 2 hours at 4°C and subsequently diluted in reaction buffer (RB). DMSO was added instead of [6]-gingerol serving as control. 18 µg protein of each sample was resolved under native conditions by a 4-20% gradient BN-PAGE. The resolved proteins were transferred electrophoretically onto PVDF membranes with the tank blot system. The membranes were destained and documented (A) prior to performing western blot. MIF, tubulin and actin were immunologically detected by primary antibodies, anti-tubulin (B), anti-MIF (C), and anti-actin (D), and HRP-conjugated secondary antibodies, followed by a chemiluminescence reaction. Condition 1: 62.5 µg [6]-gingerol with addition of reaction buffer; Condition 2: 6.25 µg [6]-gingerol with addition of reaction buffer; Condition 3: 62.5 µg [6]-gingerol without addition of reaction buffer; Condition 4: 6.25 µg [6]-gingerol without addition of reaction buffer; Condition 5: DMSO without addition of reaction buffer; M: marker.

Interestingly, there was a partial overlap of the broad signals from MIF and tubulin at around 60-280 kDa. Moreover, the detection of MIF showed a single intense broad signal without resolving single bands. Thus, a 8-16% BN-PAGE (Figure 3.4) was employed to increase resolution of protein separation and to analyse whether several distinct bands form the broadly intense signal of MIF. The same conditions were applied for this approach. In addition, to observe whether the reduction of tubulin, MIF and actin monomer signals were affected by reaction buffer, the cytosol diluted with 2X reaction buffer to a final concentration of 1X was loaded. 20 µg protein of each sample was resolved by a 8-16% BN-PAGE to obtain better resolution at the desired range (50-400 kDa). The resolved proteins on PVDF membrane stained with CBB G-250 exhibited no significant shift or differences among the samples (Figure 3.4A).

Furthermore, the western blot results demonstrated no obvious MIF-protein complex formation induced by [6]-gingerol (Figure 3.4C). When the cytosol diluted with reaction buffer was compared (condition 6) to the cytosol incubated with [6]-gingerol and diluted with reaction buffer (condition 1, 2), it was obvious that the tubulin, MIF and actin monomer signals in the samples were significantly decreased due to reaction buffer but not because of [6]-gingerol (Figure 3.4B). Since the resolution of the protein separation was increased, MIF was detected at ~36 kDa and ~272-400 kDa. Similar to the decrease of tubulin monomer signals, the MIF band at ~36 kDa (trimeric MIF) was slightly reduced due to reaction buffer compared to the samples without reaction buffer. However, the signals from actin were indistinguishable among the different conditions (Figure 3.4D).

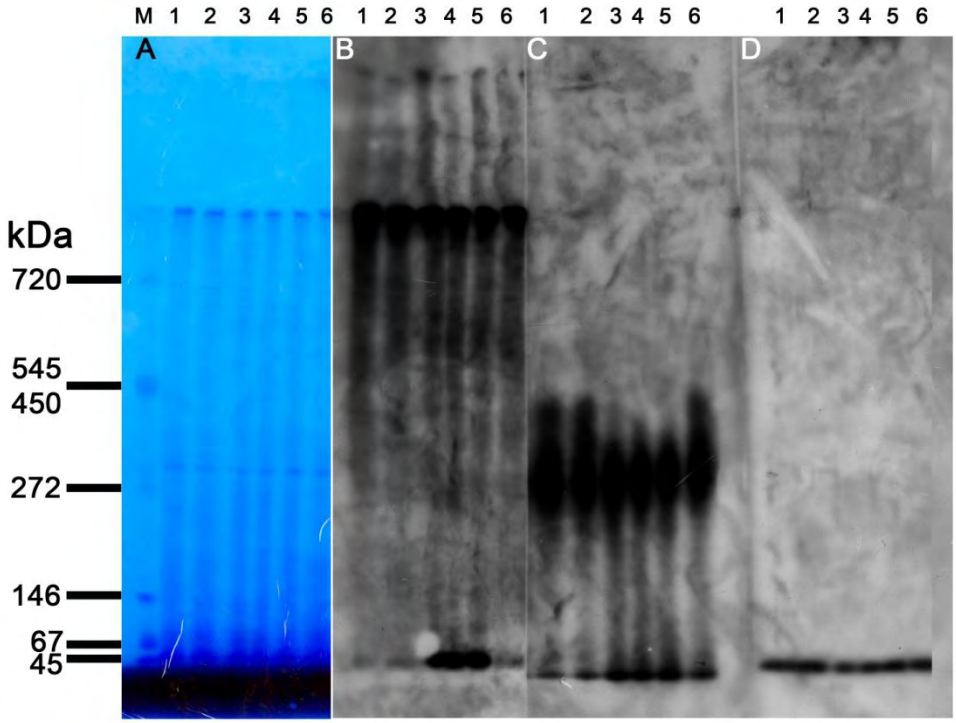

Condition	1	2	3	4	5	6
RB	+	+	-	-	-	+
6G (µg)	62.5	6.25	62.5	6.25	-	-

Figure 3.4 8-16% BN-PAGE and western blot of [6]-gingerol-dependent protein complexes

25 µL HeLa cytosol (114 µg) was incubated with 62.5 or 6.25 µg [6]-gingerol (6G) for 2 hours at 4°C followed by dilution with reaction buffer (RB). 20 µg of each sample was resolved in the native state by a 8-16% BN-PAGE. The resolved native proteins were transferred onto PVDF membranes. The membranes were destained and documented (A) prior to performing western blot. MIF, tubulin and actin were immunologically detected by primary antibodies, anti-tubulin (B), anti-MIF (C), or anti-actin (D), as well as HRP-conjugated secondary antibodies, followed by a chemiluminescence reaction. Condition 1: 62.5 µg [6]-gingerol with addition of reaction buffer; Condition 2: 6.25 µg [6]-gingerol with addition of reaction buffer; Condition 3: 62.5 µg [6]-gingerol without addition of the reaction buffer; Condition 4: 6.25 µg [6]-gingerol without addition of reaction buffer; Condition 5: DMSO without addition of reaction buffer; Condition 6: HeLa cytosol diluted with reaction buffer; M: marker.

Since it was still unclear whether MIF at molecular weights of ~200-400 kDa corresponded to covalently or non-covalently bound partners or MIF multimers, BN-PAGE under native, non-reducing and reducing conditions was conducted. 15 µL of HeLa cytosol was diluted with 3X gel buffer for native condition. For reducing and non-reducing conditions, cytosol was mixed with 2X Laemmli sample buffer with and without 2-mercaptoethanol respectively. The samples for reducing and non-reducing conditions were heated up to 95^{o}C for 5 minutes. 20 µg protein of each sample was resolved by a 8-20% BN-PAGE. The resolved proteins were electrophoretically transferred onto PVDF membrane or stained by silver staining. The proteins on the membrane were immunologically detected by anti-MIF IgG and HRP-conjugated secondary antibody, followed by a chemiluminescence reaction. Figure 3.5 shows the resolved proteins in the gel stained with silver staining and the PVDF membrane stained with CBB G-250 and the MIF western blot. The silver staining result (Figure 3.5A) showed several diffused bands of the native, non-reducing and reducing samples although the loaded proteins were titrated (1, 2 and 3 µL) suggesting that no stacking of proteins occurred. Consistently for the resolved proteins on PVDF (Figure 3.5B), under non-reducing and reducing conditions, smeared bands were detected. Under native condtion, two relevant bands were noticed at molecular weight of ~272 kDa and ~50 kDa. The result of MIF western blot (Figure 3.5C) under native condition demonstrated a broadly smeared band at molecular weights of ~272 kDa. Conversely, the results under non-reducing and reducing conditions demonstrated MIF at molecular weight of ~21 kDa. By comparing MIF western blot under native, non-reducing and reducing conditions, it can be concluded that native MIF forms non-covalently complexes with unknown proteins or to itself.

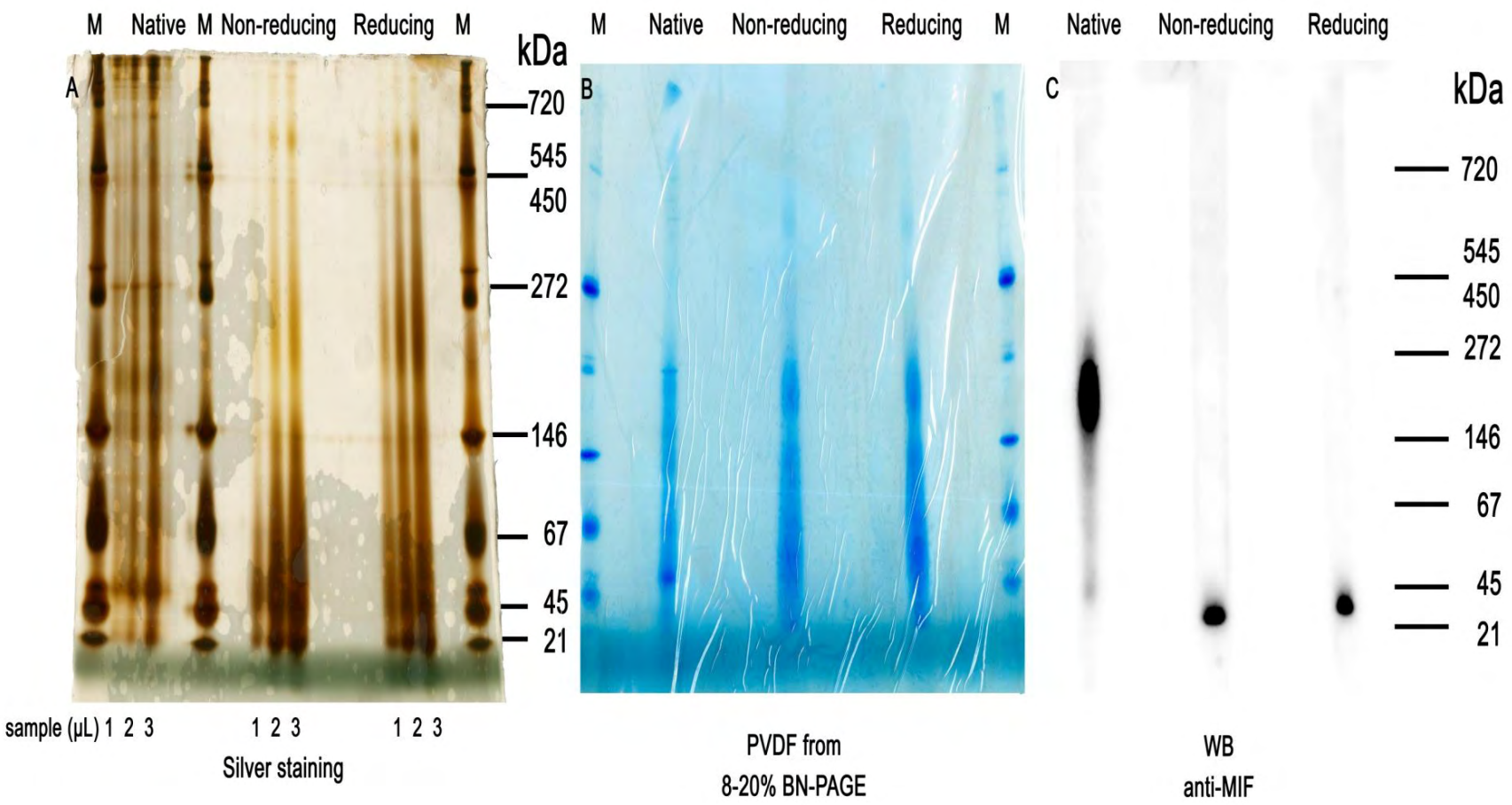

Figure 3.5 Separation of HeLa cytosolic proteins by 8-20% BN-PAGE under native and denaturing conditions (+/- reducing)

15 µL of HeLa cytosol (68 µg) was resolved under native, non-reducing and reducing conditions. For the native state, cytosol was diluted with 3X gel buffer, whereas, for denaturation, cytosol was mixed with Laemmli sample buffer with or without 2-mercaptoethanol for reducing and non-reducing condition respectively. 20 µg protein from each sample was resolved by a 8-20% BN-PAGE. The resolved proteins were either stained by silver staining (A) or blotted onto PVDF membrane (B) and analysed using primary anti-MIF IgG and HRP-conjugated secondary antibody, followed by a chemiluminescence reaction (C). For silver staining, 1, 2 and 3 µL of each sample was loaded onto the gel. M: marker.

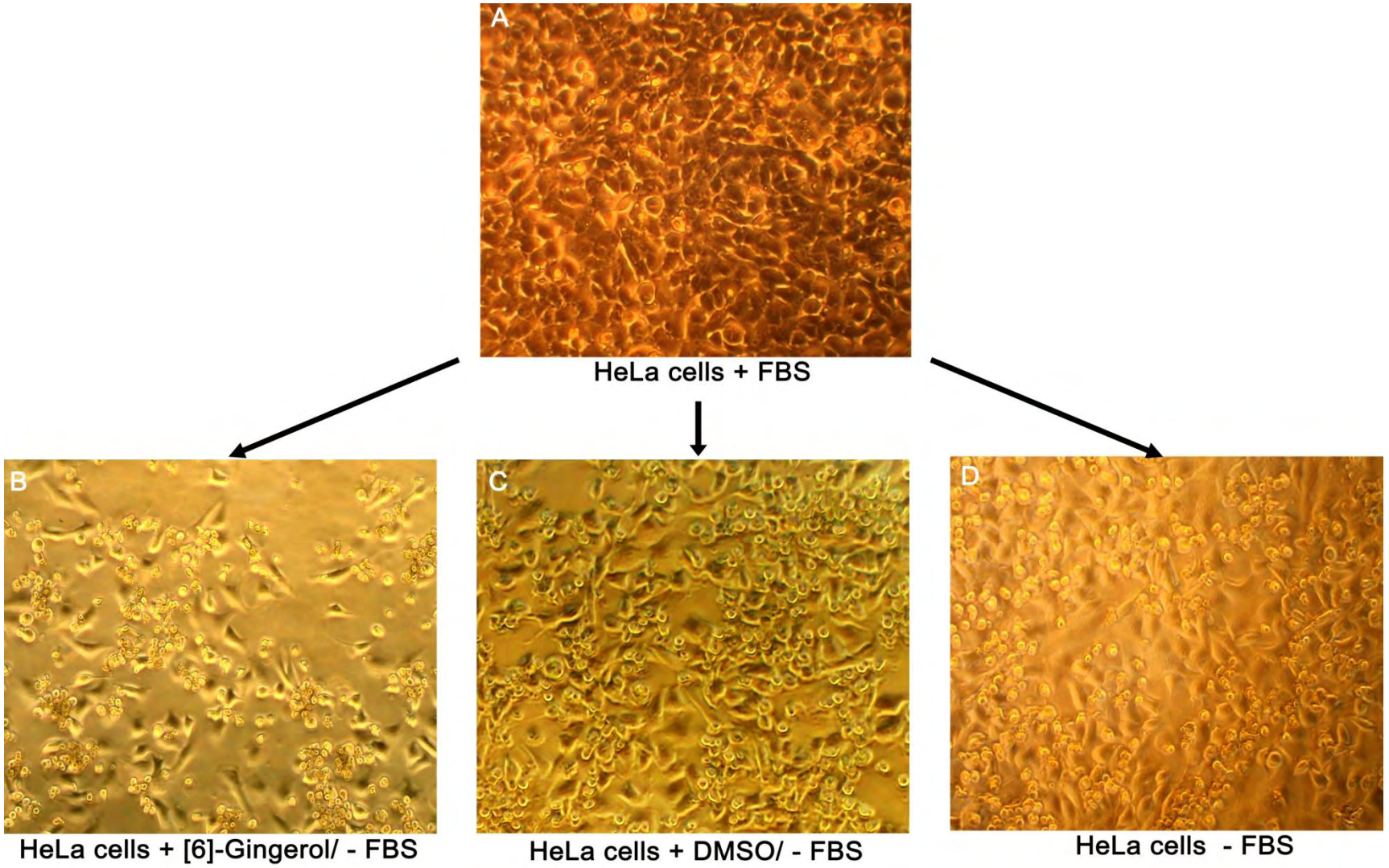

Figure 3.6 Effect of [6]-gingerol on HeLa cell morphology and cell viability

Inverted microscopic images of ~80-90% confluent HeLa cells grown for 24 hours in HeLa medium supplemented with FBS (A). Then, cells were incubated with [6]-gingerol (50 µg/mL) (B), DMSO in medium without FBS (C) and in medium without FBS (D) for 24 hours (37^{o}C, 5% CO_2). The magnification of the images is 100X.

Up to now, all experiments were performed with HeLa cytosol. Since potential complexes might be lost during preparation of PNS or not formed under the non-physiological conditions of cytosol, proteins from [6]-gingerol treated and untreated cells were investigated. HeLa cells in a 24-well culture plate with ~80-90% cell confluency were incubated with or without [6]-gingerol for 24 hours and documented by an inverted light microscope. Figure 3.6 represents the effect of [6]-gingerol on HeLa cells. Prior to incubation with [6]-gingerol (Figure 3.6A), HeLa cells formed a monolayer with typical epithelial-like morphology and slightly elongated shape at low density. After incubation with [6]-gingerol (50µg/mL) (Figure 3.6B), viability of cells was reduced and cell morphology was altered. The round-shaped cells, which are typically for cells entering the apoptosis pathway, were predominantly observed. Moreover, numerous dead, loosely attached cells were found. In contrast, cells that were treated with DMSO (Figure 3.6C) and cells with medium alone (Figure 3.6D) demonstrated a higher cell confluency and cell viability as well as a normal morphology. FBS was excluded for preventing unspecific interaction of [6]-gingerol with proteins in FBS, which might interfere with [6]-gingerol activity.

After the morphological analysis, the incubated cells were lysed with lysis buffer (50 mM Tris, 150 mM NaCl, 1 mM Pefabloc, 0.1% NP-40; pH 7.5). 40 µL of cell lysate corresponding to 0.8 cm^2 of 80% confluent cells was resolved by a 4-16% BN-PAGE. Subsequently, the resolved proteins were blotted onto a PVDF membrane. MIF was immunologically detected by western blot with anti-MIF IgG and HRP-conjugated secondary antibody, followed by a chemiluminescence reaction. Figure 3.7 represents MIF in cell lysate after *in vivo* [6]-gingerol treatment. The MIF signal intensity of cells treated by [6]-gingerol was lower than that of the controls (DMSO and untreated cells). Most likely, this was due to the difference in the total protein concentration of the loaded samples, which was lower for [6]-gingerol treated cells since it resulted in cell losses. Because the aim of the experiment was a qualitative analysis of MIF-protein complex formation induced by [6]-gingerol, thus the precise intensity of signals was not of interest. However, these results show that, in [6]-gingerol treated cells, no significant shifting of MIF-positive bands can be observed.

As the previous report by Möbus (2013) described that [6]-gingerol-conjugated matrix was able to precipitate MIF, tubulin and actin, an analysis of MIF-protein complexes induced by [6]-gingerol in presence/absence of intact microtubules was carried out. The objective of the analysis was to investigate the effect of [6]-gingerol when microtubules were completely depolymerised by nocodazole. Nocodazole is a well-known antimitotic agent that interferes with microtubule formation by binding to β−tubulin causing a change in the conformation of tubulin molecules and preventing formation of disulfide linkages between tubulin monomers (Hamel, 2008; Biswas *et al*., 1984). 136.6 µg protein of HeLa cytosol (30 µL) was incubated with 10 µM nocodazole as a final concentration. As a control, HeLa cytosol was incubated with DMSO instead. Subsequently, 45.3 µg of the pre-treated cytosol (10 µL) was further incubated with 25 µg [6]-gingerol for 2 hours and diluted with 3X gel buffer to 1X as a final concentration afterwards. The samples were subjected to a 8-20% gradient BN-PAGE. The proteins in the gels were visualised by silver staining and, in parallel, electrophoretically transferred onto PVDF membrane. An immunodetection was performed using anti-MIF IgG and HRP-conjugated secondary antibody, followed by a chemiluminescence reaction. Figure 3.8 represents the resolved proteins on PVDF membrane (Figure 3.8A), silver staining of 8-20% gradient BN-gel (Figure 3.8B) and anti-MIF western blot (Figure 3.8C). On the membrane, 5 sharp bands could be observed. There was, however, no clear shift or difference among the samples. The same is true for the silver stained gel, several sharp bands appeared in the gel indicating the effectiveness of the protein resolving by BN-PAGE. Still, there was no indication

for protein complex formation induced by [6]-gingerol. In both presence and absence of intact microtubules, MIF forms complexes of ~272 kDa, as can be concluded from the western blot result. Generally, the signals from MIF in every lane exhibited smeared bands between ~45-400 kDa. Altered MIF-protein complex formation induced by [6]-gingerol, however, was not observed regardless whether microtubules were present or not.

Since the amount of CBB G-250 in cathode buffer might lead to protein complex dissociation, a low-dye BN-PAGE approach was employed. HeLa cells were lysed in lysis buffer (50 mM NaCl, 50 mM imidazole/HCl, 2 mM ε-aminocaproic acid, 1 mM EDTA, 0.1% NP-40; pH 7.0). HeLa cell lysate and HeLa cytosol were incubated in the presence or absence of [6]-gingerol (25 µg [6]-gingerol/100 µg protein). The samples from cell lysate were divided into 2 groups: 1.) without and 2.) with addition of 5% CBB G-250, to obtain detergent/dye ratio of 8 (g/g). Approximately 20 µg protein of each sample was resolved by a 4-16% BN-PAGE with low-dye cathode buffer. After blotting onto PVDF membrane by the tank electrotransfer, the membrane was probed for MIF by immunodetection with anti-MIF IgG and HRP-conjugated secondary antibody, followed by a chemiluminescence reaction. Figure 3.9 depicts the results under low-dye BN-PAGE condition visualised by CBB G-250 (Figure 3.9A) and MIF western blot (Figure 3.9B). On the membrane, the resolved proteins stained by CBB G-250 demonstrated no significant band shift induced by [6]-gingerol. From the western blot detected by anti-MIF IgG, MIF from cell lysate had a molecular weight higher than 720 kDa, whereas MIF from cell cytosol was clearly larger than that from cell lysate. However, MIF-protein complex formation induced specifically by [6]-gingerol was not found through this approach.

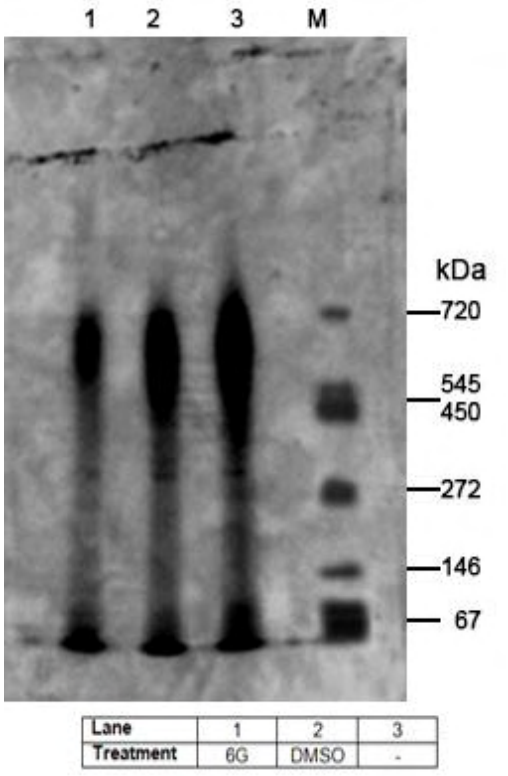

Figure 3.7 Western blot analysis of MIF after *in vivo* treatment of HeLa cells with [6]-gingerol

80-90% confluent HeLa cells were incubated with [6]-gingerol (50µg/mL), DMSO or medium alone for 24 hours in an incubator (37°C with 5% CO_2) and lysed with lysis buffer (50 mM Tris, 150 mM NaCl, 1 mM Pefabloc, 0.1% NP-40; pH 7.5). 40 µL of each sample was loaded onto a 4-16% gradient BN-PAGE. The resolved native proteins were transferred onto PVDF membrane. Immunodetection was conducted with polyclonal rabbit anti-MIF IgG and polyclonal HRP-goat anti-rabbit, followed by a chemiluminescence reaction. Lane 1: HeLa cells incubated with [6]-gingerol; Lane 2: HeLa cells incubated with DMSO; Lane 3: HeLa cells incubated with medium alone; M: marker.

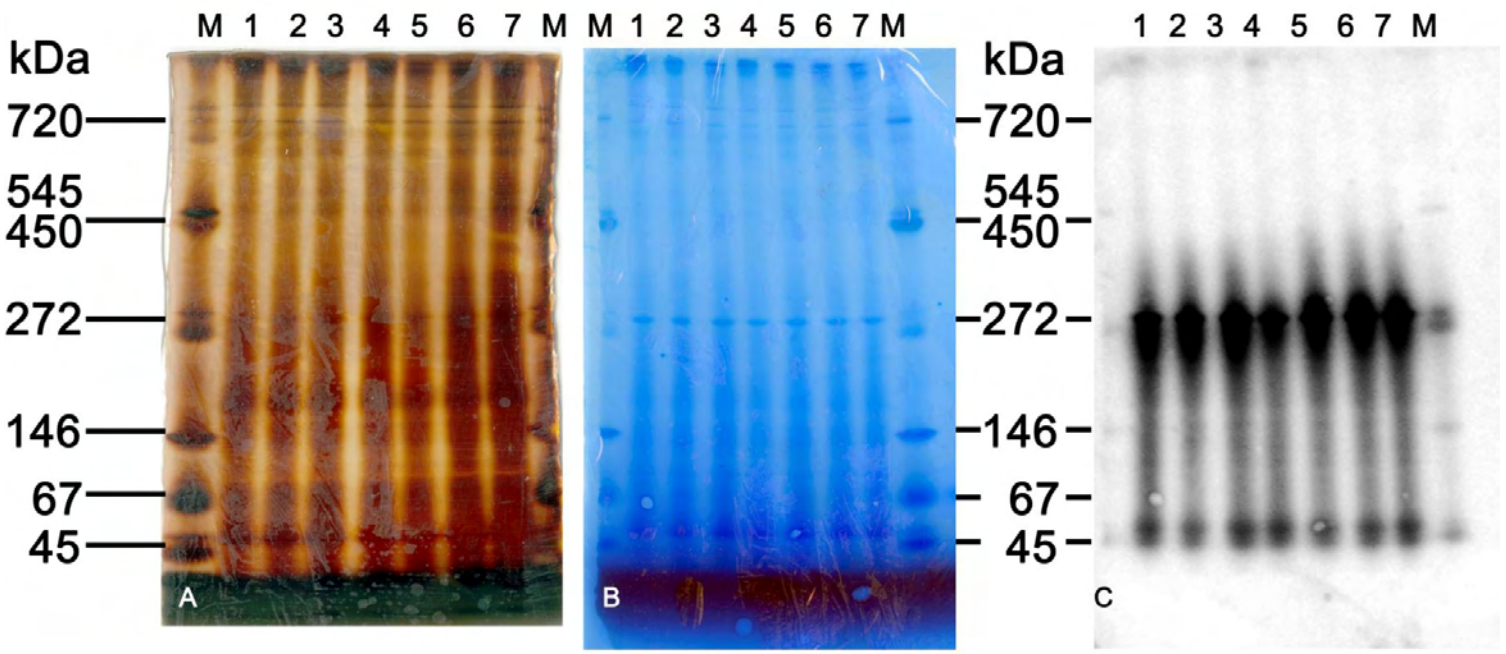

Condition	1	2	3	4	5	6	7
10 µM Nocodazole	+	+	+	-	-	-	untreated
Treatment	6G	DMSO	-	6G	DMSO	-	

Figure 3.8 Analysis of [6]-gingerol dependent-protein complex formation in presence/absence of microtubules

Microtubules in HeLa cytosol were depolymerised by incubating in 10 µM nocodazole for 30 minutes at RT. For control, cytosol was incubated with DMSO instead. Subsequently, the pre-treated cytosol was incubated with [6]-gingerol (6G) (25 µg 6G/45 µg protein) for 2 hours at 4^{o}C. As control, DMSO and none were introduced to the pre-treated cytosol. 20 µg of each sample was loaded onto a 8-20% gradient BN-PAGE. The resolved proteins were electrophoretically transferred onto PVDF membrane and further detected by using polyclonal rabbit anti-MIF IgG and polyclonal HRP-goat anti-rabbit IgG, followed by a chemiluminescence reaction. The resolved proteins were also stained by silver staining. The resolved proteins stained by silver staining (A), the resolved proteins on PVDF membrane (B) and immunodetection of MIF (C) are illustrated. Condition 1-3: nocodazole treated cytosol incubated with [6]-gingerol, DMSO and none respectively; Condition 4-6: cytosol without nocodazole incubated with [6]-gingerol, DMSO and none respectively; Condition 7: untreated (HeLa cytosol); M: marker.

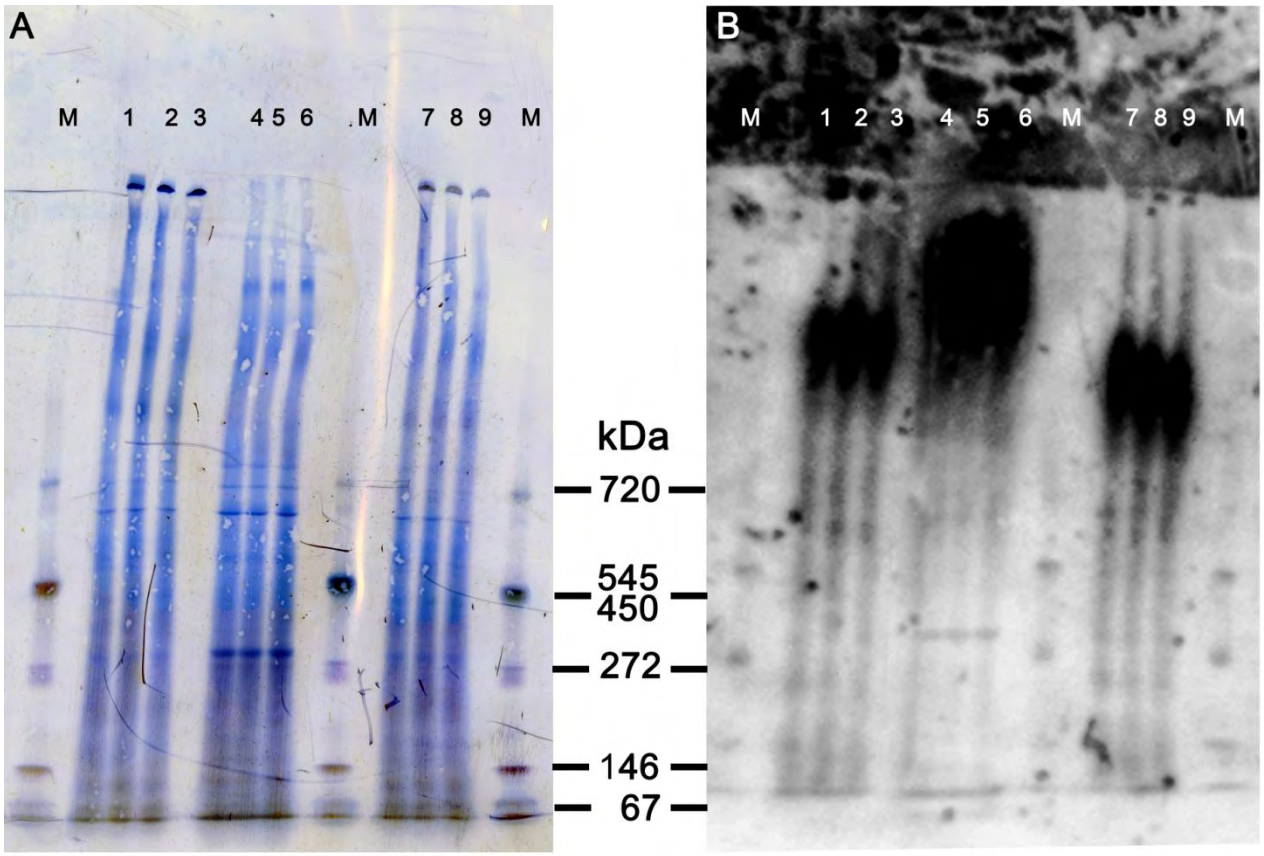

	Cell lysate			Cytosol			Cell lysate with CBB G-250		
Condition	1	2	3	4	5	6	7	8	9
Treatment	6G	DMSO	-	6G	DMSO	-	6G	DMSO	-

Figure 3.9 Low-dye BN-PAGE and western blot analysis of MIF-protein complexes induced by [6]-gingerol

Approximately 100 µg HeLa cell lyste prepared in lysis buffer (50 mM NaCl, 50 mM imidazole/HCl, 2 mM ε-aminocaproic acid, 1 mM EDTA, 0.1% NP-40; pH 7.0), and HeLa cytosol were incubated with [6]-gingerol (25 µg 6G/100 µg protein) for 2 hours at 4°C. As controls, DMSO was added to the samples. The cell lysate samples were divided into 2 groups: 1.) without and 2.) with addition of 5% CBB G-250 to obtain a detergent/dye ratio of 8 (g/g). 20 µg of each sample was loaded onto a 4-16% gradient BN-PAGE. Low-dye cathode buffer (50 mM tricine, 7.5 mM imidazole, 0.002% CBB G-250; pH ~7.0) was employed throughout the run. The resolved proteins were transferred onto PVDF membrane. Immunodetection was conducted with polyclonal rabbit anti-MIF IgG and polyclonal HRP-goat anti-rabbit IgG, followed by a chemiluminescence reaction. The resolved proteins on PVDF membrane (A) and immunodetection of MIF (B) are illustrated. Condition 1-3: treated cell lysate with [6]-gingerol, DMSO and untreated cell lysate respectively; Condition 4-6: treated HeLa cytosol with [6]-gingerol, DMSO and untreated cytosol respectively; Condition 7-9: treated cell lysate with [6]-gingerol, DMSO and untreated cell lysate respectively, followed by addition of CBB G-250; M: marker.

3.3 Co-immunoprecipitation of MIF-binding proteins from HeLa cytosol

As an alternative approach, to observe MIF-protein complex formation induced by [6]-gingerol, co-immunoprecipitation (Co-IP) was employed. HeLa cytosol was incubated with [6]-gingerol (2.5 µg [6]-gingerol/µL cytosol) for 2 hours at 4°C. One sample was diluted with 2X reaction buffer to a final concentration of 1X to mimic the affinity purification conditions from Möbus (2013). Magnetic beads were first immobilised with polyclonal rabbit anti-MIF IgG and subsequently crosslinked by disuccinimidyl suberate (DSS). DSS was applied to crosslinking antibodies to protein A/G magnetic beads, by which avoiding the problem of co-eluted antibodies. 250 µg anti-MIF IgG-magnetic beads were incubated with cytosol (135 µg) for one hour on a rotating platform. Precipitated proteins (eluate) and unbound proteins (supernatant) were resolved by a 16% SDS-PAGE. Proteins were blotted onto nitrocellulose membrane with the tank blot system and the membrane was probed for tubulin, actin and MIF using specific antibodies.

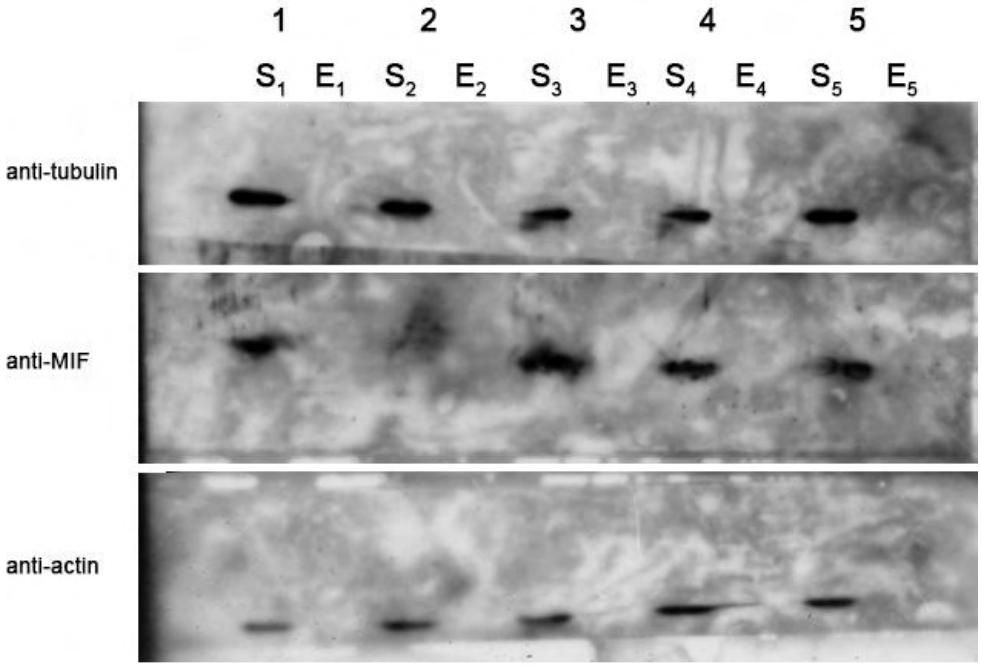

Condition	1	2	3	4	5
RB	+	-	+	-	HeLa cytosol
6G	+	+	-	-	

S: Supernatant
E: Eluate

Figure 3.10 Co-immunoprecipitation with crosslink magnetic IP/Co-IP Kit

Western blotting shows MIF, tubulin and actin in supernatant (S) and eluate (E) from Co-IP with anti-MIF-magnetic beads. Beads were first crosslinked to polyclonal anti-MIF IgG (2 µg antibody/250 µg beads used for one Co-IP reaction) by DSS. HeLa cytosol was incubated with [6]-gingerol (2.5 µg 6G/µL cytosol) for 2 hours at 4°C. For control, DMSO was added instead. Proteins were specifically precipitated by beads-coupled anti-MIF antibodies. Unbound proteins were collected, whereas the bound proteins were eluted with elution buffer. Supernatants (unbound proteins) and eluates (bound proteins) were electrophoretically resolved by a 16% SDS-PAGE. Proteins were blotted onto nitrocellulose membranes by the tank blot system. MIF, tubulin and actin were immunologically detected by primary antibodies, anti-tubulin (top), anti-MIF (middle) and anti-actin (bottom) IgGs, and HRP-conjugated secondary antibodies followed by a chemiluminescence reaction. Condition 1: [6]-gingerol (6G) and reaction buffer (RB); Condition 2: [6]-gingerol without reaction buffer; Condition 3: reaction buffer without [6]-gingerol; Condition 4: without reaction buffer and [6]-gingerol; Condition 5: HeLa cytosol.

As depicted in Figure 3.10, there was no tubulin, actin and MIF in the eluates. Conversely, in the supernatants, the target proteins could be probed by the specific antibodies. In summary, the polyclonal anti-MIF IgG used in this study (see Appendix 7.3) could not precipitate MIF from HeLa cytosol.

3.4 Crosslinking of protein complexes

To stabilise potential MIF-protein complexes inside the cells, chemical crosslinkers were employed in this study. Disuccinimidyl suberate (DSS), a cell permeable homobifunctional crosslinker, reacts readily with primary amines. In an *in vivo* approach, HeLa cells that were pre-treated with [6]-gingerol (50 µg/mL), DMSO or in HeLa medium without FBS were chemically crosslinked by incubation whole cells with DSS. Figure 3.11 depicts the effect of [6]-gingerol pretreatment followed by DSS on HeLa cells. HeLa cells incubated with [6]-gingerol predominatly entered the apoptosis pathway decreasing the cell viability as described earlier in this study (Figure 3.11A). In contrast, cells incubated with DMSO (Figure 3.11B) and cells incubated just in HeLa medium without FBS (Figure 3.11C) showed a better morphology and higher cell viability. After cells were incubated with 5 mM DSS, the [6]-gingerol pre-treated cells obviously crosslinked to each other and formed aggregated structures (Figure 3.11D).

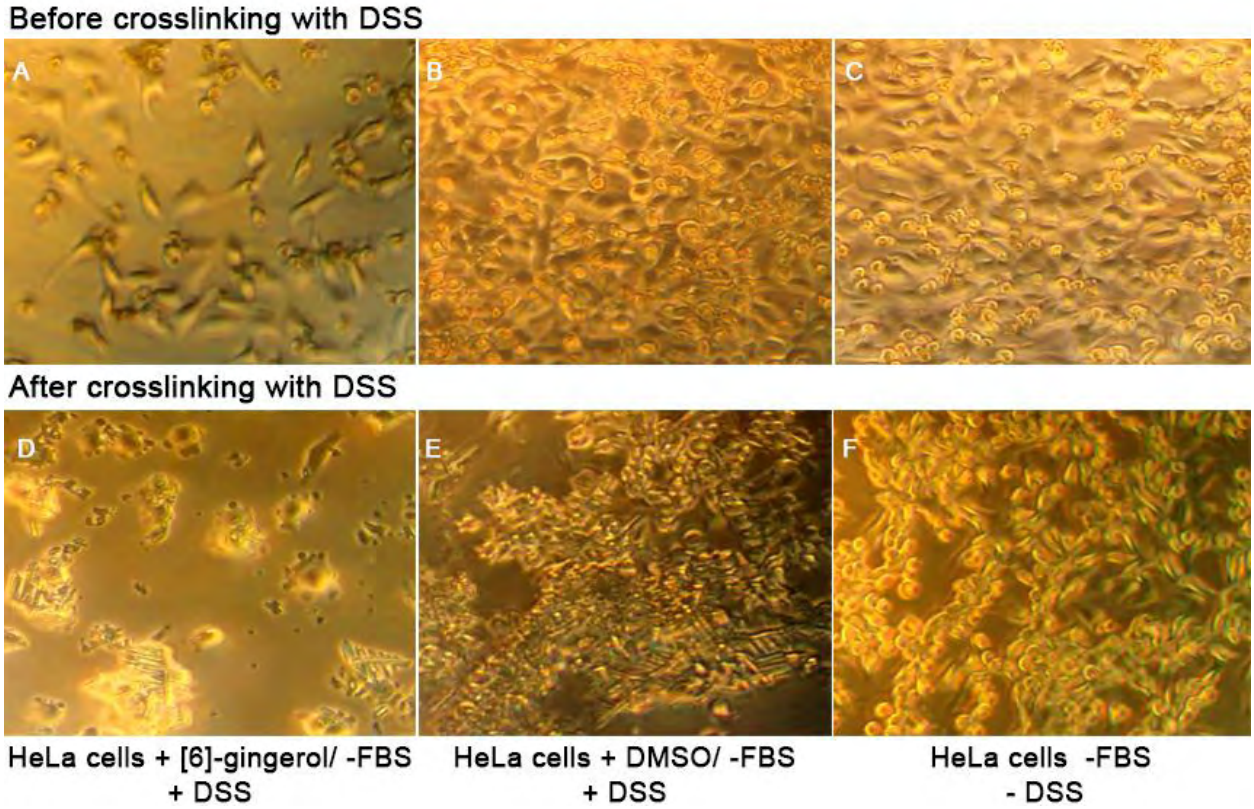

Figure 3.11 Morphological effects of DSS on +/- [6]-gingerol treated HeLa cells

The figure represents the effect of DSS on HeLa cell morphology after incubation with [6]-gingerol, DMSO or medium without FBS alone. HeLa cells were grown to ~80-90% confluence and were incubated with [6]-gingerol (50 µg/mL), DMSO diluted in medium without FBS or medium without FBS alone. Cells were further incubated for 24 hours in an incubator at 37°C with 5% CO_2. Subsequently, cells were incubated with 5 mM DSS for 60 minutes at RT. The crosslinking reaction was quenched with 50 mM Tris-HCl pH 7.5. The magnification of the images is 100X.

DMSO pre-treated cells showed larger aggregates crosslinked by DSS (Figure 3.11E) due to the difference of the cell viability and amount of intact cells prior to crosslinking as compared to [6]-gingerol treated cells. In summary, DSS crosslinked cells effectively forming huge aggregates as compared to control (Figure 3.11F) indicating the functionality of DSS in crosslinking intact cells.

The DSS crosslinked cells were lysed with Laemmli sample buffer containing 4% 2-mercaptoethanol by pipetting thoroughly. Equal volumes of each sample (40 µL) corresponding to 0.8 cm^2 of 24-well culture plate were subjected to two 12% SDS-PAGEs. The resolved proteins of one gel were blotted onto nitrocellulose membrane and the second gel was visualised by silver staining. The membrane was probed for MIF by immunodetection. Immunodetection was conducted with polyclonal rabbit anti-MIF IgG and polyclonal HRP-goat anti-rabbit IgG, followed by a chemiluminescence reaction. Figure 3.12 depicts the stained gel by silver staining (Figure 3.12A) and MIF western blotting (Figure 3.12B). On the silver stained gel, numerous bands appeared. In both, silver stain and MIF western blot, it was obvious that the signal intensity of each lane, especially condition 1-3, was different due to the varying total protein mass in each sample. At ~36 kDa of the blot, the faint protein band in this position could be MIF trimer. The slight shift in molecular weight in condition 4 suggested as MIF trimer crosslinked by DSS (368.35 Da). MIF in the monomer state was found to be the dominant form on the blot and apart from the faint signal from dimer (~24 kDa) and the trimer. However, those bands at molecular weight of ~24 kDa and ~36 kDa could be artefacts or background of the blot since SDS-PAGE system contains SDS and reducing agent resulting in the dissociation of proteins into individual polypeptides. Nevertheless, there was no relevant shift or difference induced by [6]-gingerol neither by silver staining nor by MIF western blotting.

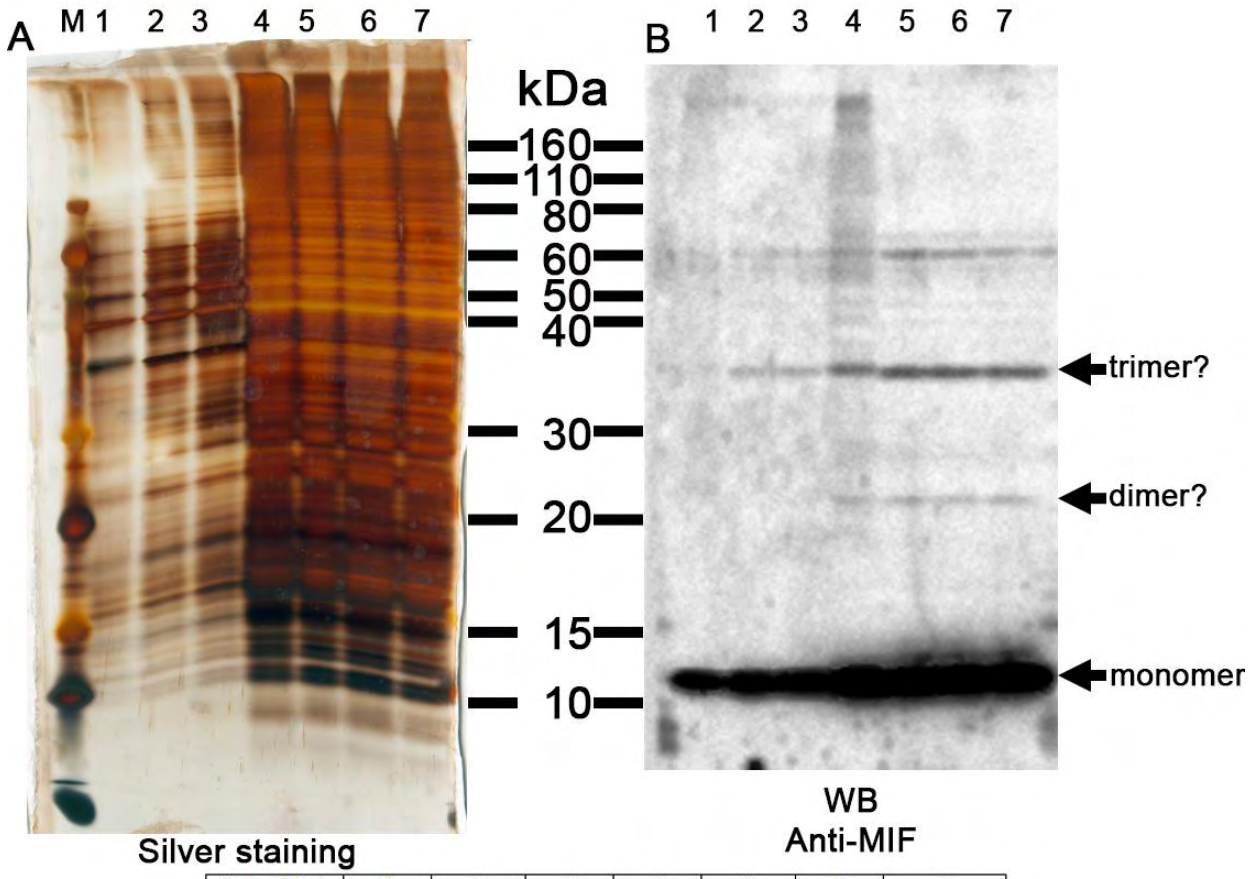

Condition	1	2	3	4	5	6	7
6G	+	+	+	-	-	-	untreated
Treatment	DSS	DMSO	-	DSS	DMSO	-	

Figure 3.12 Silver staining and anti-MIF western blotting of intact cells treated with [6]-gingerol followed by DSS crosslinking

HeLa cells treated with 50 µg/mL [6]-gingerol (6G) (24 hours) followed by DSS (60 minutes) were lysed with 2X Laemmli sample buffer containing 4% 2-mercaptoethanol. 40 µL of each sample was separated by two 12% SDS-PAGEs. The resolved proteins of one gel were blotted onto nitrocellulose membrane by the tank blot system and the other gel was stained by silver staining (A). MIF was detected by western blot with primary anti-MIF antibody followed by HRP-conjugated secondary antibody and a chemiluminescence reaction (B). Condition 1: [6]-gingerol followed by DSS; Condition 2: [6]-gingerol followed by DMSO; Condition 3: [6]-gingerol without further treatment; Condition 4: DMSO followed by DSS; Condition 5: DMSO followed by DMSO; Condition 6: DMSO without further treatment; Condition 7: untreated cell lysate; M: marker.

For the extraction of cytosolic proteins from HeLa cells by nonionic detergent, cells were grown to ~80-90% confluence in a 24-well culture plate. Cells were lysed with lysis buffer (20 mM HEPES, 150 mM NaCl, 0.05% NP-40; pH 7.08). Figure 3.13 depicts HeLa cell morphology before and after cell lysis. Before lysis, cells showed the typical HeLa cell morphology with epithelial-like and slightly elongated shape (Figure 3.13A). Because cells were lysed on ice with non-denaturing lysis buffer, they were only extracted mildly by lysis buffer thereby preserving protein complexes. The cells altered their morphology to a round shape indicating destruction of the cellular architecture upon extraction (Figure 3.13B).

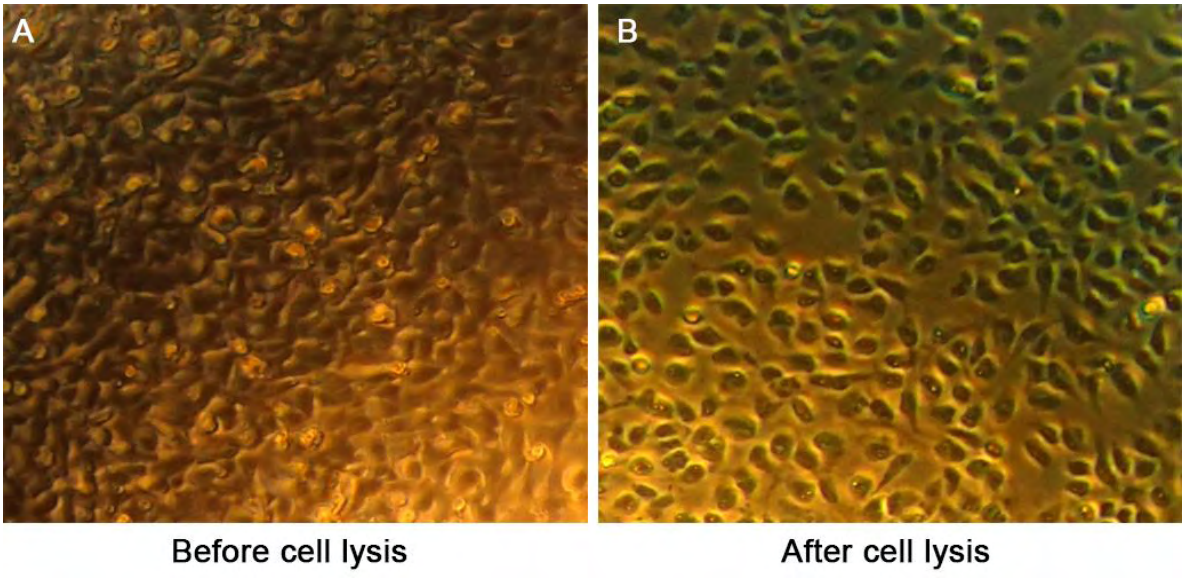

Figure 3.13 Morphology of HeLa cells A) before and B) after cell lysis
HeLa cells were proliferated until ~80-90% cell confluency was acquired in an incubator at 37°C with 5% CO_2. Cells were lysed with lysis buffer (20 mM HEPES, 150 mM NaCl, 0.05% NP-40; pH 7.08) on ice for 30 minutes. Observations were done by the inverted light microscope with 100X magnification.

The cell lysate was collected and incubated with [6]-gingerol (25 µg 6G/ 100 µg protein) or DMSO as control for 2 hours at 4°C. Then, protein complexes were crosslinked by 5 mM DSS for 60 minutes at RT and the crosslinking reaction was stopped with 50 mM Tris-HCl pH 7.5. The samples were resolved by two 12% SDS-PAGEs. Afterwards, one gel was stained by silver staining and the other was blotted onto nitrocellulose membrane. The membrane was probed for western blot analysis with polyclonal rabbit anti-MIF IgG and polyclonal HRP-secondary antibody, followed by a chemiluminescence reaction. Figure 3.14 depicts the silver stained gel (A) and MIF western blot (B). From silver staining, the stained gel exhibited a similar pattern to *in vivo* (Figure 3.12). There was a slight shift at the position of ~36 kDa from the crosslinked samples (Figure 3.14A, condition 1 and 4). Nevertheless, no significant difference induced by [6]-gingerol was noticed. MIF western blot demonstrated intense signals from MIF monomer in all conditions (Figure 3.14B). Condition 1-3 were the [6]-gingerol treated samples, however no difference induced by [6]-gingerol was detected. Only a slight shift from condition 1 and 4, in which the samples were crosslinked by DSS, was noticed at ~36 kDa. In conclusion, no MIF-protein complex formation induced by [6]-gingerol was found by this approach.

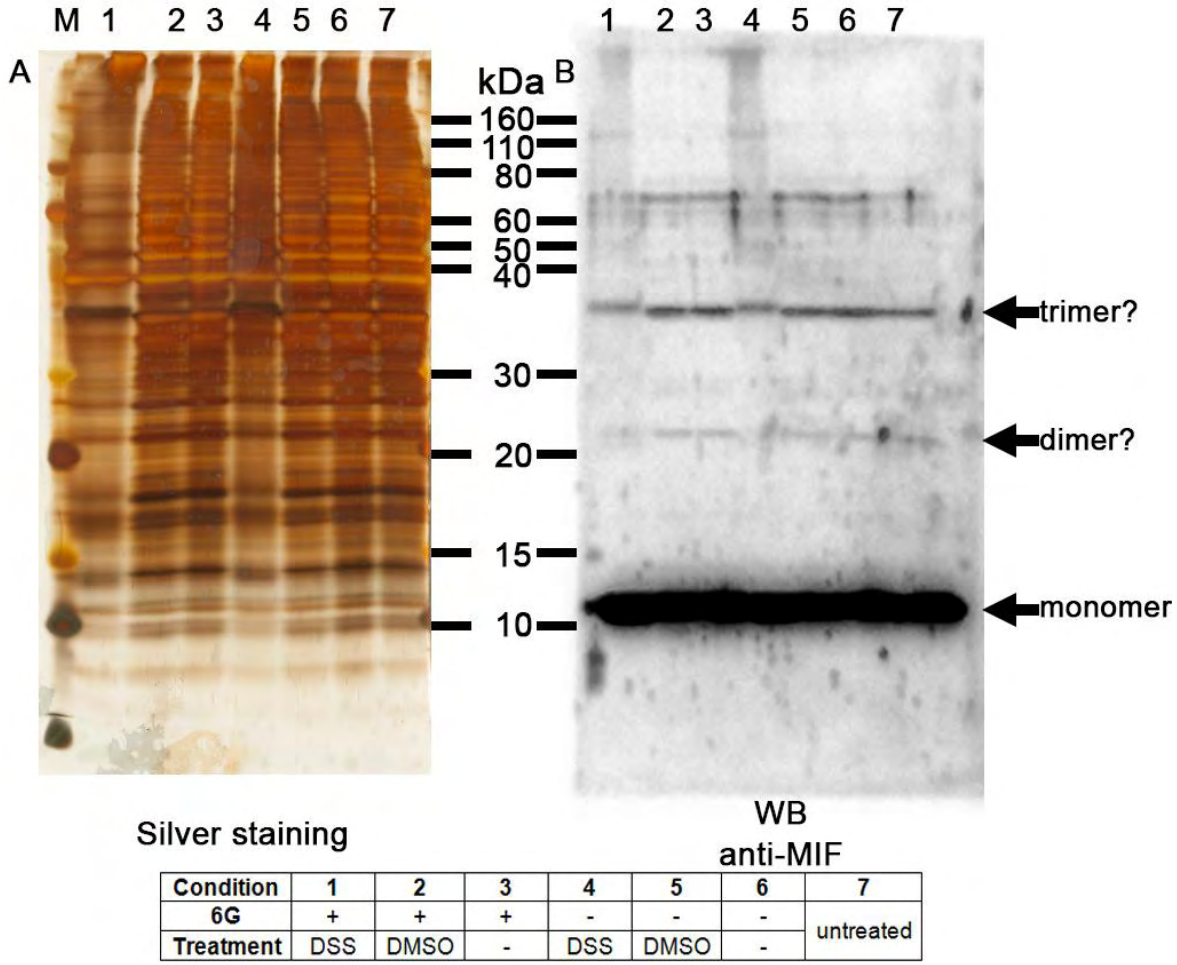

Condition	1	2	3	4	5	6	7
6G	+	+	+	-	-	-	untreated
Treatment	DSS	DMSO	-	DSS	DMSO	-	

Figure 3.14 Silver staining and anti-MIF western blotting of HeLa cell extract upon [6]-gingerol treatment, DSS crosslinking and 12% SDS-PAGE

HeLa cells were lysed with lysis buffer (20 mM HEPES, 150 mM NaCl, 0.05% NP-40; pH 7.08) on ice for 30 minutes. The cell lysate was centrifuged to remove cell debris and 100 µL the supernatant was incubated with [6]-gingerol (6G) (25 µg 6G/ 100 µg protein) at 4°C for 2 hours. The following crosslinking reaction was achieved with 5 mM DSS (60 minutes, RT) and was quenched with 50 mM Tris-HCl pH 7.5. 40 µL of the samples were resolved by 12% SDS-PAGE. The resolved proteins were either blotted onto nitrocellulose membrane by the tank blot system or stained by silver staining (A). MIF was immunodetected by primary anti-MIF antibody followed by HRP-conjugated secondary antibody and a chemiluminescence reaction (B). Condition 1: [6]-gingerol followed by DSS; Condition 2: [6]-gingerol followed by DMSO; Condition 3: [6]-gingerol without further treatment; Condition 4: DMSO followed by DSS; Condition 5: DMSO followed by DMSO; Condition 6: DMSO without further treatment; Condition 7: untreated (whole cell lysate); M: marker.

Since crosslinking with DSS *in vivo* and *in vitro* and resolving with SDS-PAGE did not reveal any [6]-gingerol-dependent MIF complex formation, the DSS crosslinking for BN-PAGE analysis was performed. DSS is a heat-stable crosslinker and should be stable under disulfide-bond cleavage conditions. However, it was hypothesised that MIF-protein complexes might be crosslinked and dissociated under reducing condition. HeLa cells with ~80-90% cell confluency were mechanically dissociated by cell scarping. Subsequently, the cell pellets were lysed with lysis buffer (20 mM HEPES, 150 mM NaCl, 0.1% NP-40, 1 mM Pefabloc; pH 7.08). The cell lysate was incubated with or without

[6]-gingerol (25 µg [6]-gingerol/100 µg protein) and treated with or without 5 mM DSS. The crosslinking reaction was stopped with 50 mM Tris-HCl pH 7.5. Samples were subjected to two 4-16% gradient BN-PAGEs. The resolved proteins of one gel were stained by silver staining and the other was transferred onto PVDF membrane. The membrane was probed by western blot analysis with polyclonal rabbit anti-MIF IgG and polyclonal HRP-secondary antibody, followed by a chemiluminescence reaction. Figure 3.15 shows the stained gel by silver staining with three different amounts of loaded proteins (2, 5 and 10 µg) and the MIF western blot. For silver staining (Figure 3.15A), there was no sign of a [6]-gingerol induced shift. For the MIF western blot (Figure 3.15B), the membrane that was probed for MIF exhibited intense signals. Comparing the sample treated with [6]-gingerol and DSS (condition 1) to the sample treated with DSS alone (condition 4), there was no significant difference. Only one high molecular weight band was less abundant in [6]-gingerol treated cell lysate compared to untreated cell lysate (Arrow in figure 3.15B). Interestingly, both conditions showed bands in a ladder pattern indicated that DSS treatment induced the MIF-containing protein complex (~680 kDa) to dissociate into smaller MIF-containing complexes. These small MIF-containing protein complexes bound non-covalently, since this pattern was not observed in the samples resolved by SDS-PAGE (Figure 3.12 and 3.14). For the samples treated with [6]-gingerol (condition 3) and the samples treated with DMSO (condition 6), one noticeable difference was detected. With DMSO treatement, the signal intensity of MIF was broader than from the samples treated with [6]-gingerol. Thus, it was likely the effect from [6]-gingerol. However, the MIF-protein complex formation induced by [6]-gingerol could not be proved by this approach. Unexpectedly, the signal intensity from whole cell lysate without both treatments showed the broadest intense MIF band at molecular weight of higher than 720 kDa.

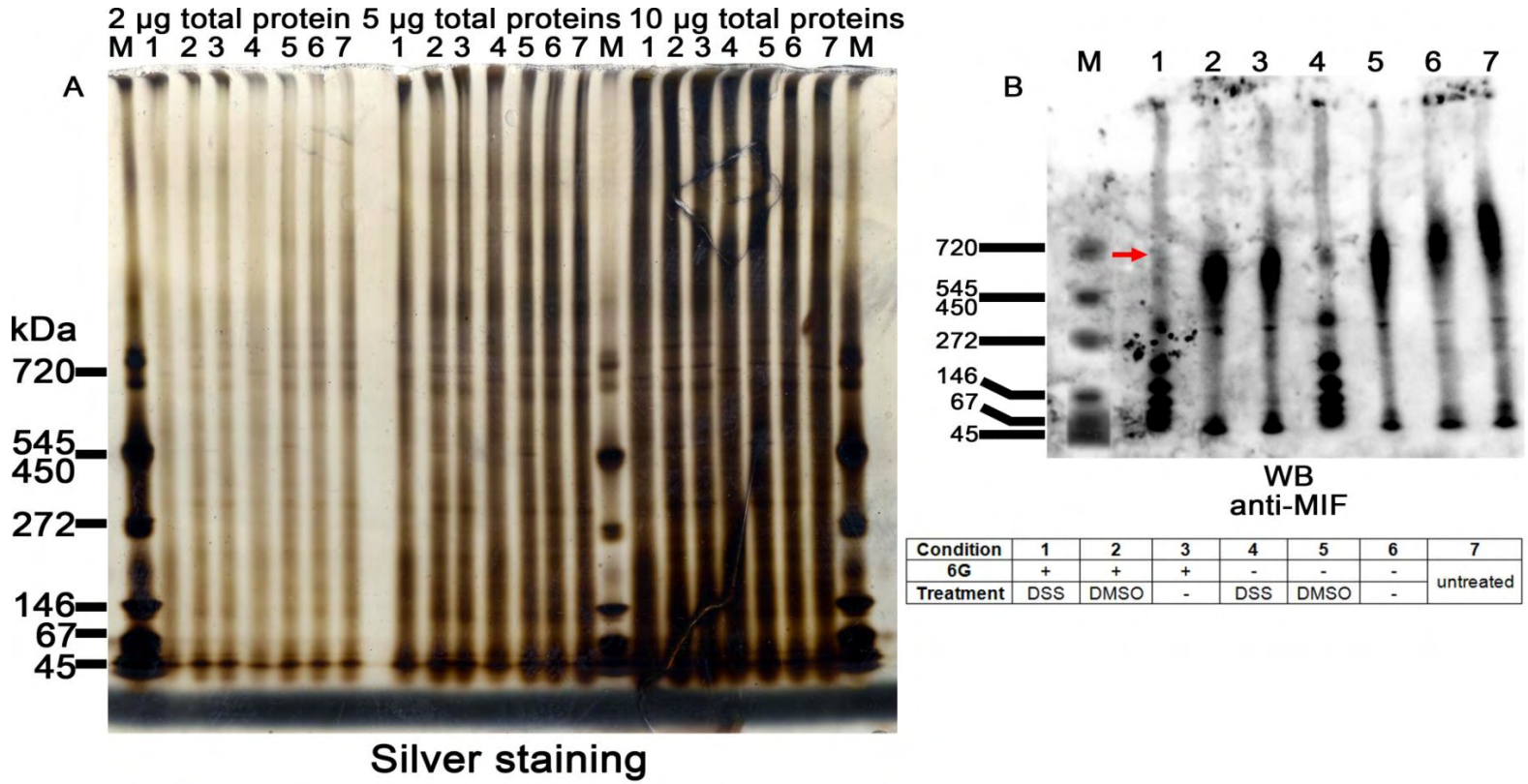

Figure 3.15 4-16% BN-PAGE followed by silver staining and anti-MIF western blotting of [6]-gingerol treated and crosslinked HeLa cell extracts

HeLa cells were grown on a petri dish (Ø 100 mm) to ~80-90% confluence. Cells were collected by cell scraping and lysed with lysis buffer (20 mM HEPES, 150 mM NaCl, 0.1% NP-40, 1 mM Pefabloc; pH 7.08). The cell lysate was centrifuged and cell debris were removed. 20 µL of cell lysate (equivalent to 2 cm^2 cell layer, 100 µg protein approximately) was incubated with [6]-gingerol (6G) (25 µg 6G/100 µg protein) at 4^oC for 2 hours. The crosslinking reaction with 5 mM DSS (60 minutes at RT) and was quenched with 50 mM Tris-HCl pH 7.5. Approximately 20 µg (for western blot) and 2, 5 and 10 µg (for silver staining) protein of the samples were resolved by two 4-16% BN-PAGEs. The resolved proteins of one gel were blotted onto PVDF membrane by the tank blot system and the other were stained by silver staining (A). MIF was immunodetected by primary anti-MIF antibody followed by HRP-conjugated secondary antibody and a chemiluminescence reaction (B). Condition 1: [6]-gingerol followed by DSS; Condition 2: [6]-gingerol followed by DMSO; Condition 3: [6]-gingerol without further treatment; Condition 4: DMSO followed by DSS; Condition 5: DMSO followed by DMSO; Condition 6: DMSO without further treatment; Condition 7: untreated (whole cell lysate); M: marker. The arrow in B indicates a band that is less abundant in [6]-gingerol treated cell lysate than in untreated cell lysate.

As the different DSS crosslinking approaches demonstrated that there were no significant [6]-induced MIF-protein complex formation, glutaraldehyde, a non-specific homobifunctional crosslinker, was employed. Crosslinking of cytosolic proteins by glutaraldehyde was performed *in vitro*. HeLa cell lysate, from cells lysed by lysis buffer (20 mM HEPES, 150 mM NaCl, 0.1% NP-40; pH 7.08), and HeLa cytosol were incubated with [6]-gingerol (25 µg [6]-gingerol/100 µg protein) at 4^{o}C for 2 hours. The samples were subsequently crosslinked with 1% or 0.1% glutaraldehyde for 10 minutes at RT and the crosslinked samples were subjected to four 12% SDS-PAGEs. Two of the gels were blotted on nitrocellulose membranes and the other two gels were stained by CBB R-250. The membranes were probed for MIF by western blot analysis with primary anti-MIF antibody followed by HRP-conjugated secondary antibody and a chemiluminescence reaction. Figure 3.16 depicts the western blot analysis and coomassie staining of [6]-gingerol treated cell lysate and cytosol crosslinking by glutaraldehyde. From the coomassie staining result of +/- [6]-gingerol treated cell lysate crosslinking by glutaraldehyde (Figure 3.16A), with 1% glutaraldehyde, proteins were crosslinked in relatively high crosslinking degree causing heavily crosslinked species that retained in the gel pockets. In contrast to 0.1% glutaraldehyde crosslinked cell lysate, the crosslinking degree was lower and crosslinked proteins were able to enter the gel indicating a concentration-dependent crosslinking of glutaraldehyde. The same is true for [6]-gingerol treated cytosol and crosslinking by 1% or 0.1% glutaraldehyde (Figure 3.16B), the degree of protein crosslinking exhibited a concentration-dependent manner. However, after protein staining by CBB R-250, there was no indication of protein complex formation induced by [6]-gingerol as compared to [6]-gingerol untreated samples under identical crosslinking conditions.

Since the two different concentrations of glutaraldehyde exerted a high protein crosslinking degree, the resolved proteins of the stacking and resolving gel were blotted onto nitrocellulose membranes to probe for MIF, which might form large aggregates and remain in the gel pockets. For cell lysate treated by +/- [6]-gingerol and followed by crosslinking with 1% or 0.1% glutaraldehyde (Figure 3.16C), large MIF complexes crosslinked to other unkown proteins were found and the complexes remained in the gel pockets. However, it was difficult to distinguish the signal intensities of MIF in the gel pockets between 1% and 0.1% glutaraldehyde concentrations due to high interferences of background. With 1% glutaraldehyde, a higher crosslinking degree was noticed as MIF formed large complexes at position of higher than 160 kDa and ~60 kDa. Conversely, with 0.1% glutaraldehyde, the formation of the complexes was noticeably lower. For cytosol treated with or without [6]-gingerol and crosslinked by 1% or 0.1% glutaraldehyde (Figure 3.16D), large MIF-protein complexes remained in the gel pockets especially for protein crosslinked by 1% glutaraldehyde. 1% glutaraldehyde showed MIF-protein complexes predominantly at the position of higher than 260 kDa and ~60 kDa. Moreover, treating the samples with 1% glutaraldehyde, several protein complexes were stabilised with various molecular weights. In contrast, by applying 0.1% glutaraldehyde, MIF-protein complexes had mostly molecular weights of larger than 260 kDa and ~120 kDa. Several MIF-protein complexes were also observed with different in molecular weights. Furthermore, MIF-protein complexes showed more distinct bands as compared to crosslinking with 1% glutaraldehyde, which showed large diffused bands. By comparing the results between the sample from cytosol and cell lysate, it was obvious that in cytosol MIF formed complexes and showed more distinct bands, whereas, for cell lysate, only two significant MIF-protein complex bands were observed. For instance, it was probably due to high DNA contents and cell debris in cell lysate that led to larger complex formation causing proteins retained on the top the gel. In summary,

MIF-protein complexes induced by [6]-gingerol could not be stabilised by glutaraldehyde since no [6]-gingerol-dependent protein complexes were detected.

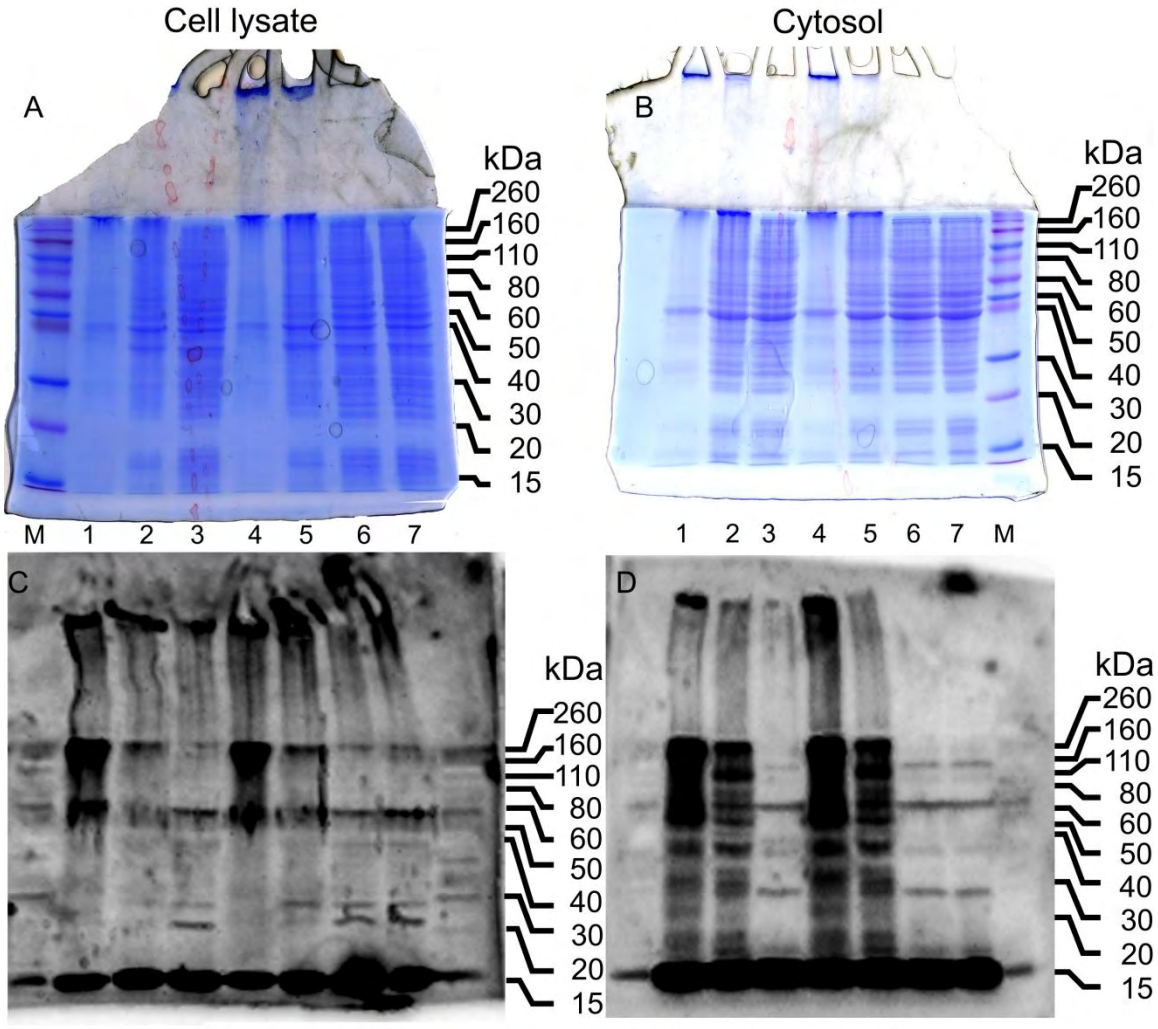

Condition	1	2	3	4	5	6	7
6G	+	+	+	-	-	-	untreated
GA (%)	1	0.1	-	1	0.1	-	

Figure 3.16 Coomassie staining and immunodetection of MIF after *in vitro* treatment of cell lysate and cytosol with [6]-gingerol and crosslinking with glutaraldehyde

20 µL of cell lysate (equivalent to 2 cm^2 cell layer, 100 µg protein approximately), from cells lysed with lysis buffer (20 mM HEPES, 150 mM NaCl, 0.1% NP-40; pH 7.08) and 22 µL of HeLa cytosol (equivalent to 100 µg protein) were incubated with [6]-gingerol (6G) (25 µg 6G/100 µg protein) at 4°C for 2 hours. For controls, DMSO was added instead. Subsequent crosslinking was achieved by 1% or 0.1% glutaraldehyde (GA) as final concentrations for 10 minutes at RT and stopped by ice-cold 100 mM Tris-HCl pH 7.5 for 5 minutes at RT. 20 µg protein of each sample was electrophoretically resolved with four 12% SDS-PAGEs. The separated proteins were either blotted onto nitrocellulose membranes or stained by CBB R-250 (cell lysate: A, cytosol: B). MIF was immunodetected by primary anti-MIF antibody followed by HRP-conjugated secondary antibody and a chemiluminescence reaction (cell lysate: C, cytosol: D). Condition 1: [6]-gingerol followed by 1% glutaraldehyde; Condition 2: [6]-gingerol followed by 0.1% glutaraldehyde; Condition 3: [6]-gingerol without glutaraldehyde; Condition 4: DMSO followed by 1% glutaraldehyde; Condition 5: DMSO followed by 0.1% glutaraldehyde; Condition 6: DMSO without glutaraldehyde; Condition 7: untreated sample (whole cell lysate or cytosol); M: marker.

Another crosslinking approach to analyse [6]-gingerol induced MIF-protein complex formation was conducted by using PFA, a zero-length, non-specific homobifunctional crosslinker. HeLa cells pre-treated with [6]-gingerol (50 µg/mL), DMSO or in HeLa medium without FBS alone were chemically crosslinked by incubation whole cells with 0.4% PFA in PBS^+. The PFA crosslinked cells were lysed with Laemmli sample buffer containing 4% 2-mercaptoethanol by pipetting thoroughly. The samples were heated up to 65°C or 99°C for 5 minutes or 10 minutes respectively, because proteins crosslinked by PFA dissociate when boiling in SDS sample buffer at high temperature (99°C). In contrast, the reaction is preserved if the proteins in SDS sample buffer are heated at lower temperature (65°C) (Klockenbusch and Kast, 2010). Approximately 20 µg protein of each sample was subjected to a 12% SDS-PAGE. The resolved proteins on the gel were blotted onto nitrocellulose membrane. The membrane was probed for immunodetection, using primary anti-MIF IgG, anti-tubulin IgG or anti-actin IgG, and HRP-conjugated secondary antibodies followed by a chemiluminescence reaction. Figure 3.17 shows the immunodetection of MIF, tubulin and actin of [6]-gingerol treated intact cells and crosslinked with 0.4% PFA. For MIF western blot (Figure 3.17A), MIF monomer bands appeared at molecular weight of 12.5 kDa. Interestingly, one MIF-protein complex band from the condition 1, in which [6]-gingerol treated cells and crosslinking by 0.4% PFA was lysed and incubated at 65°C for 5 minutes, was observed at molecular weight of ~70 kDa. The MIF-protein complex indicated [6]-gingerol induced protein complex formation, where MIF participated in. In contrast, in the same sample incubated at 99°C for 10 minutes (condition 6), the MIF-protein complex band disappeared indicating that the MIF-protein complex was dissociated when incubated at high temperature (99°C). Similarly, in the tubulin western blot (Figure 3.17B), three tubulin-protein complexes were detected with molecular weights of higher than 260 kDa, ~260 kDa and ~160 kDa when the samples were incubated at low temperature for short times (65°C for 5 minutes). In contrast, by incubating the samples at 99°C, these tubulin complexes were completely separated into tubulin monomer (55 kDa). For the actin western blot (Figure 3.17C), unexpectedly, only actin monomer was detected. Even though actin is present naturally in large microfilaments, as part of the cytoskeleton, actin complexes were not detected when proteins were crosslinked with 0.4% PFA. The MIF-protein complex induced by [6]-gingerol could, however, not be found as the experiment was repeated.

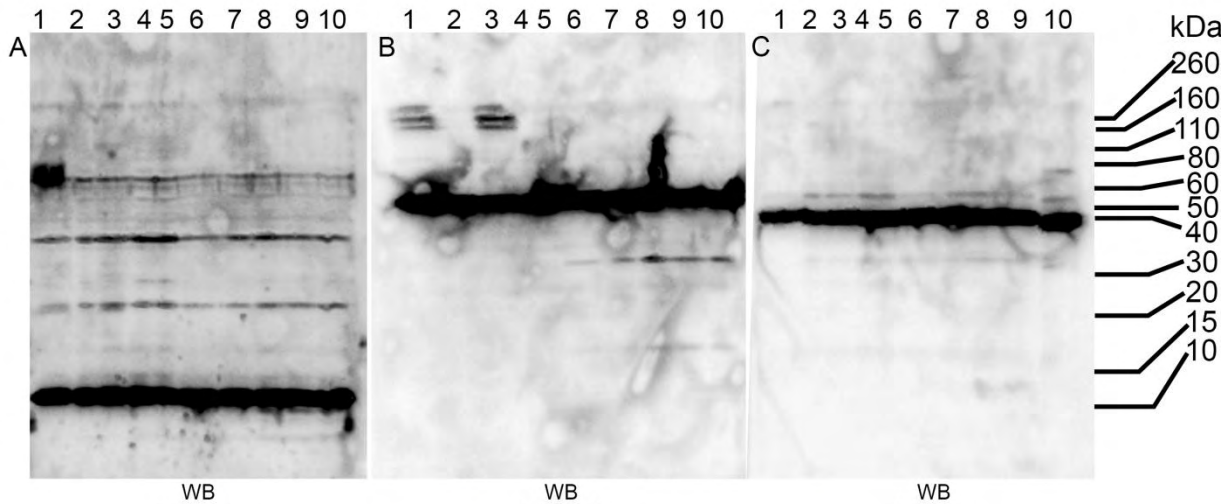

	65°C					99°C				
Condition	1	2	3	4	5	6	7	8	9	10
6G	+	+	-	-	untreated	+	+	-	-	untreated
Treatment	0.4% PFA	PBS^+	0.4% PFA	PBS^+		0.4% PFA	PBS^+	0.4% PFA	PBS^+	

Figure 3.17 12% SDS-PAGE and western blot analysis of HeLa cells treated with [6]-gingerol and crosslinked with PFA

HeLa cells were grown to ~80-90% confluence in a 24-well culture plate and were incubated with [6]-gingerol (6G) (50 µg/mL), DMSO diluted in medium without FBS or medium without FBS alone. The pre-treated cells were exposed to 200 µL of 0.4% PFA in PBS^+ (PBS^- supplemented with 0.1 M $CaCl_2$ and 0.1 M $MgCl_2$) for 10 minutes at RT. For control, cells were exposed to PBS^+ instead. PFA solution was removed and discarded and 50µL of 1.25 M glycine/PBS^- was added to quench the crosslinking reaction for 5 minutes at RT. The cells were lysed with 2X Laemmli sample buffer. The samples were heated up to 65°C or 99°C for 5 minutes or 10 minutes respectively. 20 µg protein of each sample was subjected to a 12% SDS-PAGE. The resolved proteins were blotted onto nitrocellulose membranes by the tank blot system. MIF, tubulin and actin were immunologically detected by primary antibodies, anti-MIF (A), anti-tubulin (B), and anti-actin (C), and HRP-conjugated secondary antibodies, followed by a chemiluminescence reaction. Condition 1 and 6: [6]-gingerol followed by 0.4% PFA; Condition 2 and 7: [6]-gingerol followed by PBS^+; Condition 3 and 8: DMSO followed by 0.4% PFA; Condition 4 and 9: DMSO followed by PBS^+; Condition 5 and 10: HeLa cells incubated in medium without FBS. Condition 1-5: the samples were heated up to 65°C for 5 minutes; Condition 6-10: the samples were heated up to 99°C for 10 minutes.

4. Discussion

[6]-gingerol is one of the most promising phytochemically therapeutic substances from ginger whose pharmacological effects including antimicrobial, anti-tumourigenic and anti-inflammatory activities were reported previously (Lee *et al*., 2009; Hasan *et al*., 2012). However, no cellular interaction partners and molecular mechanisms of the [6]-gingerol effects against cancer cells have been described. Only recently, a study demonstrated potential binding partners of [6]-gingerol in HeLa cytosol (Möbus, 2013). The [6]-gingerol-coupled CNBr and Epoxy matrices showed considerable direct or indirect affinity to MIF and other potential interacting proteins including tubulin and actin. Furthermore, [6]-gingerol appears to induce relocalisation of MIF into the nucleus of HeLa cells (Schäfer, unpublished). In the present study, MIF protein complexes and the potential of [6]-gingerol to induce their formation were investigated by BN-PAGE, CN-PAGE, Co-IP and chemical crosslinking.

MIF, an ubiquitous pluripotent cytokine, was first described nearly five decades ago. MIF possesses broad regulatory properties such as MIF/glucocorticoid counterregulation, inhibition of p53 tumour suppressor and promotion of angiogenesis (Bucala and Donnelly, 2007). Consequently, MIF is a critical mediator of numerous diseases as for example autoimmune disorders, inflammatory diseases, cancer promotion, and sepsis. The expression of MIF protein can be detected in various types of cells including monocytes/macrophages, lymphocytes, eosinophils, neutrophils, epithelial cells, endothelial cells and smooth muscle cells (Santos and Morand, 2009). The binding receptor of extracellular MIF for MIF signalling was identified as CD74, the cell surface form of MHC class II invariant chain. The MIF-CD74 complex further requires an additional protein, CD44, to mediate signals initiated by MIF. The MIF-CD74-CD44 complex formation leads to the activation of subsequent signalling components resulting in overexpression of important factors in inflammation and proliferation (Santos and Morand, 2009). For the tumour growth-promoting properties of MIF, several activities of MIF have been proposed contributing to carcinogenesis: MIF sustains ERK1 and ERK2 activation leading to proliferation; MIF inhibits p53-mediated growth arrest and apoptosis; MIF increases HIF-1α expression and delays tumour cell senescence; MIF increases angiogenic factor production; MIF increases MMP secretion that facilitates tumour invasion and activates CD44 enhancing metastasis (Bucala and Donnelly, 2007). Generally, human MIF monomer has a molecular mass of 12.5 kDa consisting of 115 amino acid residues. The structure of MIF monomer contains of two antiparallel α-helices packed against a four-stranded β-sheet. Three identical MIF subunits arrange to form MIF trimer containing a solvent accessible channel by three single β-sheets wrapping completely around (Sun *et al*., 1996). The inner surface of the solvent accessible channel has a positive potential, suggesting a possible binding site for negatively charged moieties (Alourfi *et al*., 2006) and small molecule ligands (Sun *et al*., 1996).

On the basis of its pleiotropic, physiologic, pathophysiologic and catalytic activities, MIF has been recognised as an attractive therapeutic target for small molecule ligands and antibody-based anticytokine drugs (Xu *et al*., 2013). MIF possesses a keto-enol tautomerase activity suggesting that biological effects of MIF rely on enzymatic action on a substrate, however no relevant substrate for MIF has been identified (Dios *et al*., 2002). Several potential plant-derived compounds have drawn attention as MIF tautomerase inhibitors. Orita and colleagues used a structure-based computer-assisted search of two databases of commercially available compounds by employing coumarin as a template and 14 novel tautomerase inhibitors were found (Orita *et al*., 2001). The catalytic site of MIF tautomerase is located in a

hydrophobic cavity between two adjacent MIF subunits of homotrimer (Lubetsky *et al*., 1999). This catalytic pocket of MIF tautomerase consists of Pro1, Met2, Ile64, Tyr95, Val106, and Phe113. Moreover, at a rim of the catalytic pocket, there is a hydrophobic surface, which consists of Pro33, Tyr36, Trp108, and Phe113 (Sugimoto *et al*., 1999). Due to the hydrophobic surface at the rim of MIF tautomerase active site, molecular modelling studies indicated that several potential MIF tautomerase inhibitors, which have aromatic rings, can interact with the hydrophobic surface (Orita *et al*., 2001). In addition, based on X-ray crystallographic studies of a potential MIF tautomerase inhibitory binding to trimeric MIF, the compound forms aromatic/hydrophobic interactions with the side-chain of Tyr-36, Ile-64 and Phe-113 (McLean *et al*., 2009). Interestingly, [6]-gingerol consists of an aromatic ring and it is considered as a hydrophobic phenolic compound due to the aromatic ring and methoxy group (Saptarini *et al*., 2013). Therefore, a potential binding site of [6]-gingerol in MIF could be either at the catalytic pocket or the hydrophobic surface at the rim of the active site via hydrophobic interaction.

4.1 Analysis of [6]-gingerol induced protein complexes by BN-PAGE

The first question was whether [6]-gingerol induced MIF-protein complexes that would form large complexes, which could be visualised when dotted onto a membrane. However, no spot-like signals indicating large MIF-containing complexes appeared on the membrane (Figure 3.1). Despite the fact that no complexes were detected via dot blot analysis, the presence of MIF in HeLa cytosol could be clearly confirmed. Furthermore, [6]-gingerol did not affect the stability and modification of MIF, tubulin and actin when analysed by SDS-PAGE (Figure 3.2). However, under the identical gel concentration, the BN-PAGE showed some differences (Figure 3.3).

The present study shows HeLa cytosol and cell lysate resolved by BN-PAGE after incubation with and without [6]-gingerol. The functionality of BN-PAGE to resolve both HeLa cell lysate and cytosol was found to be reliable. Since BN-PAGE has the ability to separate protein mixtures under native conditions, the results from BN-PAGE (Figure 3.3 and 3.4) exhibited various sizes of microtubules as broad diffused bands. Microtubules are composed of heterodimeric tubulin subunits of α- and β-tubulin, which have a molecular weight of 55 kDa each. These heterodimers form long polymers called protofilaments and thirteen of them associate laterally into a microtubule (Lodish *et al*., 2000). Microtubules radiate from the microtubule-organising centre called centrosome providing a basic organisation of cytoplasm including the localisation of organelles. Tubulin signals from western blot analysis showed differences in the intensities at monomer position of tubulin (Figure 3.3). From a control experiment, it was clear that the reaction buffer was the cause for the reduction of the tubulin signals (Figure 3.4). For instance, one reason could be the high NaCl content in the buffer, which was 150 mM. Since NaCl in samples is recommended to be kept lower than 50 mM, the high concentration of salt, as in this case, might lead to extreme stacking of proteins causing protein aggregation (Wittig *et al*., 2006; Schägger, 2001). Actin is the most abundant intracellular protein in eukaryotic cells. It is highly conserved and participates in more protein-protein interactions than any other known proteins (Dominguez and Holmes, 2011). In general, actin exists as a globular monomer named G-actin and as a linear chain of G-actin subunits forming a filamenteous polymer called F-actin. Unexpectedly, the samples analysed by BN-PAGE and detected by anti-actin IgG demonstrated actin only in monomer state, but no actin polymers were observed (Figure 3.3 and 3.4). The concentration of ε-aminocaproic acid is most likely the reason for this observation. The stability of F-actin under BN-PAGE conditions is affected considerably by the concentration of ε-aminocaproic acid in the samples. A concentration of ε-aminocaproic acid of 200 mM

leads to the complete dissociation of F-actin (Nováková *et al*., 2006). Since the concentration of ε-aminocaproic acid in the samples was 500 mM, F-actin was probably dissociated into G-actin during sample preparation.

Immunodetection of MIF after separation by BN-PAGE demonstrated that, under native conditions, MIF exists as relatively large complexes of ~272 kDa and 37.5 kDa, respectively (Figure 3.3 and 3.4). Apparently, this indicates the interaction of MIF with other unknown proteins in HeLa cytosol. Interestingly, under native conditions, no monomeric and dimeric states of MIF were detected (Figure 3.3, 3.4 and 3.5), although it was reported that MIF forms a mixture of monomers, dimers and trimers in solutions of native recombinant human or mouse MIF, with the monomer and the dimer representing the predominant species (Mischke, *et al*. 1998). Probably, MIF in HeLa cytosol exists predominantly in the trimeric state (Reidy *et al*., 2013). The BN-PAGE system is not likely to cause an artefact since BN-PAGE was able to resolve MIF monomers under reducing and non-reducing conditions (Figure 3.5). Under native conditions, MIF exhibited a broad band without the presence of monomer and dimer as compared to reducing and non-reducing conditions, in which only monomeric MIF was detected. It indicates that MIF forms non-covalent complexes at a molecular weight of ~272 kDa as well as trimeric MIF (Mischke *et al*., 1998). It has to be mentioned that the error of estimation of protein mass for BN-PAGE is commonly in the range of 10-20% (Wittig *et al*., 2006; Schägger *et al*., 1994). Thus, it could be a possible explanation why MIF monomer migrated inaccurately. Additionally, the acrylamide concentration has remarkable effects on the electromobility of proteins in BN-PAGE suggesting that proteins in the samples migrated slightly different as compared to the marker. Therefore, it is also recommended to optimise the concentration of the gel before conducting an experiment (Wittig *et al*., 2010).

Proteins resolved by BN-PAGE are commonly electrotransferred onto PVDF membranes owing to the interference of CBB G-250 during transfer to nitrocellulose membrane, which, in addition, cannot be destained since it is an organic solvent sensitive membrane (Schägger, 2001). However, several research groups successfully employed nitrocellulose membranes as solid support for blotting proteins resolved by BN-PAGE (Van Coster *et al*., 2001; Upadhaya *et al*., 2012; Willmund and Schroda, 2005). Therefore, in this study, nitrocellulose membrane was also used. The results from nitrocellulose membranes probed for MIF, tubulin and actin are not shown owing to unsatisfying transfer efficiency and low intensity of chemiluminescent signals. For MIF, only the large complexes of MIF formed with unknown proteins (~272 kDa) were detected immunologically, whereas trimeric MIF did not become visible using the same exposition times as for PVDF under the same conditions. Increasing the exposition time for detecting MIF on nitrocellulose membranes led to high background, which hampered interpretation. For actin, the chemiluminescent signal was completely invisible on nitrocellulose membrane with exposition times of 1 second to 10 minutes. Faint bands of actin were discovered only when chemiluminescence films were exposed to the membrane for several hours. In contrast, PVDF membranes demonstrated a better transfer efficiency and stronger chemiluminescent signals. Furthermore, it is convenient for partial or complete destaining with destaining solution containing methanol. According to these findings, PVDF is clearly recommended when performing BN-PAGE followed by immunodetection on membranes, in good agreement with Wittig *et al.* (2006).

Prior to transfer of proteins resolved by BN-PAGE to membranes, it has been reported that incubating the gel with a dissociating reagent can improve immunodetection. It was suggested that epitopes recognised

by antibodies might be hidden in the complexes and the high concentration of CBB G-250 bound to proteins or membranes might provoke non-specific signals or interfere with binding of antibodies to antigens (Nijtmans *et al*., 2002; Upadhaya *et al*., 2012). In the present study, the BN-gel was either equilibrated with tris-glycine electrophoresis buffer containing 0.1% SDS for 10 minutes at 65^{o}C and then transferred electrophoretically onto membranes (PVDF or nitrocellulose) or directly transferred onto the membranes after the run. The excess of CBB G-250 in the BN-gel was partly reduced by incubating with tris-glycine electrophoresis buffer. From the membranes, it was clear that the amount of CBB G-250 dye adsorbed to the membranes was lower when the gel was pre-incubated. However, from the immunodetection result (data not shown), there was no significant difference between the membranes, when resolved proteins were transferred from pre-incubated or non-incubated gels.

[6]-gingerol affects HeLa cells leading to entering the apoptosis pathway and altering the morphology (Chakraborty *et al*., 2012). This was confirmed in the present study where [6]-gingerol reduced the total number of cells as well as altered the morphology of HeLa cells (Figure 3.6). However, the *in vivo* approach using lysate from total cells instead of cytosol for analysing [6]-gingerol induced MIF complexes showed no indication of MIF complex induction (Figure 3.7). Unexpectedly, MIF in cell lysate formed larger complexes than MIF in cytosol. There are two possible explanations for different MIF complexes in cytosol and cell lysate: 1) The NaCl content in cell lysate buffer, which was 150 mM, led to extreme stacking of proteins causing the aggregation of proteins (Wittig *et al*., 2006) or 2) MIF in cell lysate participated in larger protein complexes since various compartments of cells (e.g. organelles, cell membrane and cell debris) were present in the cell lysate, whereas these compartments were completely separated during the preparation of HeLa cytosol.

Neff and Dencher reported in 1999 that the concentration of CBB G-250 in the cathode buffer of BN-PAGE is involved in the dissociation of labile subunits and complexes. Detergent solubilised CF_0F_1-ATP synthase from spinach remained intact when cathode buffer containing 0.002% CBB G-250 was employed. In contrast, using cathode buffer containing 0.02% CBB G-250 led to dissociation of CF_0F_1-ATP synthase into CF_0 and CF_1 subunits (Neff and Dencher, 1999). According to the assumption that MIF complexes might be dissociated during traditional BN-PAGE, analysis of [6]-gingerol induced MIF complexes by BN-PAGE was carried out with low dye cathode buffer. Obviously, by using the low-dye cathode buffer, MIF complexes reached their pore size limitations in the low concentration acrylamide region of the separation gel indicating MIF being part of relatively large complexes (i.e. higher than 720 kDa) (Figure 3.9). Interestingly, MIF in cytosol formed larger complexes than MIF in cell lysate. MIF complexes in cytosol reached the pore size limitations shortly after the samples had entered the gel. In contrast, MIF complexes in cell lysate were smaller suggesting that the presence of nonionic detergent (NP-40) in the samples might cause some dissociation of proteins (Wittig and Schägger, 2005; Neff and Dencher, 1999). Furthermore, the addition of CBB G-250 caused slight differences in migration as compared to the samples without addition of CBB G-250. Clearly, the minor variations of the cathode buffer and the amount of CBB G-250 have considerable effects on the principle of separation and resolution (Wittig *et al*., 2010; Neff and Dencher, 1999). Nevertheless, [6]-gingerol induced MIF complexes could not be found by BN-PAGE.

CN-PAGE is a gel-based system that works under identical conditions as BN-PAGE. One difference that alters the separation principle of the system as compared to BN-PAGE is omitting of CBB G-250 in the cathode buffer and during sample preparation. Therefore, the separation principle relies solely on intrinsic

charge and size of proteins (Schägger *et al*., 1994). Determination of molecular masses and oligomeric states of proteins and complexes depends predominantly on the p*I* value of the protein or complex of interest, which must equal or less than 5.4 (Wittig and Schägger, 2005). In addition, the resolution of CN-PAGE is considerably lower as compared to BN-PAGE (Schägger *et al*., 1994; Wittig *et al*., 2007). However, CN-PAGE offers various advantages over BN-PAGE as there is no interference of CBB G-250, therefore working under milder conditions and preserving physiological oligomer states (Wittig *et al*., 2007). The presence of CBB G-250 and a neutral detergent, as used in BN-PAGE, can mimic some properties of an anionic detergent causing dissociation of proteins (Wittig and Schägger, 2005). The result of the analysis of [6]-gingerol induced MIF complexes by CN-PAGE is not shown here since no MIF was immunologically detected. Proteins that were resolved by CN-PAGE could be visualised by CBB G-250 indicating that CN-PAGE was working properly. According to the UniProtKB/Swiss-Prot database (P14174), the theoretical p*I* value of MIF is 7.73. p*I* values of MIF described in the literature are 8.0, 7.7 (Rosengren *et al*., 1997), 7.8 and 6.98 (Magi *et al*., 1998), depending on the origin of MIF. p*I* values from both the databases and the literature suggest a major disadvantage of CN-PAGE resulting in undetectable MIF signal on the membrane. From this, it can also be concluded that [6]-gingerol did not drastically alter the p*I* value of MIF to less than or equal to 5.4. Moreover, if [6]-gingerol truely induces the complex formation of MIF with other unknown proteins, the complex definitely has a p*I* value greater than 5.4.

4.2 Co-immunoprecipitation of MIF

Co-immunoprecipitation (Co-IP) is one of the most common methods for analysing protein-protein interactions. Co-IP is a highly specific technique, relatively simple and compatible with most methods of downstream analysis (Miernyk and Thelen, 2008). In this study, Co-IP was performed by applying both traditional Co-IP (protein A-conjugated agarose gel) and Co-IP using protein A/G-conjugated magnetic beads. By combining chemical crosslinking techniques with Co-IP, heavy and light chains of antibody can be potentially excluded from the samples that are creating problems in immunodetection. MIF specific antibody was first crosslinked via covalent linkage by DSS with protein A/G-conjugated magnetic beads. Generally, the target protein within the protein complexes interacts with the specific antibody. The complex is then eluted by elution buffer and antibody-conjugated beads are separated from the eluate by magnetic force. However, in the current study, MIF could not be precipitated by the polyclonal rabbit anti-MIF IgG-crosslinked protein A/G magnetic beads (Figure 3.10) although the manufacturer's instructions were accurately followed. Furthermore, the supplier of the antibody claims that the product can be used for immunoprecipitation. MIF was observed in the supernatants (unbound proteins) by SDS-PAGE followed by immunodetection with anti-MIF IgG. This result was thought to be because of washing being too stringent. Therefore, nonionic detergent in washing buffer was 100-fold reduced (0.01% NP-40 instead of 1%). Still, no presence of MIF in the eluates was detected (data not shown). Another try without the elution step was performed as MIF might bind too strong to the antibody and the elution buffer would not elute MIF. The beads were, after forming antibody-protein complexes, directly boiled in Laemmli sample buffer containing 2-mercaptoethanol. By immunodetection of MIF (data not shown), several protein bands were observed, however also in controls, suggesting the presence of degraded antibody, released protein A/G or some encapsulated coat of the magnatic beads. Still, there was no presence of MIF in the precipitate. It indicated that using antibody crosslinked to protein A/G-conjugated magnetic beads was not preferable in this case. For instance, crosslinking of antibody to protein A/G may result in a reduction of the ability of the antibody to bind its antigen due to blocking of

the antibodies binding site by the crosslinker and conformational changes of the antibody (Huang and Kim, 2013).

For the conventional Co-IP, protein A was applied as a solid support for non-covalently immobilising the antibody. Samples containing MIF were first incubated with polyclonal rabbit anti-MIF IgG forming protein-antibody complexes. The immunocomplexes were then captured by protein A beads and separated by heating in Laemmli sample buffer containing 2-mercaptoethanol. In order to avoid background because of the presence of heavy and light chains from the rabbit antibody used for capturing, HRP-conjugated protein A was employed instead of HRP-conjugated secondary antibody against rabbit IgG. The advantage of HRP-conjugated protein A is that it binds primarily to the Fc region of antibodies providing less background signals from antibody heavy and light chains (Lal *et al*., 2005). Nevertheless, the result (data not shown) demonstrated no precipitation of MIF although the concentration of nonionic detergent (NP-40) was relatively low (0.1% during IP, 0.02% and without during washing). Unfortunately, difficulties in obtaining antibodies of high specificity and avidity are major drawbacks of Co-IP (Miernyk and Thelen, 2008). Thus, this suggests that the polyclonal rabbit anti-MIF IgG (see appendix) is not able to precipitate MIF from cytosol and cell lysate of HeLa cells under the conditions of this study.

4.3 Crosslinking of protein complexes

Due to the fact that external manipulations (e.g. sample preparation, cell lysis) of protein mixtures or intact cells are often leading to dissociation of physiologically relevant protein-protein interactions, stabilisation by chemical crosslinkers is one of the most promising approaches for revealing information of protein-protein interactions. A combination of chemical crosslinking of reactive groups in protein-protein interactions in native protein complexes with conventional (SDS-PAGE and immunodetection) or alternative downstream analysis (BN-PAGE and immunodetection) might address the aim of this study. Chemical crosslinking reaction aims at stabilising two or more proteins that reside in close proximity, depending on the spacer arm length of the crosslinker, by covalent bonds. However, this is not the only possible product of the crosslinking reaction. The possible reaction products have been classified into 4 types. (1) Derivative: only one end of the bifunctional crosslinker reacts with a crosslinkable amino acid residue, whereas the other end does not form a covalent bond with another crosslinkable residue due to insufficient proximity between those residues; (2) intra-type: crosslinks that are formed between two residues, which reside in a single polypeptide chain; (3) inter-type: crosslinks that are formed between two different peptides, which originate in the same protein; (4) trans-type: crosslinks that are covalently crosslinked between two peptides derived from two different proteins (Sutherland *et al*., 2008). The spacer arm length of crosslinkers plays an important role for the crosslinking efficiency of reactive amino acids between proteins in a complex, which undoubtly vary in proximity. Furthermore, it determines several essential properties of the crosslinker including its hydrophobicity, solubility as well as maximum distance between crosslinked residues. The longer a spacer arm is, the more likely is that two reactive groups are within the distance range of the crosslinker. However, determining theoretically the spatial distance between crosslinked residues is usually not possible (Leitner *et al*., 2010).

Disuccinimidyl suberate (DSS), a common cell permeable succinimide-type crosslinker, consists of two identical reactive sites connected through a 11.4 Å six-carbon spacer arm. The crosslinking reaction of

DSS is achieved via N-hydroxysuccinimide ester (NHS ester) that resides in both ends of DSS. NHS ester target primarily the primary amino group of lysine and N-terminus of each polypeptide with relatively high reaction specificity (Leitner *et al*., 2010). *In vivo* and *in vitro* crosslinking approaches to stabilise [6]-gingerol induced MIF complexes by DSS were conducted, however the results (Figure 3.12 and 3.14) indicated no [6]-gingerol-dependent protein complexes. DSS treated samples either with or without [6]-gingerol exhibited a minor molecular weight shift at ~36 kDa (Figure 3.12B and 3.14B). It is not clear whether these bands were trimeric MIF crosslinked by DSS or unspecific background from immunodetection. However, it is more likely that these bands were just background since Mischke and colleagues reported that crosslinking of recombinant MIF monomer by DSS was unsuccessful due to the fact that the spacer arm length is shorter than the inter-amino side chain distances of lysine and arginine residues of monomeric, dimeric and trimeric MIF (Mischke *et al*., 1998). DSS did not exert a crosslinking reaction on potential MIF complexes induced by [6]-gingerol. Despite the fact that no significant effect from [6]-gingerol was detected, the result from DSS crosslinking combined with BN-PAGE showed MIF complexes in a ladder pattern (Figure 3.15), which did not appear in the SDS-PAGE (Figure 3.14). Thus, it suggests that DSS treatment induces MIF-containing protein complexes to dissociate into smaller MIF-containing complexes where MIF binds non-covalently to unknown proteins since BN-PAGE has the ability to preserve proteins and complexes in their native states.

Another chemical crosslinker that was employed in this study was glutaraldehyde, a pungent colourless oily liquid of linear 5-carbon dialdehyde. It is used for several applications such as histochemistry, microscopy, cytochemistry, chemical stabilisation and biomedical and pharmaceutical sciences (Migneault *et al*., 2004). It is commercially available as an acidic aqueous solution with monomeric, dimeric and polymeric species at pH 3.0-4.0. The chemical crosslinking reaction of glutaraldehyde generates thermally and chemically stable crosslinking of proteins, however the target amino acid residues that react with glutaraldehyde have not been clearly understood. Glutaraldehyde has been proposed to react readily with α-amino groups of amino acids, the N-terminal amino groups of some peptides, the sulfhydryl group of cysteine, the phenolic side chain of tyrosine and the imidazole rings of histidine derivatives (Habeeb and Hiramoto, 1968), because the most reactive amino acid side chains are nucleophiles (Migneault *et al*., 2004). Therefore, glutaraldehyde was a crosslinker that could potentially stabilise MIF complexes induced by [6]-gingerol. HeLa cell lysate and cell cytosol treated by [6]-gingerol were incubated with 1% glutaraldehyde for one hour at RT according to Mischke et al. (1988) and SDS-PAGE was performed. Immunodetection of MIF (data not shown) indicated no [6]-gingerol-dependent protein complex formation and only a minor shift due to glutaraldehyde treatment was observed. The glutaraldehyde treated samples exhibited clearly less MIF signal intensity from immunodetection in comparison to the samples without glutaraldehyde treatment suggesting protein losses during the crosslinking reaction or less antibody binding due to the crosslinking. The formation of large aggregates was observed when performing protein crosslinking with glutaraldehyde. Those aggregates became visible on the top of SDS- and BN-gels. This was due to the high degree of crosslinking forming heavily crosslinked and therefore poorly soluble products as well as protein losses (Leitner *et al*., 2010). This was further supported by glutaraldehyde crosslinking followed by low-dye BN-PAGE (data not shown). During BN-PAGE, proteins are generally stained and migrate to the anode by the excess of CBB G-250 in the cathode buffer, however, glutaraldehyde crosslinked samples resolved by low-dye BN-PAGE showed almost no protein staining by CBB G-250 as compared to samples without glutaraldehyde treatment. Moreover, glutaraldehyde treatment for one hour led to dissociation of MIF

complexes into monomer and trimer, suggesting an effect of the high acidity of the commercial glutaraldehyde. Because glutaraldehyde is a highly effective protein crosslinker, which reacts rapidly with amine groups (Migneault *et al*., 2004), it is recommended to perform protein crosslinking by unspecific crosslinkers for a short reaction time and at low concentrations to avoid over-crosslinked products. Furthermore, by doing so, it allows stabilisation of transient interactions and minimises the formation of unspecific crosslinked proteins (Leitner *et al*., 2010; Klockenbusch and Kast, 2010; Silva *et al*., 2004).

Due to protein losses during crosslinking by glutaraldehyde, an optimisation of this approach was conducted by decreasing the reaction time to 10 minutes and the concentration to 0.1%. Upon decreasing both important factors (Silva *et al*., 2004), the protein losses during crosslinking decreased significantly since most of crosslinked proteins could now enter the gel and were stained by CBB R-250 (Figure 3.16). MIF and MIF complexes could be observed by immunodetection indicating the functionality of chemical crosslinking by glutaraldehyde. Comparing protein crosslinking by DSS and glutaraldehyde *in vitro*, crosslinking by glutaraldehyde showed a higher crosslinking degree and a larger variety of MIF complexes (Figure 3.14 and 3.16). An explanation might be that the commercial aqueous glutaraldehyde solution contains monomeric, dimeric and polymeric species, which have varying spacer arm lengths. Thus, they could react readily to reactive amino acid residues in varying proximity leading to unspecific crosslinking and a larger degree of complex formation (Migneault *et al*., 2004).

An additional approach to stabilise potential MIF complexes induced by [6]-gingerol was by applying formaldehyde. Chemical crosslinking by formaldehyde, a cell permeable crosslinker with a broad specificity, has been commonly used in crosslinking proteins and proteins to nucleic acids in cells, tissue, and in some instance, even for entire organisms (Sutherland *et al*., 2008; Zybailov *et al*., 2013). It is a very small bifunctional crosslinker consisting of four atoms with a relatively short spacer arm (in the range of 2.3-2.7 Å), thus it is considered as a zero-length crosslinker. One can presume that formaldehyde allows to covalently crosslink amino acid residues of two or more associated proteins in very close proximity minimising non-specific protein interactions (Sutherland *et al*., 2008). For crosslinking reaction, it has been proposed that, first, one of the functional groups links covalently with an amino acid residue forming a methylol adduct, which will then quickly dehydrate to a Schiff base. In a second step, this modified group reacts with a second amino acid, a methylene bridge, resulting in the formation of a crosslinked peptide (Klockenbusch *et al*., 2012). The reaction is reversible at elevated temperature and proceeds very quickly allowing efficient crosslinking reactions between proteins. The first-step reaction occurs primarily in crosslinking lysine and tryptophan side chains as well as secondary and primary amino groups. Moreover, the position of potentially reactive amino acid residues within the primary peptide sequence will be likely to influence the crosslinking efficiency (Sutherland *et al*., 2008). Potential MIF complexes induced by [6]-gingerol appeared to be successfully stabilised by PFA, showing a molecular weight of ~70 kDa (Figure 3.17). Moreover, the formation of tubulin complexes was detected, supporting a crosslinking reaction by PFA. Unfortunately, the result was irreproducible (data not shown) even though the crosslinking reaction itself was successful since formation of tubulin complexes was again detected. In this regard, it has been suggested that crosslinking products might often be false-positive when unspecific crosslinkers are employed (Leitner *et al*., 2010). One explanation could be that MIF and reactive amino acid residues of unknown proteins reside by chance in close proximity leading to the stabilisation of an unspecific complex (Zybailov *et al*., 2013). Alternatively, the signal resembling MIF complex could be background signal from immunodetection.

4.4 Future directions

Several analytical approaches to study protein-protein interactions were applied in this study to detect binding partner(s) of MIF induced by [6]-gingerol. Unfortunately, none of these approaches could confirm [6]-gingerol-dependent complex formation. From the author's opinion, further investigations to confirm the interaction between MIF and [6]-gingerol should be conducted before performing other analyses of MIF complex formation induced by [6]-gingerol, since analyses of protein-protein interactions are laborious and time consuming. According to the author's strategy, quenching of intrinsic fluorescence of recombinant MIF with increasing [6]-gingerol concentrations should be performed. The concept is that if MIF binds to [6]-gingerol in forming complexes, the intrinsic fluorescence intensity of MIF is reduced when [6]-gingerol molecules are situated at tryptophan or tyrosine residues (Saha *et al*., 2013), which govern ~5% of MIF amino acid sequence (UniProtKB/Swiss-Prot database (P14174)). Due to the requirements of sucessful BN-PAGE and CN-PAGE, where the separation principle is based on p*I* values, it is suggested to confirm the isoelectric focussing point of MIF from HeLa cytosol before and after [6]-gingerol treatment. The outcome would address the question whether [6]-gingerol treatment induces a change in MIF conformation or formation of complexes leading to alterations of p*I*. Furthermore, it could provide more information of MIF compatibility with BN- and other native-PAGE approaches of separation. Finally, MIF possesses a keto-enol tautomerase activity and it has been reported that MIF tautomerase activity was inhibited by several plant-derived compounds (Molnar and Garai, 2005; Healy *et al*., 2011; Xu *et al*., 2013). Therefore, [6]-gingerol might affect MIF tautomerase activity, which can be simply measured by spectrophotometric assays.

5. Summary

Ginger, the rhizome of *Zingiber officinale*, shows various pharmacological properties, which mostly rely on phenolic compounds in ginger oleoresin. [6]-gingerol is the major pungent bioactive phenolic compound that exerts pharmacological effects of ginger such as anti-inflammation, anti-oxidation and anti-cancer. The anti-cancer activities of [6]-gingerol have been studied intensively, however the exact molecular mechanisms are not well understood. From a previous study based on an affinity purification approach using [6]-gingerol-conjugated matrix, macrophage migration inhibitory factor (MIF) along with potential binding partners, tubulin and actin, were isolated from HeLa cytosol. MIF, an ubiquitous pluripotent cytokine, possesses physiological and pathogenic properties, which relate to carcinogenesis. Based on this finding, the aim of this study was to analyse [6]-gingerol induced protein complex formation of MIF with other cellular binding partners that might participate in the activities of MIF and/or [6]-gingerol. Analyses were performed *in vitro* and *in vivo* by a number of analytical methods for protein-protein interactions and protein complexes such as blue native (BN)-PAGE, clear native (CN)-PAGE and co-immunoprecipitation (Co-IP) using anti-MIF IgG. Potential protein-protein interactions were stabilised by chemical crosslinkers followed by PAGE analyses. The detection of proteins was carried out by immunodetection with specific antibodies as well as silver and coomassie staining. HeLa cells were found to be highly affected by [6]-gingerol incubation leading to inhibition of proliferation. For analysing potential MIF-containing protein complexes induced by [6]-gingerol, BN-PAGE and CN-PAGE were performed with HeLa cytosol or cell extracts followed by immunoblotting of MIF, tubulin and actin. Both analytical systems were shown to successfully resolve protein complexes, also large complexes containing MIF. However, no indication of [6]-gingerol induced MIF-protein complex formation was found. Moreover, [6]-gingerol did not show any effect on tubulin and actin and there was no sign of [6]-gingerol-dependent interaction of those three proteins. The results from Co-IP experiments demonstrated no presence of MIF after proteins from cytosol and lysate were precipitated using anti-MIF-conjugated protein A/G-magnetic beads or protein A-agarose beads. Obviously, the commercial available anti-MIF IgG was unable to precipitate the target protein. The chemical crosslinking of potential protein complexes induced by [6]-gingerol were conducted with disuccinimidyl suberate (DSS), glutaraldehyde and paraformaldehyde. The results demonstrated efficient crosslinking as several protein complexes were observed. Crosslinking by glutaraldehyde was found to show the highest degree of protein crosslinking. However, protein complex formation induced specifically by [6]-gingerol was not detected and there was no indication of a physical connection of MIF to tubulin and actin. In conclusion, by employing several technical approaches for analysing protein complexes, MIF complexes induced by [6]-gingerol could not be detected. Further investigations should focus on direct and indirect interactions between [6]-gingerol and MIF.

6. References

Alourfi, Z., Ray, D. W. and Donn, R. 2006. Section 14: Macrophage Migration Inhibitory Factor (MIF). In: K. Vandenbroeck, ed. *Cytokine Gene Polymorphisms in Multifactorial Conditions.* Boca Raton: CRC Press, pp. 191-205.

Al-Tahtawy, R. H. M., El-Bastawesy, A. M., Monem, M. G. A., Zekry, Z. K., Al-Mehdar, H. A. and El-Merzabani, M. M. 2011. Antioxidant activity of the volatile oils of *Zingiber officinale* (ginger). *Spatula DD.,* 1(1), pp. 1-8.

Avramease, S. 1969. Coupling of enzymes to proteins with glutaraldehyde. Use of the conjugates for the detection of antigens and antibodies. *Immunochemistry,* 6(1), pp. 43-52.

Bailey-Shaw, Y., Williams, L. A., Junor, G. A., Green, C. E., Hibbert, S. L., Salmon, C. N. and Smith, A. M. 2008. Changes in the Contents of Oleoresin and Pungent Bioactive Principles of Jamaican Ginger (*Zingiber officinale* Roscoe.) during Maturation. *J. Agric. Food Chem.,* 56(14), pp. 5564–5571.

Berger, A. 1999. What are leukotrienes and how do they work in asthma?. *BMJ,* 319(90), pp. 1.

Bériault, R., Chénier, D., Singh, R., Middaugh, J., Mailloux, R. and Appanna, V. 2005. Detection and purification of glucose 6-phosphate dehydrogenase, malic enzyme, and NADP-dependent isocitrate dehydrogenase by blue native polyacrylamide gel electrophoresis. *Electrophoresis,* 26(15), pp. 2892-2897.

Biswas, B. B., Sen, K., Ghosh Choudhury, G. and Bhattacharyya, B. 1984. Molecular biology of tubulin: Its interaction with drugs and genomic organization. *J. Biosci.,* 6(4), pp. 431-457.

Bode, A. M. and Dong, Z. 2011. The Amazing and Mighty Ginger. In: I. Benzie and S. Wachtel-Galor, eds. *Herbal Medicine: Biomolecular and Clinical Aspects.* 2nd ed. Boca Raton: CRC Press, pp. 131-156.

Booz, M. L. 2007. Electrophoresis. In: A. S. Gerstein, ed. *Molecular Biology Problem Solver: A Laboratory Guide*. New York: John Wiley & Sons, pp. 331-372.

Bortner, C. D., Oldenburg, N. B. and Cidlowski, J. A. 1995. The role of DNA fragmentation in apoptosis. *Trends Cell Biol.,* 5(1), pp. 21–26.

Bradford, M. M. 1976. A Rapid and Sensitive Method for the Quantitation of Microgram Quantities of Protein Utilizing the Principle of Protein-Dye Binding. *Anal. Biochem.,* 72, pp. 248-254.

Bucala, R. and Donnelly, S. C. 2007. Macrophage Migration Inhibitory Factor: A Probable Link between Inflammation and Cancer. *Immunity.,* 26(3), pp. 281-285.

Chakraborty, D., Bishayee, K., Ghosh, S., Biswas, R., Mandal, S. K. and Khuda-Bukhsh, A. R. 2012. [6]-Gingerol induces caspase 3 dependent apoptosis and autophagy in cancer cells: Drug–DNA interaction and expression of certain signal genes in HeLa cells. *Eur. J. Pharmacol.,* 694(1-3), pp. 20-29.

Chakraborty, D., Mukherjee, A., Sikdar, S., Paul, A., Ghosh, S. and Khuda-Bukhsh, A. R. 2012. [6]-Gingerol isolated from ginger attenuates sodium arsenite induced oxidative stress and plays a corrective role in improving insulin signaling in mice. *Toxicol. Lett.*, 210(1), pp. 34-43.

Chen, X., Wang, S., Wu, N. and Yang, C. 2004. Leukotriene A4 Hydrolase as a Target for Cancer Prevention and Therapy. *Curr. Cancer Drug Targets*, 4(3), pp. 267-283.

Cheng, X. L., Liu, Q., Peng, Y. B. and Qi, L. W. 2011. Steamed ginger (*Zingiber officinale*): Changed chemical profile and increased anticancer potential. *Food Chem.*, 129(4), pp. 1785–1792.

Chevallet, M., Luche, S. and Rabilloud, T. 2006. Silver staining of proteins in polyacrylamide gels. *Nat Protoc.*, 1(4), pp. 1852–1858.

Chrubasik, S., Pittler, M. and Roufogalis, B. 2005. *Zingiberis rhizoma*: A comprehensive review on the ginger effect and efficacy profiles. *Phytomedicine*, 12(9), pp. 684-701.

Compton, S. J. and Jones, C. G. 1985. Mechanism of dye response and interference in the Bradford protein assay. *Anal. Biochem.*, 151(2), pp. 369–374.

Dios. A., Mitchell, R. A., Aljabari, B., Lubetsky, J., O'Connor, K., Liao, H., Senter, P. D., Manogue, K. R., Lolis, E., Metz, C., Bucala, R., Callaway, D. J. and Al-Abed, Y. 2002. Inhibition of MIF bioactivity by rational design of pharmacological inhibitors of MIF tautomerase activity. *J. Med. Chem.*, 45(12), pp. 2410-2416.

Dominguez, R. and Holmes, K. C. 2011. Actin structure and function. *Annu. Rev. Biophys.*, 40, pp. 169-186.

DuBois, R. N., 2003. Leukotriene A4 Signaling, Inflammation, and Cancer. *J. Natl. Cancer Inst.*, 95(14), pp. 1028-1029.

Dugasani, S., Pichika, M. R., Nadarajah, V. D., Balijepalli, M. K., Tandra, S. and Korlakunta, J. N. 2010. Comparative antioxidant and anti-inflammatory effects of [6]-gingerol, [8]-gingerol, [10]-gingerol and [6]-shogaol. *J. Ethnopharmacol.*, 127(3), pp. 515-520.

Dunn, M. J. 2002. Detection of Proteins in Polyacrylamide Gels. In: J. M. Walker, ed. *The Protein Protocols Handbook.* 2nd ed. Totowa: Humana Press, pp. 265-271.

Ekundayo, O. 1988. Composition of Ginger (*Zingiber oflcinale* Roscoe) Volatile Oils from Nigeria. *Flavour Frag. J.*, 3(2), pp. 85-90.

Elmore, J. M. and Coaker, G. 2011. Biochemical Purification of Native Immune Protein Complexes. *Methods Mol Biol.*, 712, pp. 31-44.

Gallagher, S., Winston, S. E., Fuller, S. A. and Hurrell, J. G. 2008. Immunoblotting and Immunodetection. *Curr. Protoc. Mol. Biol.*, 83, pp. 10.8.1-10.8.28.

Gaoa, D. and Zhang, Y. 2010. Comparative antibacterial activities of crude polysaccharides and flavonoids from *Zingiber officinale* and their extraction. *Asian J. Tradit. Med.*, 5(6), pp. 235-238.

Giriraju, A. and Yunus, G. 2013. Assessment of antimicrobial potential of 10% ginger extract against *Streptococcus mutans*, *Candida albicans*, and *Enterococcus faecalis*: an in vitro study. *Indian J. Dent. Res.,* 24(4), pp. 397-400.

Gupta, S. and Ravishankar, S. 2005. A Comparison of the Antimicrobial Activity of Garlic, Ginger, Carrot, and Turmeric Pastes Against *Escherichia coli* O157:H7 in Laboratory Buffer and Ground Beef. *Foodborne Pathog. Dis.,* 2(4), pp. 330-340.

Habeeb, A. and Hiramoto, R. 1968. Reaction of proteins with glutaraldehyde. *Arch. Biochem. Biophys.,* 126(1), pp. 16-26.

Halvorsen, B. L., Holte, K., Myhrstad, M. C., Barikmo, I., Hvattum, E., Remberg, S. F., Wold, A. B., Haffner, K., Baugerød, H., Andersen, L. F., Moskaug, Ø., Jacobs, D. R. Jr and Blomhoff, R. 2002. A Systematic Screening of Total Antioxidants in Dietary Plants. *J. Nutr.,* 132(3), pp. 461-471.

Hamel, E. 2008. An Overview of Compounds That Interact with Tubulin and Their Effects on Microtubule Assembly. In: A. T. Fojo, ed. *The Role of Microtubules in Cell Biology, Neurobiology, and Oncology.* Totowa: Humana Press, pp. 1-19.

Hasan, H. A., Rasheed Raauf, A. M., Abd Razik, B. M. and Rasool Hassan, B. A. 2012. Chemical Composition and Antimicrobial Activity of the Crude Extracts Isolated from *Zingiber Officinale* by Different Solvents. *Pharmaceut. Anal. Act.,* 3(9), doi: 10.4172/2153-2435.1000184.

Healy, Z. R., Liu, H., Holtzclaw, W. D. and Talalay, P. 2011. Inactivation of Tautomerase Activity of Macrophage Migration Inhibitory Factor by Sulforaphane: a Potential Biomarker for Anti-inflammatory Intervention. *Cancer Epidemiol. Biomarkers Prev.,* 20(7), pp. 1516-1523.

Heuberger, E. H., Veenhoff, L. M., Duurkens, R. H., Friesen, R. H. and Poolman, B. 2002. Oligomeric state of membrane transport proteins analyzed with blue native electrophoresis and analytical ultracentrifugation. *J. Mol. Biol.,* 317(4), pp. 591-600.

Heukeshoven, J. and Dernick, R. 1985. Simplified method for silver staining of proteins in polyacrylamide gels and the mechanism of silver staining. *Electrophoresis,* 6(3), pp. 103-112.

Huang B. X. and Kim, H-Y. 2013. Effective Identification of Akt Interacting Proteins by Two-Step Chemical Crosslinking, Co-Immunoprecipitation and Mass Spectrometry. PLoS ONE, 8(4): e61430. doi:10.1371/journal.pone.0061430

Ippoushi, K., Azuma, K., Ito, H., Horie, H. and Higashio, H. 2003. [6]-Gingerol inhibits nitric oxide synthesis in activated J774.1 mouse macrophages and prevents peroxynitrite-induced oxidation and nitration reactions. *Life Sci.,* 73(26), pp. 3427-3437.

Ivanković, M., Cukusić, A., Gotić, I., Skrobot, N., Matijasić, M., Polancec, D. and Rubelj, I. 2007. Telomerase activity in HeLa cervical carcinoma cell line proliferation. *Biogerontology,* 8(2), pp. 163-172.

Jeena, K., Liju, V. B. and Kuttan, R. 2013. Antioxidant, Anti-inflammatory and Antinociceptive Activities of Essential Oil from Ginger. *Indian J Physiol Pharmacol.,* 57(1), pp. 51-62.

Jeong, C., Bode, A. M., Pugliese, A., Cho, Y. Y., Kim, H. G., Shim, J. H., Jeon, Y. J., Li, H., Jiang, H. and Dong, Z. 2009. [6]-Gingerol Suppresses Colon Cancer Growth by Targeting Leukotriene A4 Hydrolase. *Cancer Res.*, 69(13), pp. 5584-5591.

Johansen, K. and Svensson, L. 2002. Immunoprecipitation. In: J. M. Walker, ed. *The Protein Protocols Handbook.* Totowa: Humana Press, pp. 1097-1106.

Jolad, S. D., Lantz, R. C., Chen, G. J., Bates, R. B. and Timmermann B. N. 2005. Commercially processed dry ginger (*Zingiber officinale*): Composition and effects on LPS-stimulated PGE2 production. *Phytochem.*, 66(13), p. 1614–1635.

Kim, J. K., Kim, Y., Na, K. M., Surh, Y. J. and Kim, T. Y. 2007. [6]-Gingerol prevents UVB-induced ROS production and COX-2 expression *in vitro* and *in vivo*. *Free Radic. Res.*, 41(5), pp. 603-614.

Kiuchi, F., Iwakami, S., Shibuya, M., Hanaoka, F. and Sankawa, U. 1992. Inhibition of Prostaglandin and Leukotriene Biosynthesis by Gingerols and Diarylheptanoids. *Chem. Pharm. Bull. (Tokyo)*, 40(2), pp. 387-391.

Klockenbusch, C. and Kast, J. 2010. Optimization of Formaldehyde Cross-Linking for Protein Interaction Analysis of Non-Tagged Integrin β1. *J. Biomed. Biotechnol.*, 2010(2010), doi:10.1155/2010/927585.

Klockenbusch, C., O'Hara, J. E. and Kast, J. 2012. Advancing formaldehyde cross-linking toward quantitative proteomic applications. *Anal. Bioanal. Chem.*, 404(4), pp. 1057-1067.

Koh, E. M., Kim, H. J., Kim, S., Choi, W. H., Choi, Y. H., Ryu, S. Y., Kim, Y. S., Koh, W. S. and Park, S. Y., 2009. Modulation of Macrophage Functions by Compounds Isolated from *Zingiber officinale*. *Planta Med.*, 75(2), pp. 148-151.

Krause, F., 2006. Detection and analysis of protein-protein interactions in organellar and prokaryotic proteoms by native gel electrophoresis: (Membrane) protein complexes and supercomplexes. *Electrophoresis*, 27(13), pp. 2759-2781.

Ladig, R., Sommer, M. S., Hahn, A., Leisegang, M. S., Papasotiriou, D. G., Ibrahim, M., Elkehal, R., Karas, M., Zickermann, V., Gutensohn, M., Brandt, U., Klösgen, R. B. and Schleiff, E. 2011. A high-definition native polyacrylamide gel electrophoresis system for the analysis of membrane complexes. *Plant J.*, 67(1), pp. 181-194.

Lal, A., Haynes, S. R. and Gorospe, M. 2005. Clean western blot signals from immunoprecipitated samples. *Mol. Cell. Probes.*, 19, pp. 385-388.

Lantz, R., Chen, G. J., Sarihan, M., Sólyom, A. M., Jolad, S. D. and Timmermann, B. N. 2007. The effect of extracts from ginger rhizome on inflammatory mediator production. *Phytomedicine*, 14(2-3), pp. 123-128.

Lechner, M., Lirk, P. and Rieder, J. 2005. Inducible nitric oxide synthase (iNOS) in tumor biology: the two sides of the same coin. *Semin. Cancer Biol.*, 15(4), pp. 277-289.

Lee, H. W., Kyung, T., Yoo, J., Kim, T., Chung, C., Ryu, J. Y., Lee, H., Park, K., Lee, S., Jones, W. D., Lim, D. S., Hyeon, C., Heo, W. D. and Yoon, T. Y. 2013. Real-time single-molecule coimmunoprecipitation of weak protein-protein interactions. *Nat. Protoc.,* 8, pp. 2045–2060.

Lee, S. H., Cekanova, M. and Baek, S. J. 2008. Multiple Mechanisms Are Involved in 6-Gingerol-Induced Cell Growth Arrest and Apoptosis in Human Colorectal Cancer Cells. *Mol. Carcinog.,* 47(3), pp. 197–208.

Lee, T. Y., Lee, K. C., Chen, S. Y. and Chang, H. H. 2009. 6-Gingerol inhibits ROS and iNOS through the suppression of PKC-alpha and NF-kappaB pathways in lipopolysaccharide-stimulated mouse macrophages. *Biochem. Biophys. Res. Commun.,* 382(1), pp. 134-139.

Leitner, A., Walzthoeni, T., Kahraman, A., Herzog, F., Rinner, O., Beck, M. and Aebersold, R. 2010. Probing Native Protein Structures by Chemical Cross-linking, Mass Spectrometry, and Bioinformatics. *Mol. Cell. Proteomics,* 9(8), pp. 1634-1649.

Lin, R. J., Chen, C. Y., Chung, L. Y. and Yen, C. M. 2010. Larvicidal activities of ginger (*Zingiber officinale*) against Angiostrongylus cantonensis. *Acta Trop.,* 115(1-2), pp. 69-76.

Lodish, H., Berk, A., Matsudaira, P., Kaiser, C. A., Krieger, M., Zipursky, L. and Darnell, J. 2000. Section 19.1 Microtubule Structures. In: *Molecular Cell Biology.* New York: W. H. Freeman.

Lodish, H., Berk, A., Zipursky, S. L., Matsudaira, P., Baltimore, D. and Darnell, J. 2003. Section 5.5 Purification of Cells and Their Parts. In: *Molecular Cell Biology.* 5th ed. New York: W. H. Freeman and Company, pp. 178-184.

Lubetsky, J. B., Swope, M., Dealwis, C., Blake, P. and Lolis, E. 1999. Pro-1 of macrophage migration inhibitory factor functions as a catalytic base in the phenylpyruvate tautomerase activity. *Biochemistry,* 38(22), pp.7346-7354.

Lukas, J., Bartek, J. and Hansen, K. 2006. Chapter 31: Immunoprecipitation of Proteins under Nondenaturing Conditions. In: J. E. Celis, *et al*. eds. *Cell Biology A Laboratory Handbook.* Oxford: Academic Press, pp. 253-258.

Lv, L., Chen, H., Soroka, D., Chen, X., Leung, T. and Sang, S. 2012. 6-Gingerdiols as the Major Metabolites of 6-Gingerol in Cancer Cells and in Mice and Their Cytotoxic Effects on Human Cancer Cells. *J. Agric. Food. Chem.,* 60(45), pp. 11372–11377.

Magi, B., Bini, L., Liberatori, S., Marzocchi, B., Raggiaschi, R., Arcuri, F., Tripodi, S. A., Cintorino, M., Tosi, P. and Pallini, V. 1998. Charge heterogeneity of macrophage migration inhibitory factor (MIF) in human liver and breast tissue. *Electrophoresis,* 19(11), pp. 2010-2013.

Mahady, G. B., Pendland, S. L., Yun, G. S., Lu, Z. Z. and Stoia, A. 2003. Ginger (*Zingiber officinale* Roscoe) and the Gingerols Inhibit the Growth of Cag A+ Strains of *Helicobacter pylori*. *Anticancer Res.,* 23(5A), pp. 3699–3702.

Malhotra, S. and Singh, A. P. 2003. Medicinal properties of Ginger (*Zingiber officinale* Rosc.). *Nat. Prod. Rad.,* 2(6), pp. 296-301.

McLean, L. R., Zhang, Y., Li, H., Li, Z., Lukasczyk, U., Choi, Y. M., Han, Z., Prisco, J., Fordham, J., Tsay, J. T., Reiling, S., Vaz, R. J. and Li, Y. 2009. Discovery of covalent inhibitors for MIF tautomerase via cocrystal structures with phantom hits from virtual screening. *Bioorg. Med. Chem. Lett*., 9(23), pp. 6717-6720

Miernyk, J. A. and Thelen, J. J. 2008. Biochemical approaches for discovering protein–protein interactions. *Plant J.,* 53(4), pp. 597-609.

Migneault, I., Dartiguenave, C., Bertrand, M. J. and Waldron, K. C. 2004. Glutaraldehyde: behavior in aqueous solution, reaction with proteins, and application to enzyme crosslinking. *Biotechniques,* 37(5), pp. 790-802.

Mischke, R., Kleemann, R., Brunner, H. and Bernhagen, J. 1998. Cross-linking and mutational analysis of the oligomerization state of the cytokine macrophage migration inhibitory factor (MIF). *FEBS Lett.,* 427(1), pp. 85-90.

Mitchell, R. A. and Bucula, R. 2000. Tumor growth-promoting properties of macrophage migration inhibitory factor (MIF). *Semin. Cancer Biol.,* 10(5), pp. 359-366.

Möbus, L. 2013. *Identifizierung eines Interaktionspartners von 6-Gingerol in HeLa-Zellen mittels Affinitätschromatographie,* Hamburg: Unpublished.

Molnar, V. and Garai, J. 2005. Plant-derived anti-inflammatory compounds affect MIF tautomerase activity. *Int. Immunopharmacol.,* 5(5), pp. 849-856.

Nakazawa, T. and Ohsawa, K. 2002. Metabolism of [6]-gingerol in rats. *Life Sci.,* 70(18), pp. 2165–2175.

Naora, K., Ding, G., Hayashibara, M., Katagiri, Y., Kano, Y. and Iwamoto, K. 1992. Pharmacokinetics of [6]-gingerol after intravenous administration in rats with acute renal or hepatic failure. *Chem. Pharm. Bull. (Tokyo).,* 40(5), pp. 1295-1298.

Neff, D. and Dencher, N. A. 1999. Purification of multisubunit membrane protein complexes: isolation of chloroplast F_0F_1-ATP synthase, CF_0 and CF_1 by blue native electrophoresis. *Biochem. Biophys. Res. Commun.,* 259(3), pp. 569-75.

Nijtmans, L. G., Henderson, N. S. and Holt, I. J. 2002. Blue Native electrophoresis to study mitochondrial and other protein complexes. *Methods,* 26(4), pp. 327-334.

Nováková, Z., Man, P., Novák, P., Hozák, P. and Hodný, Z. 2006. Separation of nuclear protein complexes by blue native polyacrylamide gel electrophoresis. *Electrophoresis,* 27(7), pp. 1277-1287.

Orita, M., Yamamoto, S., Katayama, N., Aoki, M., Takayama, K., Yamagiwa, Y., Seki, N., Suzuki, H., Kurihara, H., Sakashita, H., Takeuchi, M., Fujita, S., Yamada, T. and Tanaka, A. 2001. Coumarin and chromen-4-one analogues as tautomerase inhibitors of macrophage migration inhibitory factor: discovery and X-ray crystallography. *J. Med. Chem.* 44(4), pp 540-547

Park, Y. J., Wen, J., Bang, S., Park, S. W. and Song, S. Y. 2006. [6]-Gingerol Induces Cell Cycle Arrest and Cell Death of Mutant p53-expressing Pancreatic Cancer Cells. *Yonsei Med. J.,* 47(5), pp. 688-697.

Puck, T. T., Marcus, P. I. and Cieciura, S. J. 1956. Clonal growth of mammalian cells *in vitro*; Growth characteristics of colonies from single HeLa cells with and without a "FEEDER" layer. *J. Exp. Med.*, 103(2), pp. 273-284.

Rabilloud, T. 1990. Mechanisms of protein silver staining in polyacrylamide gels: A 10-year synthesis. *Electrophoresis*, 11(10), pp. 785-794.

Rakoff-Nahoum, S. 2006. Why Cancer and Inflammation?. *Yale J Biol Med.*, 79(3-4), pp. 123-130.

Reidy, T., Rittenberg, A., Dwyer, M., D'Ortona, S., Pier, G. and Gadjeva, M. 2013. Homotrimeric MIF drives inflammatory responses in the corneal epithelium by promoting caveolin-rich platform assembly in response to infection. *J. Biol. Chem.*, 288(12), pp. 8269-8278.

Ren, L., Emery, D., Kaboord, B., Chang, E. and Qoronfleh, M. W. 2003. Improved immunomatrix methods to detect protein:protein interactions. *J. Biochem. Biophys. Methods.*, 57(2), pp. 143-157.

Renger, M. 2013. *Charakterisierung der inhibierenden Wirkung von Ingwer-Fraktionen auf HeLa-Zellen*, Hamburg: Unpublished.

Rosengren, E., Aman, P., Thelin, S., Hansson, C., Ahlfors, S., Björk, P., Jacobsson, L. and Rorsman, H. 1997. The macrophage migration inhibitory factor MIF is a phenylpyruvate tautomerase. *FEBS Lett.*, 417(1), pp. 85-88.

Rützel, K. 2012. *Analyse der inhibierenden und stimulierenden Effekte von Ingwer auf das Wachstum von Säugetierzellen*, Hamburg: Unpublished.

Saha, P., Das, B. and Chaudhuri, K. 2013. Role of 6-Gingerol in Reduction of Cholera Toxin Activity *In Vitro* and *In Vivo*. *Antimicrob. Agents Chemother.*, 57(9), pp. 4373-4380.

Sambrook, J. and Russell, D. W. 2001. *Molecular Cloning: A Laboratory Manual.* 3rd ed. New York: Cold Spring Harbor Laboratory Press.

Santos, L. L. and Morand, E. F. 2009. Macrophage migration inhibitory factor: a key cytokine in RA, SLE and atherosclerosis. *Clin. Chim. Acta.*, 399(1-2), pp. 1-7.

Saptarini, N. M., Sitorus, E. Y. and Levita, J. 2013. Structure-Based in Silico Study of 6-Gingerol, 6-Ghogaol, and 6-Paradol, Active Compounds of Ginger (*Zingiber officinale*) as COX-2 Inhibitors. *Int. J. Chem.*, 5(3), pp. 12-18.

Schägger, H. 2001. Blue-Native Gels to Isolate Protein Complexes from Mitochondria. In: L. A. Pon and E. A. Schon, eds. *Method in Cell Biology: Mitochondria.* San Diego: Acedemic Press, pp. 231-244.

Schägger, H. and von Jagow, G. 1991. Blue Native Electrophoresis for Isolation of Membrane Protein Complexes in Enzymatically Active Form. *Anal. Biochem.*, 199(2), pp. 223-231.

Schägger, H., Cramer, W. A. and von Jagow, G. 1994. Analysis of Molecular Masses and Oligimeric States of Protein Complexes by Blue Native Electrophoresis and Isolation of Membrane Protein Complexes by Two-Dimensional Native Electrophoresis. *Anal. Biochem.*, 217(2), pp. 220-230.

Scherer, W. F., Syverton, J. T. and Gey, G. O. 1953. Studies on the propagation *in vitro* of poliomyelitis viruses IV. Viral multiplication in a stable strain of human malignant epithelial cells (strain HeLa) derived from an epidermoid carcinoma of the cervix. *J. Exp. Med.,* 97(5), pp. 695–710.

Shi, Q. and Jackowski, G. 1998. One-dimensional polyacrylamide gel electrophoresis. In: B. D. Hames, ed. *Gel Electrophoresis of Proteins : A Practical Approach.* New York: Oxford University Press, pp. 1-50.

Silva, C. J. S. M., Sousa, F., Gübitz, G. and Cavaco-Paulo, A. 2004. Chemical Modifications on Proteins Using Glutaraldehyde. *Food Technol. Biotechnol.,* 42(1), pp. 51-56.

Singh, R., Chénier, D., Bériault, R., Mailloux, R., Hamel, R. D. and Appanna, V. D. 2005. Blue native polyacrylamide gel electrophoresis and the monitoring of malate- and oxaloacetate-producing enzymes. *J. Biochem. Biophys. Methods,* 64(3), pp. 189-199.

Stephenson, E. 1982. Locomotory invasion of human cervical epithelium and avian fibroblasts by HeLa cells in vitro. *J. Cell Sci.,* 57, pp. 293–314.

Stoilova, I., Krastanov, A., Stoyanova, A., Denev, P. and Gargovaa, S. 2007. Antioxidant activity of a ginger extract (*Zingiber officinale*). *Food. Chem.,* 102(3), pp. 764–770.

Sugimoto, H., Taniguchi, M., Nakagawa, A., Tanaka, I., Suzuki, M. and Nishihira, J. 1999. Crystal structure of human D-dopachrome tautomerase, a homologue of macrophage migration inhibitory factor, at 1.54 Å resolution. *Biochemistry,* 38(11), pp. 3268-3279.

Sun, H. W., Bernhagen, J., Bucala, R. and Lolis, E. 1996. Crystal structure at 2.6-Å resolution of human macrophage migration inhibitory factor. *Proc. Natl. Acad. Sci. U S A.,* 93(11), pp. 5191-5196.

Surh, Y. J. 1999. Molecular mechanisms of chemopreventive effects of selected dietary and medicinal phenolic substances. *Mutat Res.,* 428(1-2), pp. 305-327.

Sutherland, B. W., Toews, J. and Kast, L. 2008. Utility of formaldehyde cross-linking and mass spectrometry in the study of protein-protein interactions. *J. Mass. Spectrom.,* 43(6), pp. 699-715.

Switzer, R. C. 3rd., Merril, C. R. and Shifrin, S. 1979. A highly sensitive silver stain for detecting proteins and peptides in polyacrylamide gels. *Anal. Biochem.,* 98(1), pp. 231-237.

Tagoe, D., Baidoo, S., Dadzie, I., Kangah, V. and Nyarko, H. 2009. A Comparison Of The Antimicrobial (Antifungal) Properties Of Garlic, Ginger And Lime On *Aspergillus Flavus*, *Aspergillus Niger* And *Cladosporium Herbarum* Using Organic And Water Base Extraction Methods. *J. Trop. Med.,* 7(1).

Thannickal, V. J. and Fanburg, B. L. 2000. Reactive oxygen species in cell signaling. *Am. J. Physiol. Lung Cell Mol. Physiol.,* 279(6), pp. L1005-1028

Tripathi, S., Bruch, D. and Kittur, D. S. 2008. Ginger extract inhibits LPS induced macrophage activation and function. *BMC Complement. Altern. Med.,* 8(1).

Tripathi, S., Maier, K. G., Bruch, D. and Kittur, D. S. 2007. Effect of 6-Gingerol on Pro-Inflammatory Cytokine Production and Costimulatory Molecule Expression in Murine Peritoneal Macrophages. *J. Surg Res.,* 138(2), pp. 209-213.

Tulp, A., Verwoerd, D. and Neefjes, J. 1999. Electromigration for separations of protein complexes. *J. Chromatogr. B Biomed. Sci. Appl.,* 722(1-2), pp. 141-151.

Upadhaya, A. R., Lungrin, I., Yamaguchi, H., Fändrich, M. and Thal, D. R. 2012. High-molecular weight Aβ oligomers and protofibrils are the predominant Aβ species in the native soluble protein fraction of the AD brain. *J. Cell Mol. Med.,* 16(2), pp. 287-295.

Van Coster, R., Smet, J., George, E., De Meirleir, L., Seneca, S., Van Hove, J., Sebire, G., Verhelst, H., De Bleecker, J., Van Vlem, B., Verloo, P. and Leroy, J. 2001. Blue Native Polyacrylamide Gel Electrophoresis: A Powerful Tool in Diagnosis of Oxidative Phosphorylation Defects. *Pediatr. Res.,* 50(5), pp. 658-665.

Walker, J. M., 2002. SDS Polyacrylamide Gel Electrophoresis of Proteins. In: J. M. Walker, ed. *The Protein Protocols Handbook.* 2nd ed. Totowa: Humana Press, pp. 61-68.

Wang, X., Baek, S. J. and Eling, T. E. 2013. The diverse roles of nonsteroidal anti-inflammatory drug activated gene (NAG-1/GDF15) in cancer. *Biochem. Pharmacol.,* 85(5), pp. 597-606.

Weiss, U. 2008. Inflammation. *Nature,* 454(7203), p. 427.

Williams, N. 2010. Prize for the HeLa cell story. *Curr. Biol.,* 20(23), pp. R1003-R1004.

Willmund, F. and Schroda, M. 2005. HEAT SHOCK PROTEIN 90C is a bona fide Hsp90 that interacts with plastidic HSP70B in Chlamydomonas reinhardtii. *Plant Physiol.,* 138(4), pp. 2310-2322.

Winkler, C., Denker, K., Wortelkamp, S. and Sickmann, A. 2007. Silver- and Coomassie-staining protocols: detection limits and compatibility with ESI MS. *Electrophoresis,* 28(12), pp. 2095-2099.

Wittig, I. and Schägger, H. 2005. Advantages and limitations of clear-native PAGE. *Proteomics,* 5(17), pp. 4338-4346.

Wittig, I., Beckhaus, T., Wumaier, Z., Karas, M. and Schägger, H. 2010. Mass Estimation of Native Proteins by Blue Native Electrophoresis. *Mol. Cell. Proteomics.,* 9(10), pp. 2149-2161.

Wittig, I., Braun, H. P. and Schägger, H. 2006. Blue native PAGE. *Nat. Protoc.,* 1(1), pp. 418-428.

Wittig, I., Karas, M. and Schägger, H. 2007. High Resolution Clear Native Electrophoresis for In-gel Functional Assays and Fluorescence Studies of Membrane Protein Complexes. *Mol. Cell Proteomics,* 6(7), pp. 1215-1225.

Wohlmuth, H., Leach, D., Smith, M. and Myers, S. 2005. Gingerol content of diploid and tetraploid clones of ginger (*Zingiber officinale* Roscoe). *J. Agric. Food. Chem.,* 53(14), pp. 5772-5778.

Xu, L., Li, Y., Sun, H., Zhen, X., Qiao, C., Tian, S. and Hou, T. 2013. Current developments of macrophage migration inhibitory factor (MIF) inhibitors. *Drug Discov. Today.,* 18(11-12), p. 592–600.

Young, H. Y., Luo, Y. L., Cheng, H. Y., Hsieh, W. C., Liao, J. C. and Peng, W. H. 2005. Analgesic and anti-inflammatory activities of [6]-gingerol. *J. Ethnopharmacol.*, 96(1-2), pp. 207-210.

Yu, Y., Zick, S., Li, X., Zou, P., Wright, B. and Sun, D. 2011. Examination of the Pharmacokinetics of Active Ingredients of Ginger in Humans. *AAPS J.*, 13(3), pp. 417-426.

Zachariah, T. 2008. Gigner. In: V. A. Parthasarathy, B. Chempakam and T. J. Zachariah, eds. *Chemistry of Spices.* London: CAB International, pp. 70-96.

Zancan, K. C., Marques, M. O., Petenate, A. J. and Meireles, M. A. A. 2002. Extraction of ginger (*Zingiber officinale* Roscoe) oleoresin with CO2 and co-solvents: a study of the antioxidant action of the extracts. *J. Supercrit. Fluids.*, 24(1), pp. 57–76.

Zybailov, B. L., Glazko, G. V., Jaiswal, M. and Raney, K. D. 2013. Large Scale Chemical Cross-linking Mass Spectrometry Perspectives. *J. Proteomics Bioinform.,* Volume S2: 001.

6.1 Internet references

American Cancer Society 2010. *Ginger.* [Online]
Available at:
http://www.cancer.org/treatment/treatmentsandsideeffects/complementaryandalternativemedicine/herbsvitaminsandminerals/ginger
[Accessed 3 March 2014].

Amersham Biosciences n.d. *Automated Silver and Coomassie Staining of Polyacrylamide Gels.* [Online]
Available at:
https://www.gelifesciences.com/gehcls_images/GELS/Related%20Content/Files/1314716762536/litdoc80634334AB_20110830181131.pdf
[Accessed 16 March 2014].

Bio-Rad Laboratories, Inc. n.d. *Clarity Western ECL Substrate Instruction Manual, Rev A.* [Online]
Available at: http://www.bio-rad.com/webroot/web/pdf/lsr/literature/10026389.pdf
[Accessed 15 March 2014].

EMD Millipore Corporation 2014. *Western Blotting Protocols - A Comprehensive List.* [Online]
Available at:
http://www.millipore.com/life_sciences/flx4/western_blotting&tab1=7&tab2=2#tab2=2:tab1=7
[Accessed 15 March 2014].

LI-COR, Inc. 2008. *Technical Note: Protein Electrotransfer Methods and the Odyssey®Infrared Imaging Systems.* [Online]
Available at: http://biosupport.licor.com/docs/bt0609_LI-COR_final_Electrotransfer_methods.pdf
[Accessed 17 March 2014].

National Institutes of Health 2013. *Ginger.* [Online]
Available at: http://www.nlm.nih.gov/medlineplus/druginfo/natural/961.html#
[Accessed 3 March 2014].

7. Appendices

7.1 List of figures

7.2 List of tables

7.3 Materials

7.3.1 Instruments

Instrument	Manufacturer
Air displacement micropipette	Gilson, Inc.
Analytical balance LE244S	Satorius AG
Autoclave	Systec GmbH
CO_2 incubator	Binder, Inc.
Digital camera	Olympus Corporation
Electric bag sealer	Severin Elektrogeräte GmbH
Electrophoresis Power Supply-EPS 601	GE Healthcare
Freezer (-20^{o}C)	Liebherr-International AG
FUSION-FX7 Advance-Multi-Imaging Instrument	Vilber Lourmat Deutschland GmbH
GE Healthcare Imagescanner III	GE Healthcare
Inverted microscope	Carl Zeiss AG
Laboratory glassware washer	Miele, Inc.
Mini Trans-Blot electrophoretic transfer cell	Bio-Rad Laboratories, Inc.
Mini-PROTEAN Tetra Cell	Bio-Rad Laboratories, Inc
MiniSpin plus with rotor F-45-12-11	Eppendorf AG
Multifuge 3SR Plus with microlitre rotor AL 24x1.5/2ml (75003332) and swing-out rotor 4 place (75006445)	Heraeus Holding GmbH
MultiTemp III Thermostatic circulator	GE Healthcare
Optima TL Ultracentrifuge, Rotor TLA 100	Beckman Coulter, Inc.
pH-Meter	WTW GmbH
Pipetting aid	BRAND GmbH + Co. KG.
Refrigerator (4^{o}C)	Liebherr-International AG
Rocking shaker	European Molecular Biology Laboratory
Rotating platform	Labortechnik Fröbel GmbH
Sterile workbench class 2	Thermo Electron Corporation
Top-Loading Balances TE1502S	Satorius AG
Trans-Blot system with plate electrodes	Bio-Rad Laboratories, Inc.
Ultra-low temperature freezer	Heraeus Holding GmbH
Ultrapure water system	Millipore Corporation
UV/Vis photometer	Eppendorf AG
Vertical electrophoresis apparatus (SE 600 RUBY)	GE Healthcare
Vertical electrophoresis apparatus and accessories	European Molecular Biology Laboratory
Water bath (37^{o}C)	Gesellschaft für Labortechnik GmbH

7.3.2 Equipments

Equipment	Manufacturer
24-well tissue culture test plates	TPP Techno Plastic Products AG
75 cm^2 Tissue culture flasks	TPP Techno Plastic Products AG
Blotting filter papers	Bio-Rad Laboratories, Inc.
Conical centrifuge tubes (15, 50 mL)	BD Biosciences
Disposable pasteur pipettes (3 mL)	Carl Roth GmbH + Co.KG
epT.I.P.S.-pipette tips (20, 200, 1000 µL)	Eppendorf AG
Gel staining trays	Carl Roth GmbH + Co.KG
High performance chemiluminescence films	GE Healthcare
Immun-Blot PVDF membrane	Bio-Rad Laboratories, Inc.
Microscope slide	Carl Roth GmbH + Co.KG
Protran nitrocellulose membranes (0.45 µm)	GE Healthcare
Reaction tubes (1 mL, 2 mL)	Eppendorf AG
Rotilabo-disposable weighing trays	Carl Roth GmbH + Co.KG
Rotilabo-syringe filters	Carl Roth GmbH + Co.KG
Serological pipettes	TPP Techno Plastic Products AG
Standard disposable cuvettes	BRAND GmbH + Co. KG.
Syringes and needles	B. Braun Melsungen AG
Thickwall polycarbonate centrifuge tube, 230 µL, (7 x 21 mm)	Beckman Coulter, Inc.
Tissue culture dishes (100 x 20 mm.)	Thermo Fisher Scientific Inc.
Tissue culture dishes (96 x 21 mm.)	TPP Techno Plastic Products AG

7.3.3 Chemicals and biochemicals

Chemical and biochemical	Manufacturer or supplier
[6]-Gingerol ≥ 98% (HPLC)	Sigma-Aldrich Co. LLC.
1 M HEPES buffer	Biochrom AG
10% (wt/v) Nonidet P-40 (NP-40)	F. Hoffmann-La Roche Ltd.
2-Mercaptoethanol ≥ 99.0%	Sigma-Aldrich Co. LLC.
7.5% Sodium bicarbonate	Biochrom AG
Acetic acid 99-100%,≥ 99%, for synthesis	Carl Roth GmbH + Co.KG
Acrylamide 2X	Serva Electrophoresis GmbH
Albumin Fraction V	Carl Roth GmbH + Co.KG
Ammonium peroxydisulphate (APS)	Carl Roth GmbH + Co.KG
Ammunium persulphate (APS)	GE Healthcare
Bromophenol blue sodium salt	Carl Roth GmbH + Co.KG
Calcium chloride dihydrate ≥ 99 %, p.a., ACS	Carl Roth GmbH + Co.KG
Carestream Kodak Processing chemicals Developer	Sigma-Aldrich Co. LLC.
Carestream Kodak Processing chemicals Fixer	Sigma-Aldrich Co. LLC.
Coomassie blue G-250	Serva Electrophoresis GmbH
Coomassie blue R-250	Serva Electrophoresis GmbH
D(+)Saccharose	Carl Roth GmbH + Co.KG
Dimethyl sulfoxide. p.a., ACS reagent, ≥99.9% (GC)	Sigma-Aldrich Co. LLC.
Dimethyl sulfoxide (DMSO)	Carl Roth GmbH + Co.KG
Disuccinimidyl suberate (DSS)	Thermo Fisher Scientific Inc.
DL-Dithiothreitol	Sigma-Aldrich Co. LLC.
Dodecylsulfate·Na-salt in Pellets research grade	Serva Electrophoresis GmbH
Dulbecco`s MEM (10x)	Biochrom AG
Ethanol denatured ≥ 98 %, with ca. 1 % MEK	Carl Roth GmbH + Co.KG
Ethylenediaminetetraacetic acid (EDTA)	Carl Roth GmbH + Co.KG
Fetal bovine serum	Sigma-Aldrich Co. LLC.
Formaldehyde solution (37%)	Carl Roth GmbH + Co.KG
Glutaraldehyde (25%)	Carl Roth GmbH + Co.KG
Glycerol ≥ 86%	Carl Roth GmbH + Co.KG
Glycine	Serva Electrophoresis GmbH
Hydrochloric acid 37%, extra pure	Carl Roth GmbH + Co.KG
Hydrochloric acid fuming, ROTIPURAN, 37%, p.a., ACS, ISO	Carl Roth GmbH + Co.KG
Imidazole	Sigma-Aldrich Co. LLC.
Imidazole	Serva Electrophoresis GmbH
L-Glutamine	Biochrom AG
Magnesium chloride hexahydrate	Carl Roth GmbH + Co.KG
Methanol ≥ 99%, for synthesis	Carl Roth GmbH + Co.KG
Methanol ROTIPURAN, ≥ 99.9%, p.a., ACS, ISO	Carl Roth GmbH + Co.KG
N,N,N',N'-Tetramethyl-ethylenediamine (TEMED)	Serva Electrophoresis GmbH
N,N´-Methylene bisacrylamide 2X	Serva Electrophoresis GmbH
Nocodazole	Sigma-Aldrich Co. LLC.
Non-essential amino acids (NEA)	Biochrom AG
Novex Sharp Pre-stained Protein Standard	Thermo Fisher Scientific Inc.
Paraformaldehyde powder 95%	Sigma-Aldrich Co. LLC.
PBS Dulbecco (without Ca^{2+} without Mg^{2+})	Biochrom AG

Chemical and biochemical	Manufacturer or supplier
Pefabloc SC-Protease-Inhibitor	Carl Roth GmbH + Co.KG
Penicillin/Streptomycin (10.000 Units/ml; 10.000 µg/ml)	Thermo Fisher Scientific Inc.
Pierce Crosslink Magnetic IP/Co-IP Kit (# 88805)	Thermo Fisher Scientific Inc.
Ponceau S for electrophoresis	Sigma-Aldrich Co. LLC.
Powdered milk blotting grade, powdered, low fat	Carl Roth GmbH + Co.KG
Protein A-Agarose lyophilized powder (P1406)	Sigma-Aldrich Co. LLC.
Protein A–Peroxidase from Staphylococcus aureus/horseradish	Sigma-Aldrich Co. LLC.
Rotiphorese Gel 30 (37.5:1): 30 % acrylamide/bisacrylamide	Carl Roth GmbH + Co.KG
Roti-Quant (5x)	Carl Roth GmbH + Co.KG
SERVANativ Marker Liquid Mix for BN/CN	Serva Electrophoresis GmbH
Silver nitrate	Carl Roth GmbH + Co.KG
Sodium acetate	Carl Roth GmbH + Co.KG
Sodium carbonate anhydrous	Carl Roth GmbH + Co.KG
Sodium chloride	Carl Roth GmbH + Co.KG
Sodium hydroxide	Carl Roth GmbH + Co.KG
Sodium thiosulphate pentahydrate	Carl Roth GmbH + Co.KG
Sodium-Pyruvate	Biochrom AG
SuperSignal West Dura Extended Duration Substrate	Thermo Fisher Scientific Inc.
Tricine	Serva Electrophoresis GmbH
Tris(hydroxymethyl)aminomethane	Sigma-Aldrich Co. LLC.
Trypsin/EDTA solution (0.05%/0.02 % in PBS, without Ca^{2+}, Mg^{2+})	Biochrom AG
Tween 20 (Polyoxyethylenesorbitanmonolaurate)	GE Healthcare
ε-Aminocaproic acid	Serva Electrophoresis GmbH

7.3.4 Antibodies

Antibody (Product No.)		Manufacturer or supplier
Polyclonal HRP-goat anti-mouse	(115-035-146)	Dianova GmbH
Polyclonal HRP-goat anti-rabbit	(111-035-144)	Dianova GmbH
Monoclonal mouse anti-Actin	(DLN-07274)	Dianova GmbH
Monoclonal mouse anti-Tubulin	(T 6199)	Sigma-Aldrich Co. LLC.
Polyclonal rabbit anti-MIF	(sc-20121)	Santa Cruz Biotechnology, Inc

7.3.5 Software

Software	Developer
SilverFastAi 6.6	Lasersoft Imaging, Inc.
FUSION-CAPT	Vilber Lourmat Deutschland GmbH
Microsoft office 2007	Microsoft Corporation
Adobe Photoshop CS6	Adobe Systems Inc.

7.4 Abbreviations

× *g*	Times gravity
µg	Microgram
µL	Microlitre
6G	[6]-Gingerol
AKT	Protein kinase B
APS	Ammonium persulfate
BAX	Bcl-2-associated X protein
Bcl2	B-cell lymphoma 2
BN-PAGE	Blue native polyacrylamide gel electrophoresis
cAMP	Cyclic adenosine monophosphate
CAT	Catalase
CBB G-250	Coomassie brillant blue G-250
CBB R-250	Coomassie brillant blue R-250
Cdk	Cyclin-dependent kinase
cm	Centimetre
cm^2	Square centimetre
CNBr	Cyanogen bromide
cNOS	Constitutive nitric oxide synthase
CN-PAGE	Clear native polyacrylamide gel electrophoresis
Co-IP	Co-immunoprecipitation
COX-2	Cyclooxygenase-2 or Prostaglandin-endoperoxide synthase 2
Da	Dalton
ddH_2O	Deionised distilled water or ultra pure water
DMSO	Dimethyl sulfoxide
DNA	Deoxyribonucleic acid
DPPH	di(phenyl)-(2,4,6-trinitrophenyl)iminoazanium
DSS	Disuccinimidyl suberate
DTT	Dithiothreitol
e.g.	*exempli gratia*
EDTA	Ethylenediaminetetraacetic acid
ELISA	Enzyme-linked immunosorbent assay
ERK	Extracellular signal-regulated kinase
FBS	Fetal bovine serum
GA	Glutaraldehyde
GPx	Glutathione peroxidise
GSH	Glutathione
GSK-3	Glycogen synthase kinase 3
HEPA	High-efficiency particulate absorption
HEPES	4-(2-Hydroxyethyl)piperazine-1-ethanesulfonic acid
HIF-1α	Hypoxia-inducible factor 1-alpha
HPLC	High performance liquid chromatography
HRP	Horseradish peroxidise

HSB	High salt buffer
i.e.	*id est*
IgG	Immunoglobulin G
IL	Interleukin
iNOs	Inducible nitric oxide synthase
kDa	kilodalton
LC-MS/MS	Liquid chromatography-tandam mass spectrometry
LDL	Low-density lipoprotein
LPS	Lipopolysaccharide
LTA_4H	Leukotriene A_4 Hydrolase
M	Molar
mA	Milliampere
MCP-1	Monocyte chemotactic protein-1
mg	Milligram
MHC II	Major histocompatibility complex II
MIC	Minimum inhibitory concentration
MIF	Macrophage migration inhibitory factor
mL	Millilitre
mm	Millimetre
mM	Millimolar
mRNA	Messenger RNA
NF-κB	Nuclear factor kappa-light-chain-enhancer of activated B cells
ng	Nanogram
nm	Nanometre
NP-40	Nonidet P-40 or Igepal CA-630
^oC	Degree celcius
PBS^-	Phosphate buffered saline without Ca^{2+} and Mg^{2+}
PBS^+	PBS^- supplemented with 0.1 M $CaCl_2$ and 0.1 M $MgCl_2$
PBST	Phosphate buffered saline containing 0.1% Tween 20
PFA	Paraformaldehyde
PGE_2	Prostaglandin E_2
p*I*	Isoelectric point
PI3K	Phosphatidylinositol-3-kinase
PKC-ε	Protein kinase C
PNS	Post nuclear supernatant
pRb	Phosphorylated retinoblastoma protein
PVDF	Polyvinylidene fluoride
RANTES	Regulated on activation, normal T cell expressed and secreted
RB	Reaction buffer
Rb	Retinoblastoma protein
ROS	Reactive oxygen species
Rpm	Revolutions per minute
RT	Room temperature
SDS-PAGE	Sodium dodecyl sulfate polyacrylamide gel electrophoresis

SOD	Superoxide dismutase
TEMED	N,N,N',N'-tetramethylenediamine
TNF-α	Tumor necrosis factor alpha
Tris	Tris(hydroxymethyl)aminomethane
V	Voltage
WB	Western blot
wt/v	Weight by volume

7.5 Statutory declaration

I hereby confirm that I am the author of the thesis presented. I have written the thesis as applied for previously unassisted by others, using only the sources and references stated in the text.

Hamburg, 6 June 2014

Treewut Rassamegevanon